Thermomechanical Layout of the NET First Wall Assembly

NET Contract No. 150/84-3/FU-D/NET

S.B. MUKHERJEE

IPP 2/273

January 1985

MAX-PLANCK-INSTITUT FÜR PLASMAPHYSIK

8046 GARCHING BEI MÜNCHEN

MAX-PLANCK-INSTITUT FÜR PLASMAPHYSIK

GARCHING BEI MÜNCHEN

Thermomechanical Layout of the NET First Wall Assembly

NET Contract No. 150/84-3/FU-D/NET

S.B. MUKHERJEE

IPP 2/273 January 1985

Die nachstehende Arbeit wurde im Rahmen des Vertrages zwischen dem Max-Planck-Institut für Plasmaphysik und der Europäischen Atomgemeinschaft über die Zusammenarbeit auf dem Gebiete der Plasmaphysik durchgeführt.

Abstract

The 2D-finite element (FE) method is applied for the NET first wall structure to compute the quasi-harmonic steady-state temperature distribution within the wall and to determine the nonlinear elastic stresses under thermomechanical loads. 26 different cases (as proposed) have been investigated for the structure containing plane wall, grooved wall and thin wall concepts, respectively. The wall's support condition and the nonlinear material and thermal parameters are varied. The computations are carried out once with water coolant and then with high pressure helium coolant. The results are documented in this final report.

The FE analyses show that the first wall is subjected to high bending stresses, if it is mounted on the blanket. Under the assumed conditions the wall with grooves reaches high stresses due to stress concentrations at the groove regions, while the plane wall concept appears to be relatively sound. Using the martensitic steel (1.4914) the stresses can be dropped by more than 30 % when compared with the austenitic steel (316L). For large wall stresses, this may be significant reduction. Since the high stresses are mainly due to bending moments, some support-stiffness between the first wall and the blanket might be necessary to reduce such moments and the reaction forces, transmitted from the blanket to the first wall.

The stresses at the rounded corners of the rectangular breeder ducts are rather considerable, especially for the plane wall concept. The reaction forces, transmitted from the blanket, are collected locally in the wall at the duct's corners. The grooved wall, in contrast, reduces these corner stresses; but this is again at the cost of high stress concentrations in the grooved regions of the wall. The consideration for circular-shaped ducts instead of rectangular ones may be worthwhile for better distribution of reaction forces within the first wall. Also hoop stresses around the ducts, induced by the pressure load, could be uniformly distributed if they are circular.

C O N T E N T S

1. Introduction

The NET team is currently considering two alternative blanket concepts /7,13/, one employing a water cooled liquid breeder and another one with a helium cooled solid ceramic breeder. For both concepts first wall designs have been elaborated and roughly analyzed which should meet the high priority requirements of reliability and safety. The approach towards high reliability expresses in the choice of poloidal coolant tubes of circular cross-section resulting in the lowest number of tubes possible. The request for high safety is met by providing double containment of the high pressure coolant which is a specific demand in the case of water cooling.

First one dimensional analyses /3/ showed that is might be difficult to operate either of the two first wall structures within the temperature and stress limitations, prescribed by the characteristic properties of the breeder or multiplier and the structural material. Melting points, chemical compatibility, and strength of the materials are the properties of major concern.

The aim of this engineering study, therefore, is to determine the steady-state two-dimensional temperature and stress distributions within a representative part of the cross-section of the first wall assembly using finite element (FE) method and to prove the feasibility of the basic first wall concepts for the two applications. The water and the helium cooled concepts are to be treated separately.

With the water cooled first wall the coolant tube is contained in a closed structural box, the interspace being filled with 17Li83Pb eutectic breeder material in liquid phase. This provides good thermal bonding and contributes additionally to the tritium breeding capability of the blanket. Inlet and outlet temperature of the water coolant are assumed to be 240 and 280^{o} C.

The original helium cooled first wall is of similar design. The structural box is, however, of bigger radial extension, carries two

coolant tubes instead of one, and the interspace is filled with pure lead which should remain solid during the operation. Because of the relatively thick lead layer this first wall structure acts as a neutron multiplier for a solid ceramic blanket attached to it. However, this concept is dropped from the present FE computations. This is due to the uncertainty with the helium's working temperatures for efficient operation and for maintaining the solid state of the pure lead multiplier at the same time. A rough estimate showed that the lead multiplier could stay only in the solid state (i.e. less than 327^{o} C, the melting point of pure lead), if the maximum helium coolant temperature did not exceed 220^{o} C. These difficulties have already been recognized by the NET team and alternative design solutions are underway.

Investigations with an alternative helium coolant concept are carried out instead. In this concept the original water-cooled first wall is now assumed to be helium cooled. The coolant occupies the entire cross-section of the rectangular duct.

There are three types of the first wall configuration considered by the NET team for FE computations:
The plane wall, the grooved wall and the thin wall. Special emphasis is devoted to the idea of grooving the first wall by cutting slots, with rounded bottom, to the surface exposed to the plasma. This means should lead to acceptable temperature and stress conditions within the bearing structure behind the grooves. The sacrificial layer in between the grooves is being subject to erosion and its higher stress values could be afforded.

The thin wall configuration is considered for studying the distribution of wall stresses when the sacrificial layer in between the grooves disappeared through erosion. Of bigger importance are these results, however, as a first approach for the case that the thin metallic first wall structure is protected against erosion by a non-metallic layer or tiles.

316L austenitic stainless steel is assumed as the reference structural material. Alternatively the 1.4914 martensitic steel is considered and that should yield appreciably lower temperature gradients and thermal stresses.

Within the NET contract period of 6 months, the first half has been involved with the work of finite element modelling and mesh generation for the water cooled austenitic first wall structure in three basic configurations: without grooves, with grooves, and with partly closed grooves. The FE computations have then been performed for 2D quasi-harmonic problems of the steady-state temperature distributions within the wall's cross-section and the corresponding nonlinear elastic problems with the wall structure being fully supported on the blanket. The first results for this design on temperature, displacement and stress field have been documented in the intermediate report /1/.

In the second half of the period FE computations have been proposed for the plane wall, the grooved wall and for the thin wall respectively, with varying the support parameters and the material parameters, once with the water cooling (and the breeder duct being subjected to the internal hydrostatic pressure of the liquid lead) and then with the high pressure helium cooling. Altogether 26 combinations of cases (see Appendix 1) have been investigated and are documented in this final report.

2. FE Computations of the First Wall

The finite element models for the representative cross-section of the first wall strutcure are produced by the mesh generator of the code STRUDL /2/. Detailed description about mesh generation is made in the intermediate report /1/. There are three variations of the water cooled first wall configuration and these are the plane wall, the grooved wall and the thin wall respectively. For the helium cooling, the first wall cross-section is identical to that of the water cooling with the only difference that the liquid lead and the coolant

tubes are removed and the rectangular ducts are then used for the helium coolant flow as mentioned before. The 2D parabolic isoparametric elements are used for the models. Each element contains 8 nodes and each node has 2 degrees of freedom (plane strain problem). There are a total of 560 elements and 2008 nodal points (maximum) for the water cooled grooved wall (Fig. 1) and they vary as the configuration of the wall's cross-section changes.

To support the representative part of the first wall structure, three different types have been considered so far:

a) Side support only

Here the wall is actually allowed for free two-dimensional expansion under thermal load. To simulate this effect the wall is only supported sidewise at A-A as shown in Sketch 1. All the points on A-A do not move in the x-direction but they are free to more in the xy direction only. The point B is fixed both in x and in y directions respectively. This type of side support is necessary for the FE computation, if it is required to simulate the free expansions of the wall in both directions (for the plane strain problem). The free wall has to be supported somewhat, otherwise the determinant of the structural stiffness matrix will be singular and this means that an application of any form of external loading will result in the system moving as a rigid body. It is to be mentioned again that the point B is fixed in both directions; otherwise if y is free, the representative wall will move away in the y direction since all other points on A-A are free to move in that direction. Again if the point B is free in the x direction only, then this point B will move in x direction leaving a gab there in the wall.

This type of side support is different from the cantilever type support, in which a beam is rigidly fixed at one side. In this case all the points along the supported side are fixed not only in the x direction but also in the y direction as well.

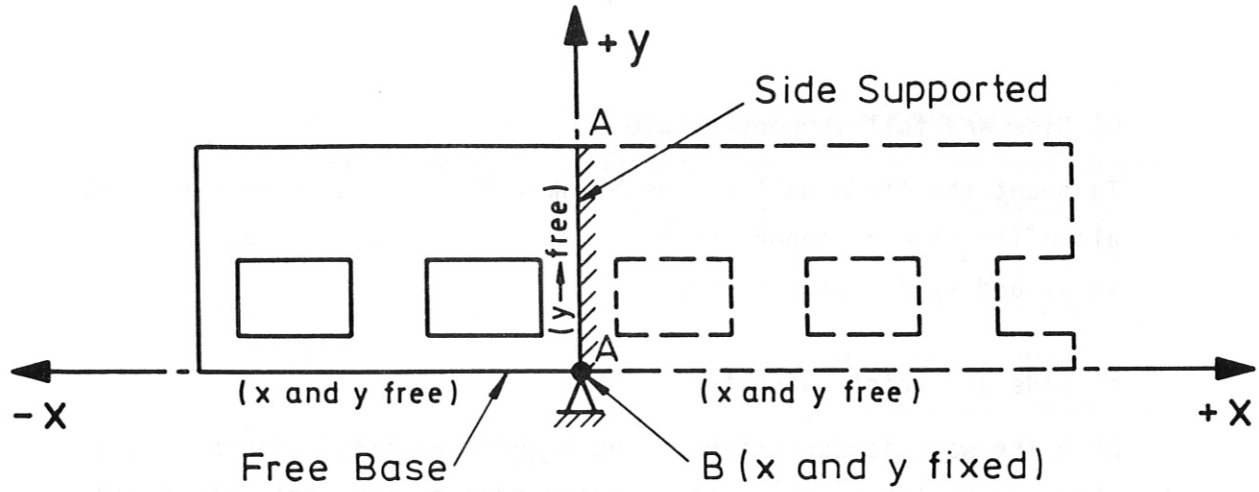

Sketch 1: Side Support only

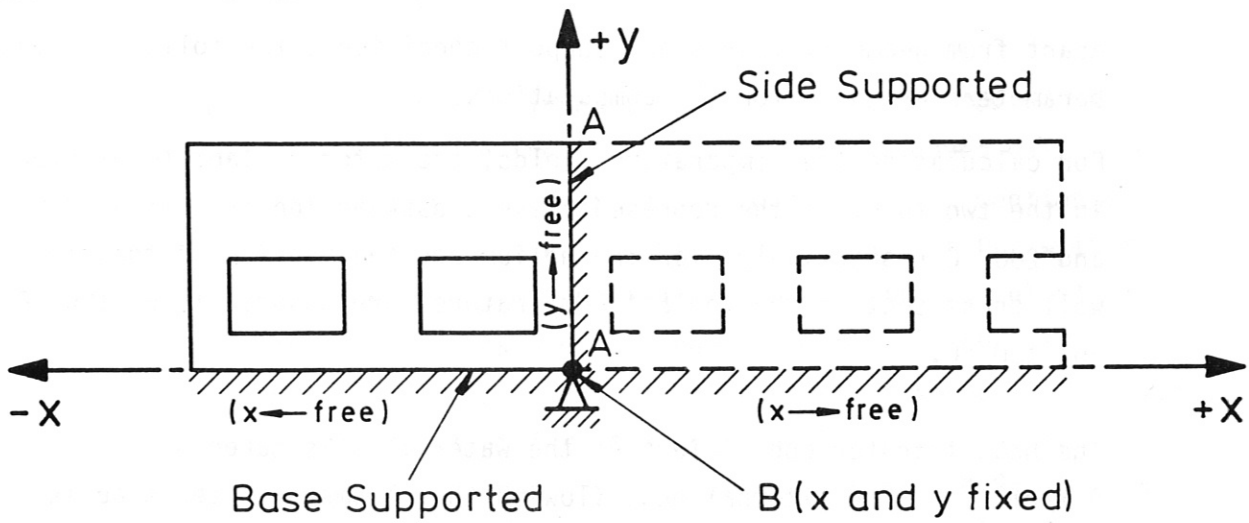

Sketch 2: Side and Base Supported

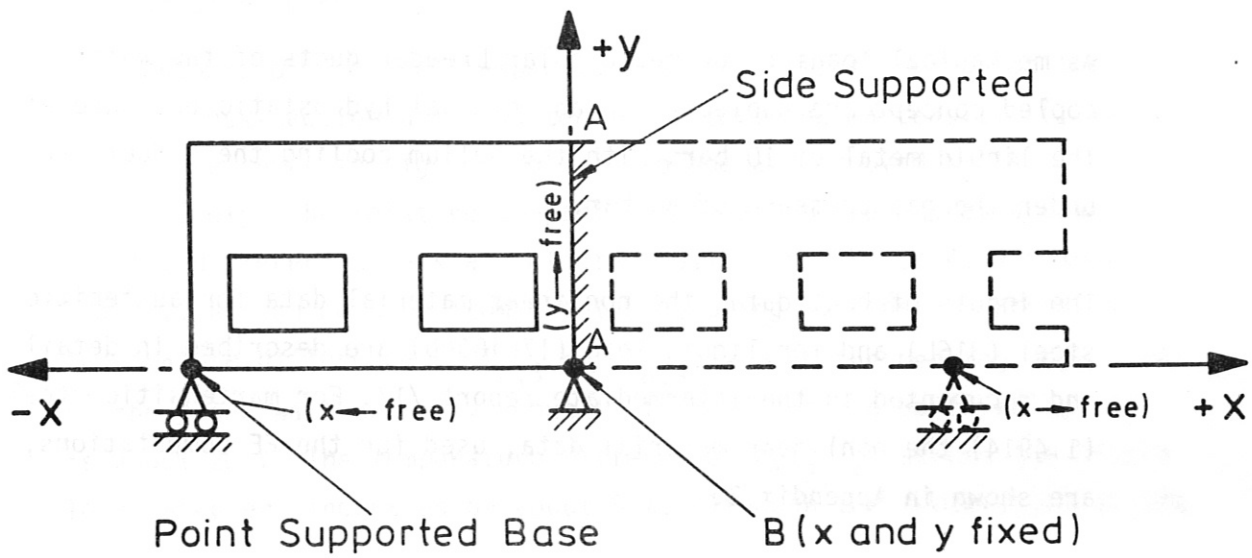

Sketch 3: Side and Point Supported Base

b) Side and full supported base

To mount the first wall on the blanket the structure is supported all along its base as shown in Sketch 2. Here the wall is allowed to move in -x and +y directions only.

c) Side and point supported base

Here the wall is supported on the blanket at fixed points only as shown in Sketch 3. The wall is again free to move only at -x and +y directions. The FE computations with this support concept are done only for two cases and they will be discussed later.

Apart from geometry models and support conditions, the following load parameters are used for the computations:

For calculating the temperature fields, the water coolant temperatures in the two tubes of the representative cross-section are set at 240^{o} C and 280^{o} C respectively. For the helium cooling version of the same wall cross-section the coolant temperatures are assumed to be 100^{o} C and 300^{o} C.

The heat transfer coefficient of the water flow is taken as 5 W/cm^2 ^{o} C. The external heat flow on the plasma oriented side is 13 W/cm^2. The power density distribution within the wall is shown in Appendix 2. This corresponds to a neutron wall loading of about 1.3 MW/m^2.

As mechanical loading the rectangular breeder ducts of the water cooled concept are subjected to an internal hydrostatic pressure of the liquid metal of 10 bar. With the helium cooling these ducts are under the gas pressure of 80 bar.

The inputs of heat data, the nonlinear material data for austenitic steel (316L) and for liquid lead (17Li83Pb) are described in detail and documented in the intermediate report /1/. For martensitic steel (1.4914) the nonlinear material data, used for the FE computations, are shown in Appendix 3.

The 2D quasi-harmonic problems of the steady-state temperature distributions within the first wall cross-section and the corresponding nonlinear elastic problems together with the pressure load for different wall-support conditions are computed by the FE code STRUDL /2/. For calculation of the stiffness matrix of the wall structure, the liquid lead elements are removed. All coolant tube elements are also eliminated, since they are assumed to stand alone for themselves within the ducts after removal of the liquid lead elements.

3. Water Cooled First Wall

10 different cases have been investigated for the water cooled first wall concept. These include the plane wall and the grooved wall. They are supported with three different support conditions as mentioned before (Sketches 1 to 3). The calculations are done at first with the austenitic steel and they are repeated with martensitic steel. As far as thermomechanical stresses are concerned, the discussions of results are carried out mainly with the von Mises equivalent stresses. The von Mises stresses are important for structural analysis to find out whether the failure will occur anywhere within the structure through plastic yielding. A detailed study of the component stresses using austenitic steel has been done in /1/.

3.1 Discussion of Results

The contours of isotherm temperature distributions throughout the wall's cross-section using austenitic (316L) and martensitic (1.4914) steels are shown in Figs. 2 to 5 for plane and grooved walls respectively. The relative comparison of wall temperatures are made for two different steels at selected positions, Sketch 4, and shown in Table 1. As can be seen from the table, using martensitic steel the temperature difference ($\triangle T_{2,3}$ or $\triangle T_{8,9}$) across the bearing structure of the plane wall drops by about 17 % and for the grooved wall, this is about 20 %. The temperature difference ($\triangle T_{3,4}$) across the liquid lead, however, increases by about 8 %. Although the temperature at the

TABLE 1: Comparison of Water-Cooled Wall Temperatures for Austenitic and Martensitic Steels.

	Temperature Locations	Wall	Austenitic(3162)	Martensitic(1.4914)	Difference
Coolant 240° C	T_1	plane grooved	538°C 530°C	495°C 487°C	
	$(T_2 - T_3)$ Across wall	plane grooved	$\Delta T_{2,3}$ = 209°C $\Delta T_{2,3}$ = 71°C	$\Delta T_{2,3}$ = 173°C $\Delta T_{2,3}$ = 57°C	- 17.2 % - 19.7 %
	$(T_3 - T_4)$ Across Liquid Lead	plane grooved	$\Delta T_{3,4}$ = 38°C $\Delta T_{3,4}$ = 36°C	$\Delta T_{3,4}$ = 41°C $\Delta T_{3,4}$ = 39°C	+ 7.9 % + 8.3 %
	$(T_4 - T_5)$ Across Coolant Tube	plane grooved	$\Delta T_{4,5}$ = 37°C $\Delta T_{4,5}$ = 35°C	$\Delta T_{4,5}$ = 28°C $\Delta T_{4,5}$ = 26°C	- 24.3 % - 25.7 %
	T_6 Min. Liquid Lead Temp.	plane grooved	252°C 252°C	250°C 250°C	
Coolant 280° C	T_7 Max. Steel Temp.	plane grooved	556°C 557°C	515°C 517°C	
	$(T_8 - T_9)$ Across Wall	plane grooved	$\Delta T_{8,9}$ = 192°C $\Delta T_{8,9}$ = 64°C	$\Delta T_{8,9}$ = 158°C $\Delta T_{8,9}$ = 51°C	- 17.7 % - 20.3 %
	$(T_9 - T_{10})$ Across Liquid Lead	plane grooved	$\Delta T_{9,10}$ = 34°C $\Delta T_{9,10}$ = 32°C	$\Delta T_{9,10}$ = 35°C $\Delta T_{9,10}$ = 33°C	+ 2.9 % + 3.1 %
	$(T_{10} - T_{11})$ Across Coolant Tube	plane grooved	$\Delta T_{10,11}$= 33°C $\Delta T_{10,11}$= 31°C	$\Delta T_{10,11}$= 24°C $\Delta T_{10,11}$= 24°C	- 27.3 % - 22.6 %
	T_{12} Max. Liquid Lead Temp.	plane grooved	396°C 395°C	385°C 385°C	

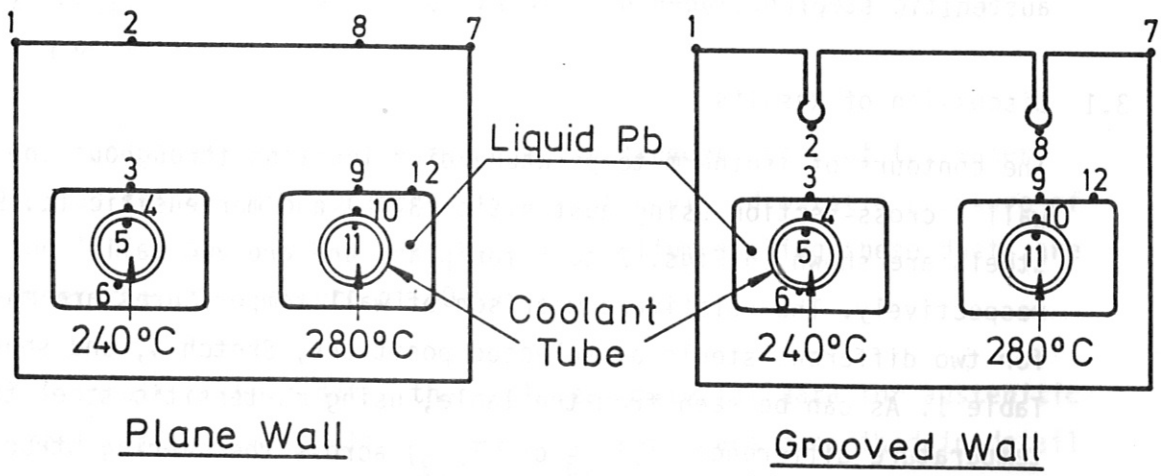

Sketch 4 (Temperature Locations. Water Cooled Wall)

interface between liquid lead and martensitic steel is lower than in case of using austenitic steel, the lower lead temperature increases the thermal resistance of liquid lead. The maximum temperature of the structural steel occurs at T_7. The maximum liquid lead temperature, never exceeds 450°C (the highest limit). The minimum liquid temperature, T_6, is above the melting point of 235°C in all cases.

As far as stresses are concerned, these include thermal stresses and mechanical stresses due to the hydrostatic pressure of the liquid lead. Since this pressure is only 10 bar, the contribution of mechanical stresses is rather low and the thermal stresses are predominant. The contours of stresses due to the hydrostatic liquid lead pressure is shown in Fig. 6. These are hoop stresses in nature and have low values. The outer leg of the free wall end is subjected to bending stresses due to the pressure. The deflection of the wall under the liquid lead pressure is shown in Fig. 7. The outer leg is deflected only by 0.003 mm. The edges of the inner leg remain parallel due to the equal pressure from both side. Fig. 8 shows the total deformation pattern both due to the temperature and pressure. The deformation of the wall is dominated by the temperature rise within the wall. The total deformation patterns for other support conditions are shown in Figs. 9 to 13. for the austenitic steel only. With the martensitic steel the deformation patterns are similar.

For different support conditions the thermomechanical stresses are obtained for the locations as shown in Sketch 5. A comparison of these stresses is shown in Table 2 for the plane and the grooved walls with the two different structural steels. σ_7 represents the stress where the temperature of the steel is maximum. σ_{12} represents the stress of the wall where the liquid lead temperature attains its maximum value. Only these wall stresses are tabulated for comparison. All other wall stresses in the corners of the rectangular breeder ducts are shown in Figs. 14 to 23. As shown in Table 2 and also in the contours of von Mises stresses, the stresses developed both for austenitic and for martensitic steels are rather low if the wall is supported only sidewise (i.e. for the free expansion of the wall). The contours

TABLE 2: Comparison of Water Cooled Wall Stresses (von Mises) using Different Supports for Austenitic and Martensitic Steels.

Stress Locations	Wall	Austenitic Steel (316 L)			Martensitic Steel (1.4914)	
		Side Support only	Side and Base Supported	Side and Point Supported Base	Side Support only	Side and Base Supported
σ_1 (MPa)	plane	1.4 (538°C)	3 (538°C)	2 (538°C)	1 (495°C)	2 (495°C)
	grooved	2 (530°C)	2 (530°C)	2 (530°C)	1 (487°C)	1 (487°C)
σ_2 (MPa)	plane	32 (539°C)	48 (539°C)	25 (539°C)	22 (497°C)	34 (497°C)
	grooved	159 (396°C)	428 (396°C)	306 (396°C)	102 (377°C)	288 (377°C)
σ_3 (MPa)	plane	64 (330°C)	153 (330°C)	128 (330°C)	34 (324°C)	93 (324°C)
	grooved	94 (325°C)	228 (325°C)	164 (325°C)	62 (320°C)	153 (320°C)
σ_7 (MPa) Steel Temp. Max.)	plane	14.6 (556°C)	189 (556°C)	201 (556°C)	11.9 (515°C)	127 (515°C)
	grooved	35 (557°C)	33 (557°C)	25 (557°C)	24 (517°C)	22 (517°C)
σ_8 (MPa)	plane	12 (552°C)	172 (552°C)	159 (552°C)	10 (511°C)	117 (511°C)
	grooved	257 (420°C)	549 (420°C)	568 (420°C)	153 (401°C)	355 (401°C)
σ_9 (MPa)	plane	90 (360°C)	264 (360°C)	253 (360°C)	51 (353°C)	167 (353°C)
	grooved	149 (356°C)	264 (356°C)	278 (356°C)	91 (350°C)	169 (350°C)
σ_{12} (MPa) Ref. only (Liquid Lead Temp. Max.)	plane	123 (396°C)	413 (396°C)	443 (396°C)	75 (385°C)	267 (385°C)
	grooved	82 (395°C)	82 (395°C)	109 (395°C)	51 (385°C)	51 (385°C)

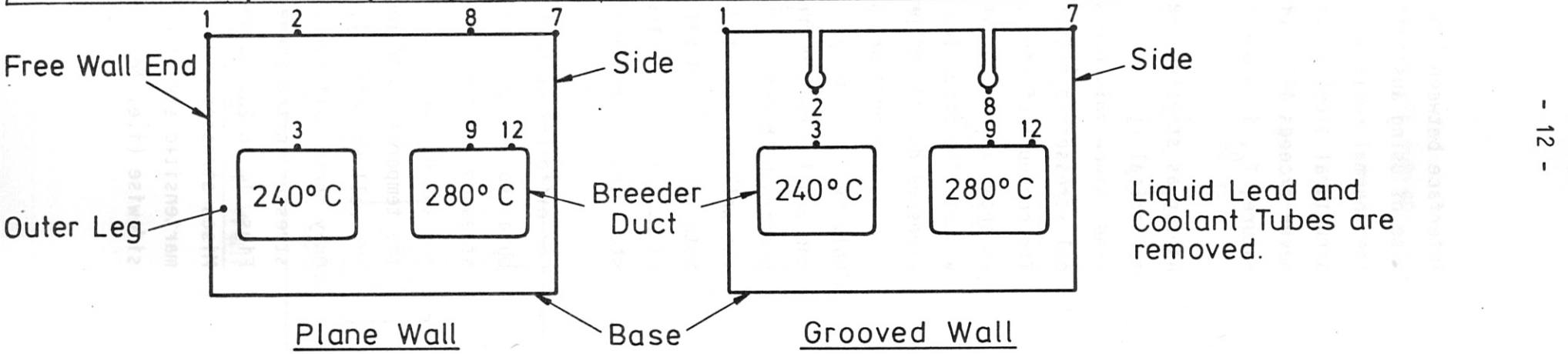

Sketch 5 (Stress Locations. Water Cooled Wall)

of these stresses are the interlayer stresses acting within the plane wall due to temperature variations. When the wall is grooved, all these interlayer stresses now concentrate mainly at and around the rounded part of a groove. With no groove the maximum stress within the wall width σ_9 attains 90 MPa for austenitic (and 51 MPa for martensitic). For the grooved wall the maximum stress σ_8 in the groove region amounts to 257 MPa for austenitic (and 153 MPa for martensitic). It is to be mentioned that σ_{12} (shown in Table 2 for reference only) belongs to the corner stresses of the rectangular breeder ducts and for which the discussions will be carried out later in this report.

If the wall is supported at the base, the maximum stresses both for the grooved and for the plane wall (σ_8 and σ_9 respectively) now increase by factor 2 to 3. These increase in stress is due to the additional bending stresses now acting in the first wall. When the wall expands freely (Fig. 9 for the side support only), it expands also downward at the base (0.176 mm deformation for the plan wall). If this expansion at the base is now constrained (i.e. the base is supported) a bending moment is induced. An estimate is made for the plane wall with the point supported base (Sketch 3 and Fig. 10) and the maximum bending stress is worked out to be about 300 MPa (Appendix 4). The FE computations also show the high bending stresses acting in the plane wall and in the grooved wall when supported. Figs. 11 and 12 show the deformation plots for the grooved wall. With full base support the grooves are further squeezed when compared with the deformation where the base is free. The high stress concentration in a grooved wall has also been detected by G. Vieider in his analytical model /3/.

The grooved wall has less resistance to bending. The area moment (I) of the wall is locally reduced when it is grooved. The flexural rigidity of the wall EI (where E is the elastic modul) towards bending is now determined by the material left over behind the groove. Further, the grooved wall does not reduce the thermal resistance when compared with the plane wall having the same width. Instead the grooves induce

stress concentrations even when the wall is free to expand (Fig. 17 and Table 2). The induced bending moment then intensifies these stress concentrations by further squeezing the grooves. It is not likely that the bigger groove radius could reduce these stress concentrations considerably as long as the squeezing occurs. The comparison of the wall stresses in Table 2 shows that the plane wall (although highly stressed when supported on the blanket) is relatively better off than the grooved wall for the given support conditions. The maximum stress within the plane wall (σ_9) is always less than then maximum groove stress (σ_8) by factor 2 or more for the water cooled first wall structure.

The stresses in the rounded corners of the breeder duct for the plane wall are rather high, even when the wall is free to expand (Fig. 14). The outer leg is most heavily loaded. This is due to the nonuniform deformation of the plane wall (Fig. 9) imposing axial thrust on the outer leg. When the wall is supported at the base, the induced bending moment increases the stresses at the corners of the breeder ducts. On the outer leg the stresses become even higher by factor 2 or more (Fig. 15). The outer leg actually represents the free end condition of the first wall. The higher stiffness of the outer leg would of course reduce these stresses. Splitting the plane wall (i.e. grooving the wall), of course, reduces the stresses in the outer leg by more than half the value and also the stresses at the rounded corners of the breeder ducts drop (Figs. 17 and 18) when compared with the plane wall (Figs. 14 and 15). But this is at the cost of high stress concentrations in the grooved regions of the wall. Further the wall with thin grooves (1 mm width) may not be easy to fabricate. It may be easier and cheaper to put bigger radius at the corner of a rectangular duct. This would, of course, reduce the volume of the breeding materials. It might even be better to reduce the wall thickness for releasing these corner stresses. Reduction of the wall thickness leads to less thermal resistance and induced bending moment.

As far as the material for the wall structure is concerned, the martensitic steel seems to be a good performer. It has higher thermal conductivity (Appendix 3) within the temperature range of 0^{o} to $600^{o}C$

and thus the temperature difference across the wall decreases when compared with the austenitic steel. Also the coefficient of thermal expansion for martensitic steel is lower than the austenitic steel and this makes the thermal expansion of the wall by a factor of 1.5 smaller. Comparing the stresses in Table 2, the stresses within the wall drop by 30 % or more using martensitic. Thus, the higher the thermal loads the more suitable this steel would be to bring down the stresses when compared with austenitic. Also the Young's modulus E for martensitic is higher than for austenitic. This means that the martensitic steel offers greater structural stiffness and thus less deflection under mechanical load.

When talking about reduction of stresses, the correct supporting of the wall plays a very important role. A structure under thermal load is sensitive to support conditions. Ideally, if the wall could be simply hanged from one end (to simulate the free expansion), this would have produced least stresses within the plane wall. Technically this would not likely to be feasible, since this arrangement would drift the wall towards the plasma. If the first wall is now point supported on the blanket (Sketch 3), the stress concentrations could be as high as 883 MPa at the supported points (Fig. 16). The stresses within the grooved wall structure for point support is shown in Fig. 19. Only sensible mounting of the wall on the blanket may be to support the wall all along its base. In the present FE computations the base of the wall is rigidly fixed all along. This has caused high support reactions. These reactions could be reduced if the first wall is propped all along its base, i.e. if some support stiffness is introduced between the wall and the blanket. This support stiffness could be simulated using boundary spring elements as shown in Sketch 6, for the FE computations. With this support stiffness condition the induced bending moment may be less and thus the first wall may then be subjected to less superimposed bending stresses, especially in the regions of the rectangular ducts.

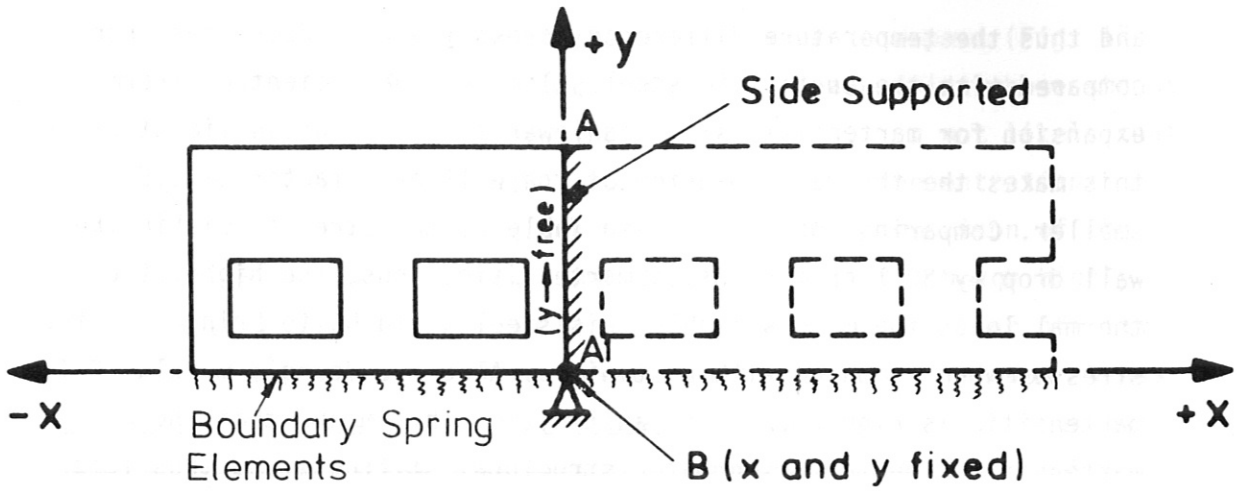

Sketch 6: Simulation of Support Stiffness
using Boundary Spring Elements.

3.2 Conclusion

The FE analysis for the water cooled first wall structure (using both austenitic and martensitic steels respectively) shows that due to the high stress concentration problem, "the grooving concept" might not be a sound engineering approach for reducing the thermal stresses, superimposed by the bending stresses, within the wall structure as long as the wall is supported on the blanket. The wall with grooves may be difficult to manufacture and there are always stress concentrations to be expected. The plane wall on the other hand (although highly stressed) appears to be relatively friendly as far as stresses within the plan wall width are concerned. From the fatigue's point of view the grooves are undesirable for a structure subjected to high temperature, since they tend to initiate cracks.

As mentioned before, for the choice between austenitic and martensitic steels, the latter appears to be more attractive. This steel offers relatively low thermal resistance towards heat flow, causes less thermal deformation, gives higher structural stiffness against mechanical load and the stresses drop by more than 30 % when compared with the austenitic steel. The martensitic (1.4914) is a good engineering

material for high thermal stresses. But the high stresses within the first wall structure are mainly the bending stresses acting in it as shown in Appendix 4. If a means is found to minimize the induced bending moment and thereby to reduce the high wall stresses, it is then perhaps worthwhile to make specific consideration between the martenitic and the austenitic steels.

For the plane wall the corner stresses of the breeder ducts are most problematic. Bigger corner radii to bring down the stresses will be at the cost of the breeder volume. Instead of grooving, it may be suitable to reduce the wall thickness to release some stresses. In fact the feasibility of shortening the wall thickness has already been discussed by W. Daenner in /4/. Also it may be interesting to make an interplay between the wall thickness reduction and the support stiffness variation. This may produce fruitful results to optimize not only the wall stresses but also the breeder-duct corner stresses. Perhaps an alternative design of the breeder-duct may solve this problem altogether.

4. Helium Cooled First Wall

The water cooled first wall is simply converted into a helium cooled one by removing the liquid breeder and coolant tubes and using the duct for helium coolant flow as mentioned before. There are again 8 different cases investigated for this concept. These include the wall with grooves and no grooves as before with austenitic and martensitic steels respectively. The helium pressure of 80 bar is now included as the mechanical load and the thermal load in the structure remained unaltered as for the water cooled concept (Appendix 2). The coolant temperatures are assumed to be 100^{o} C and 300^{o} C. Here also the comparison of stresses are based on von Mises only. The wall supports of two types: a) Side support only (Sketch 1) and b) Side and Base supported (Sketch 2), are considered.The FE computations with the helium cooled first wall are performed mainly for academic reasons, to get some basic ideas about the stress response within the wall

structure using the low heat transfer coefficient of 0.5 $W/cm^2\ ^oC$ for helium under pressure, with varying the support and material parameters.

4.1 Discussion of Results

Figs. 24 and 27 are showing the contours of temperature distributions for helium cooled grooved and plane walls using austenitic and martensitic steels respectively. Table 3 shows the comparison of temperatures. Using martensitic steel the temperature difference across the plane wall drops by 22 to 25 % when compared with the austenitic steel. For FE computations the helium coolant temperatures are only assumed values. Since they are not yet positively decided, a direct comparison with the water cooled wall would be incorrect. This is because, the material properties as function of temperatures are nonlinear in character.

For the FE computation of wall stresses the helium pressure of 80 bar is included which is higher than the liquid lead hydrostatic pressure (10 bar) used for the water cooled concept. Fig. 28 shows the deflection of the free end of the plane wall due to the gas pressure alone with the wall supported at one side only. Fig. 29 shows the total deflection due to the thermal and the mechanical (pressure) load. The helium pressure is causing hoop stresses which are distributed mainly around the rectangular helium-ducts (Fig. 35). The plane wall is hardly affected. The outer leg of the wall end is subjected to bending stresses and the von Mises stresses are as high as 177 MPa. Fig. 36 shows the stresses due to the thermal load alone. Fig. 37 shows the combined thermomechanical stresses. The upper part of the plane wall is slightly affected by the hoop stresses. Near the helium-duct regions the stresses are affected differently by the superposition of the hoop stresses (due to gas pressure) on the thermal stresses. Some are gone up high and others are down especially at the corner regions.

For the plane wall with the side and the base supported, the deflection pattern due to the helium pressure alone is shown in Fig. 30. The

TABLE 3: Comparison of Helium Cooled Wall Temperatures for Austenitic and Martensitic Steels.

	Temp. Locations	Wall	Austenitic (3162)	Martensitic (1.4914)	Difference
Coolant 300°C / Coolant 100°C	T_1	plane	411°C	362°C	
		grooved	383°C	332°C	
	$(T_2 - T_3)$	plane	$\Delta T_{2,3}$ = 233°C	$\Delta T_{2,3}$ = 181°C	- 22.3 %
		grooved	$\Delta T_{2,3}$ = 72°C	$\Delta T_{2,3}$ = 54°C	- 25 %
	$(T_4 - T_5)$	plane	$\Delta T_{4,5}$ = 149°C	$\Delta T_{4,5}$ = 113°C	- 24.2 %
		grooved	$\Delta T_{4,5}$ = 41°C	$\Delta T_{4,5}$ = 29°C	- 29.3 %
	T_6 (Max. Steel Temp.)	plane	517°C	475°C	
		grooved	537°C	498°C	

TABLE 4: Comparison of Helium Cooled Wall Stresses (von Mises) using Different Supports for Austenitic and Martensitic Steels.

		Austenitic Steel (316L)		Martensitic Steel (1.4914)	
Stress Locations	Wall	Side Support Only	Side and Base Supported	Side Support Only	Side and Base Supported
σ_1 (MPa)	plane	2 (411°C)	3 (411°C)	1 (362°C)	2 (362°C)
	grooved	2 (383°C)	2 (383°C)	1 (332°C)	1 (332°C)
σ_2 (MPa)	plane	27 (425°C)	37 (425°C)	11 (377°C)	24 (377°C)
	grooved	269 (256°C)	553 (256°C)	178 (241°C)	358 (241°C)
σ_3 (MPa)	plane	123 (192°C)	191 (192°C)	88 (196°C)	124 (196°C)
	grooved	218 (184°C)	362 (184°C)	165 (187°C)	254 (187°C)
σ_4 (MPa)	plane	22 (504°C)	84 (504°C)	19 (461°C)	31 (461°C)
	grooved	124 (394°C)	234 (394°C)	17.5 (377°C)	60 (377°C)
σ_5 (MPa)	plane	118 (355°C)	219 (355°C)	82 (348°C)	129 (348°C)
	grooved	140 (353°C)	182 (353°C)	80 (348°C)	96 (348°C)
σ_6 (MPa)	plane	30 (517°C)	56 (517°C)	26 (475°C)	3 (475°C)
	grooved	38 (537°C)	48 (537°C)	25 (498°C)	34 (498°C)

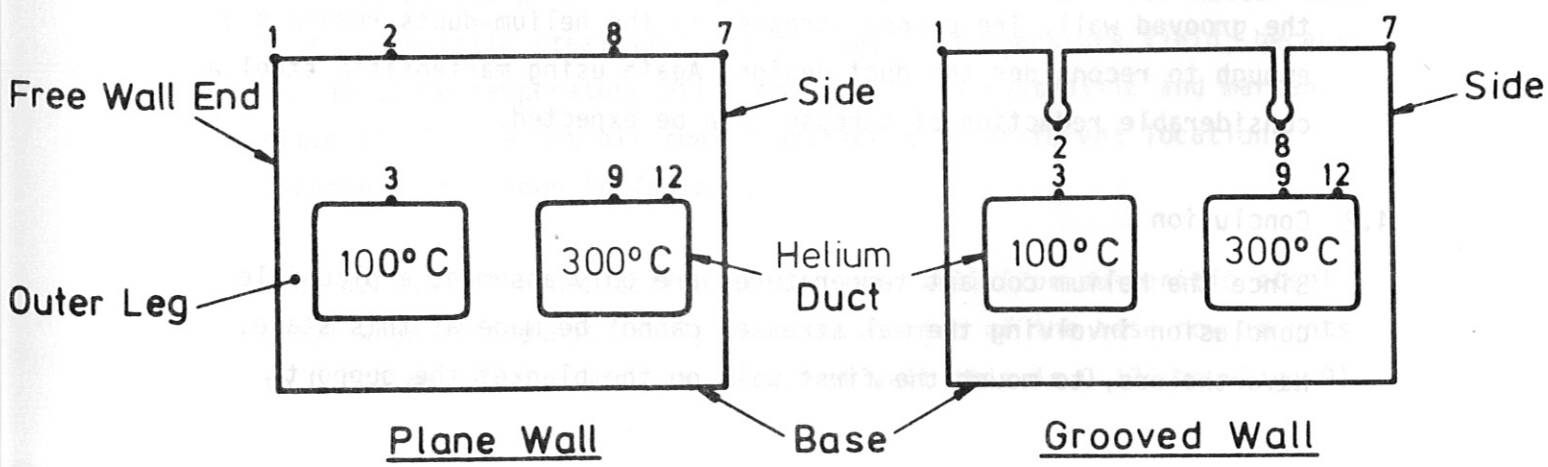

Sketch 7 (Temp. and Stress Locations. Helium Cooled Wall)

helium pressure causes more trouble at the end of the wall than anywhere else. A helium-duct, except at the end, is subjected to hoop stress mainly. The inner legs of the wall structure are balanced by the pressure from both sides. At the wall end the outer leg is deflected outward by the helium pressure. The outer leg is subjected to bending stresses and the maximum value in 210 MPa. Also there is an axial pull acting along the length of the wall as shown. These bending stresses would, however, be less with thicker outer leg. Fig. 31 shows the total deformation due to the thermal and pressure loads combined. The deflection of the grooved wall with side and base supported and under the helium pressure is shown in Fig. 32. The helium pressure tends to open up the groove on the right hand side of the wall but the groove at the end is squeezed. The wall under thermal load (with induced bending moment due to the base support) is shown in Fig. 33. Here both grooves are squeezed. The combined deformation due to the thermo-mechanical loads is shown in Fig. 34. The groove near the wall end is now more squeezed (giving higher stress concentration) while the other one is to some extent released from the thermal squeezing due to helium pressure. All deformation plots are shown for the austenitic steel only. They are similar with martensitic steel.

The comparison of the wall stresses with different support conditions using austenitic and martensitic steel is shown in Table 4. As can be seen from the table the groove stress σ_2 is greater than the groove stress σ_4 for all support conditions and for different-steel materials. The contours of von Mises stresses for all eight different cases with thermo-mechanical loads are shown in Figs. 37 to 44. Here also the maximum stress within the plane wall is less than that for the grooved wall. The corner stresses in the helium-ducts remain high enough to reconsider the duct design. Again using martensitic steel a considerable reduction of stresses can be expected.

4.2 Conclusion

Since the helium coolant temperatures are only assumed, a plausible conclusion involving thermal stresses cannot be made at this stage. Nevertheless, to mount the first wall on the blanket the support

stiffness consideration in necessary to reduce the superimposed bending stresses. The helium pressure with 80 bar causes hoop stresses. These stresses coupled with the thermal stresses are affecting the ducts differently. For better distributions of hoop stresses an alternative design of helium duct may be worthwhile.

As far as the structural steel is concerned, the martensitic (1.4914) seems to be as before a potential material.

5. Water and Helium Cooled Thin Wall

For these concepts altogether 8 different cases have been investigated. With the thin wall configuration the original wall width is reduced by 11 mm. The thin wall is then exposed to the plasma heat and the corresponding wall loading is adjusted accordingly. All other parameters remained unchanged as for the water cooling and for the helium cooling as well. The aim of these FE computations are to document the relative changes in temperature and stress contours when the wall width becomes thin under the same boundary and material parameters.

5.1 Discussion of Results

For the water cooled thin wall the contours of temperature distribution are shown in Figs. 45 and 46 using austenitic and martensitic steels respectively. As shown in Table 5, using martensitic steel the temperature difference across the plane thin wall drops by about 22 %. Actually at low wall resistance to heat flow, it does not matter much that martensitic steel improves the wall's temperature field; because the absolute temperature differences between austenitic and martensitic steels are not all that significant at different locations (Sketch 8) as shown in Table 5.

Fig. 47 shows the deflection of the thin wall (for austenitic steel only) when it expands freely. The deflection of the base now amounts to 0.044 mm whereas with the original wall this is 0.176 mm (Fig. 9).

TABLE 5: Comparison of Water Cooled Thin Wall Temperatures for Austenitic and Martensitic Steels

	Temperature Locations	Austenitic (316L)	Martensitic (1.4914)	Difference
Coolant 240° C	T_1	356 °C	340 °C	
	$(T_2 - T_3)$ Across Wall	$\Delta T_{2,3}$ = 44°C	$\Delta T_{2,3}$ = 34°C	- 22.7 %
	$(T_3 - T_4)$ Across Liquid Lead	$\Delta T_{3,4}$ = 24°C	$\Delta T_{3,4}$ = 25°C	+ 4 %
	$(T_4 - T_5)$ Across Coolant Tube	$\Delta T_{4,5}$ = 22°C	$\Delta T_{4,5}$ = 18°C	- 18.2 %
	T_6 Min. Liquid Lead Temp.	253°C	251°C	
Coolant 280° C	T_7 Max. Steel Temp.	391°C	375°C	
	$(T_8 - T_9)$ Across Wall	$\Delta T_{8,9}$ = 41°C	$\Delta T_{8,9}$ = 32°C	- 22 %
	$(T_9 - T_{10})$ Across Liquid Lead	$\Delta T_{9,10}$ = 20°C	$\Delta T_{9,10}$ = 21°C	+ 5 %
	$(T_{10} - T_{11})$ Across Coolant Tube	$\Delta T_{10,11}$ = 21°C	$\Delta T_{10,11}$ = 16°C	- 24 %
	T_{12} Max. Liquid Lead Temp.	358°C	350°C	

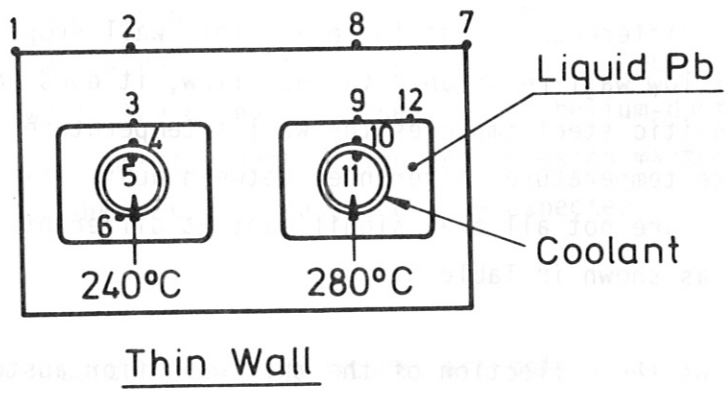

Sketch 8 (Temp. Locations. Water Cooled Thin Wall)

TABLE 6: Comparison of Water Cooled Thin Wall Stresses (von Mises) using Different Supports for Austenitic and Martensitic Steels.

	Austenitic Steel (316L)		Martensitic Steel (1.4914)	
Stress Locations	Side Support only	Side and Base Supported	Side Support only	Side and Base Supported
σ_1 (MPa)	3 (356°C)	2 (356°C)	2 (340°C)	1 (340°C)
σ_2 (MPa)	30 (339°C)	51 (339°C)	20 (326°C)	34 (326°C)
σ_3 (MPa)	44 (295°C)	62 (295°C)	32 (292°C)	44 (292°C)
σ_7 (MPa) (Steel Temp.Max.)	5 (391°C)	28 (391°C)	1 (375°C)	15 (375°C)
σ_8 (MPa)	32 (370°C)	49 (370°C)	18 (357°C)	29 (357°C)
σ_9 (MPa)	47 (329°C)	50 (329°C)	30 (325°C)	32 (325°C)
σ_{12}(MPa) Ref.only (Liquid Lead Temp. Max.)	41 (358°C)	58 (358°C)	23 (350°C)	34 (350°C)

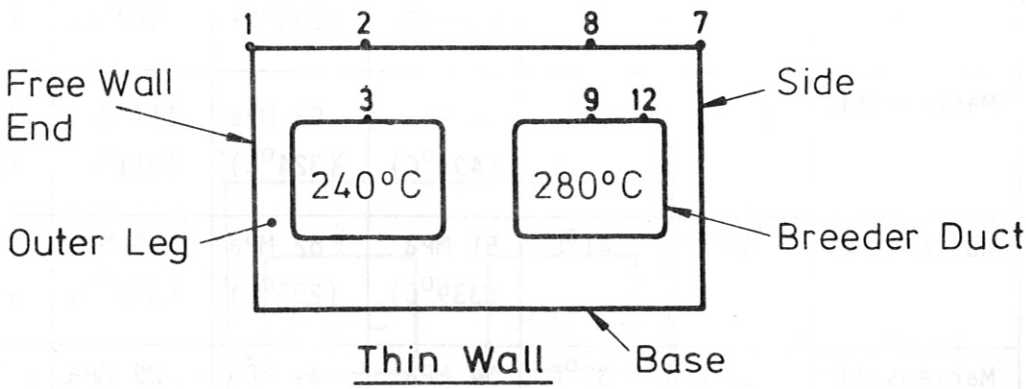

Sketch 9 (Stress Locations. Water Cooled Thin Wall)

Therefore, when the thin plane wall is supported on the blanket, Fig. 48, the induced bending moment is greatly reduced. The FE computation are carried out with Point-Supported Base (Sketch 3) for the thin wall and for the original plane wall respectively. The results show a reduction of the induced bending moment by 94 % when the thin wall concept is used.

The contours of von Mises stresses for the water cooled concept are shown in Figs. 49 to 52. The stress results show that, the corner-stresses of the breeder ducts decrease by 70 to 80 % with the thin wall concept when compared with the original plane wall concept. The comparison of the wall stresses with different support conditions using austenitic and martensitic steels is shown in Table 6. Table 7 shows the comparison of temperatures and stresses at the location numbers (Sketch 9) between the water cooled original plane wall (15 mm wide) and the thin wall (4 mm wide) using two different steels.

TABLE 7: Comparison between the Original Plane Wall and the Thin Wall, Water Cooled.

Wall	steel	(T_2-T_3)	(T_8-T_9)	σ_2	σ_3	σ_8	σ_9
Original plane wall (15 mm)	Austenitic	209°C	192°C	48 MPa (539°C)	153 MPa (330°C)	172 MPa (552°C)	264 MPa (360°C)
	Martensitic	173°C	158°C	34 MPa (497°C)	93 MPa (324°C)	117 MPa (511°C)	167 MPa (353°C)
Thin wall (4 mm)	Austenitic	44°C	41°C	51 MPa (339°C)	62 MPa (295°C)	49 MPa (370°C)	50 MPa (329°C)
	Martensitic	34°C	32°C	34 MPa (326°C)	44 MPa (292°C)	29 MPa (357°C)	32 MPa (325°C)

(See Sketch 9 for the stress location numbers)

TABLE 8: Comparison of Helium Cooled Thin Wall Temperatures for Austenitic and Martensitic Steels.

	Temp. Locations	Austenitic (361L)	Martensitic (1.4914)	Difference
Coolant 100°C	T_1	185°C	171°C	
	$T_2 - T_3$	$\Delta T_{2,3} = 44°C$	$\Delta T_{2,3} = 31°C$	- 29.5 %
Coolant 300°C	$T_4 - T_5$	$\Delta T_{4,5} = 30°C$	$\Delta T_{4,5} = 21°C$	- 30 %
	T_6	374°C	363°C	

TABLE 9: Comparison of Helium Cooled Thin Wall Stresses (von Mises) using Different Supports for Austenitic and Martensitic Steels.

	Austenitic Steel (316L)		Martensitic Steel (1.4914)	
Stress Locations	Side Support only	Side and Base Supported	Side Support only	Side and Base Supported
σ_1 (MPa)	6 (185°C)	6 (185°C)	5 (171°C)	5 (171°C)
σ_2 (MPa)	83 (191°C)	90 (191°C)	64 (181°C)	67 (181°C)
σ_3 (MPa)	161 (147°C)	166 (147°C)	137 (150°C)	138 (150°C)
σ_4 (MPa)	3 (363°C)	4 (363°C)	10 (351°C)	11 (351°C)
σ_5 (MPa)	81 (333°C)	85 (333°C)	65 (330°C)	67 (330°C)
σ_6 (MPa)	34 (374°C)	67 (363°C)	36 (363°C)	66 (363°C)

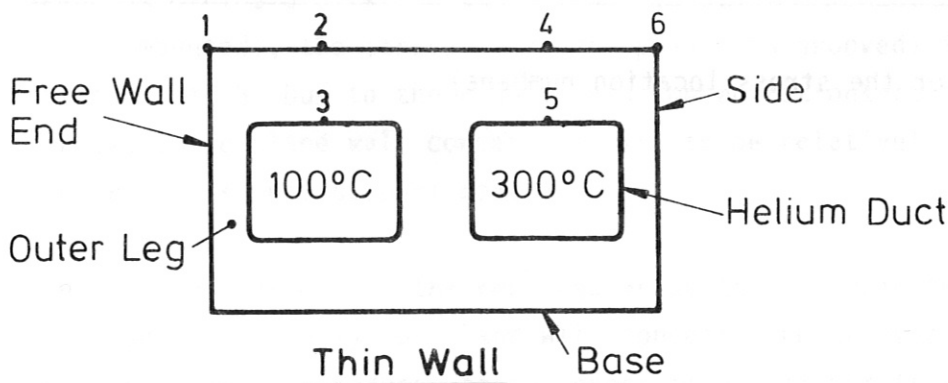

Sketch 10 (Temp. and Stress Locations. Helium Cooled Thin Wall)

For the helium cooled wall the contours of temperature distributions are shwon in Figs. 53 and 54. The wall deformation plots for austenitic steel are shown in Figs. 55 to 58. The contours of von Mises stresses are shown in Figs. 59 to 62. The comparison of temperatures and stresses are shown in Tables 8 and 9 respectively. Table 10 shows the comparison with respect to temperatures and stresses between the helium cooled original plane wall and the thin wall at the location numbers indicated in Sketch 10.

TABLE 10: Comparison between the Original Plane Wall and the Thin Wall, Helium Cooled.

	steel	(T_2-T_3)	(T_4-T_5)	σ_2	σ_3	σ_4	σ_5
Original plane wall (15 mm)	Austenitic	233°C	149°C	37 MPa (425°C)	191 MPa (192°C)	84 MPa (504°C)	219 MPa (355°C)
	Martensitic	181°C	113°C	24 MPa (377°C)	124 MPa (196°C)	31 MPa (461°C)	129 MPa (348°C)
Thin wall (4 mm)	Austenitic	44°C	30°C	90 MPa (191°C)	166 MPa (147°C)	4 MPa (363°C)	85 MPa (333°C)
	Martensitic	31°C	21°C	67 MPa (181°C)	138 MPa (150°C)	11 MPa (351°C)	67 MPa (330°C)

(See Sketch 10 for the stress location numbers)

5.2 Conclusion

Reducing the wall thickness brings down the bending stresses within the wall. The corner-stresses in the rectangular ducts also diminish accordingly. Using martensitic steel the temperature and stress distributions within the thin wall structure, however, improve. If the wall resistance to heat flow is considerably low (by thinning the wall thickness), the actual differences in temperatures and stresses are less significant between the austenitic and the martensitic steels.

6. Summary

The FE computations are carried out for the water cooled version of the first wall structure and include plane, grooved and thin wall concepts respectively. For different wall support conditions and material parameters with inclusion of pressure loads in the ducts the computations are firstly done for the water coolant and then for helium coolant flow (after removing the liquid lead and the water coolant tubes from the ducts) respectively. There are altogether 26 different cases investigated and documented. Here is the summary of the main results:

- The first wall when mounted on the blanket, is subjected to high bending stresses. If it is not supported on the blanket, the stresses are mainly due to the wall's temperature variations and these are rather low within the plane wall width. Grooving the wall leads to the concentration of these stresses around the rounded regions of the grooves. With the induced bending moment on the wall (when mounted), the stress (for both plane and grooved) increase by factor 2 to 3. Due to the high stress concentrations at the grooves, the plane wall concept appears to be relatively better under the assumed support conditions.

- The rounded corners of the rectangular ducts are subjected to high stresses, especially for plane wall concept. The grooved wall, however, however, reduces these corner stresses; but this is at the

cost of high stress concentrations in the grooved regions of the wall. Also due to the pressure load, the induced hoop stresses are not uninformly distributed around the rectangular-shaped ducts. The concentration of hoop stresses are considerable using the high pressured helium coolant (80 bar). The stresses due to the hydrostatic liquid lead pressure (of 10 bar) may be neglected.

- The martensitic steel appears to be a good engineering material. This steel (1.4914) offers relatively low thermal resistance towards heat flow, causes less thermal deformation, gives higher structural stiffness against mechanical load and the stresses drop by more than 30 % when compared with the austenitic steel (316L). For highly stressed structure, the wall structure are, however, mainly due to the bending stresses. The FE computations for the thin wall concept show that, for the low wall stresses the actual difference of stresses using austenitic and martensitic steels are not all that significant. Therefore, if a means is found to minimize the induced bending moment, the choice between the austenitic and the martensitic steels may be more specific.

7. Consideration for Circular Duct within First Wall

The circular ducts are proposed here for better distribution of reaction forces and stresses within the wall structure.

According to the FE computations as mentioned before, the mounted wall structure under thermomechanical loads is highly stresses and especially critical in the corner regions of the rectangular ducts. The pressure load develops hoop stresses around the ducts and because of their rectangular shapes these stresses are not evenly distributed. Under thermal load when the wall structure is mounted on the blanket, the reaction forces from the base of the wall are transmitted through the legs of the rectangular ducts on to the plane wall. These forces are then mainly concentrated locally on the wall and causing high stresses at the corners of the ducts.

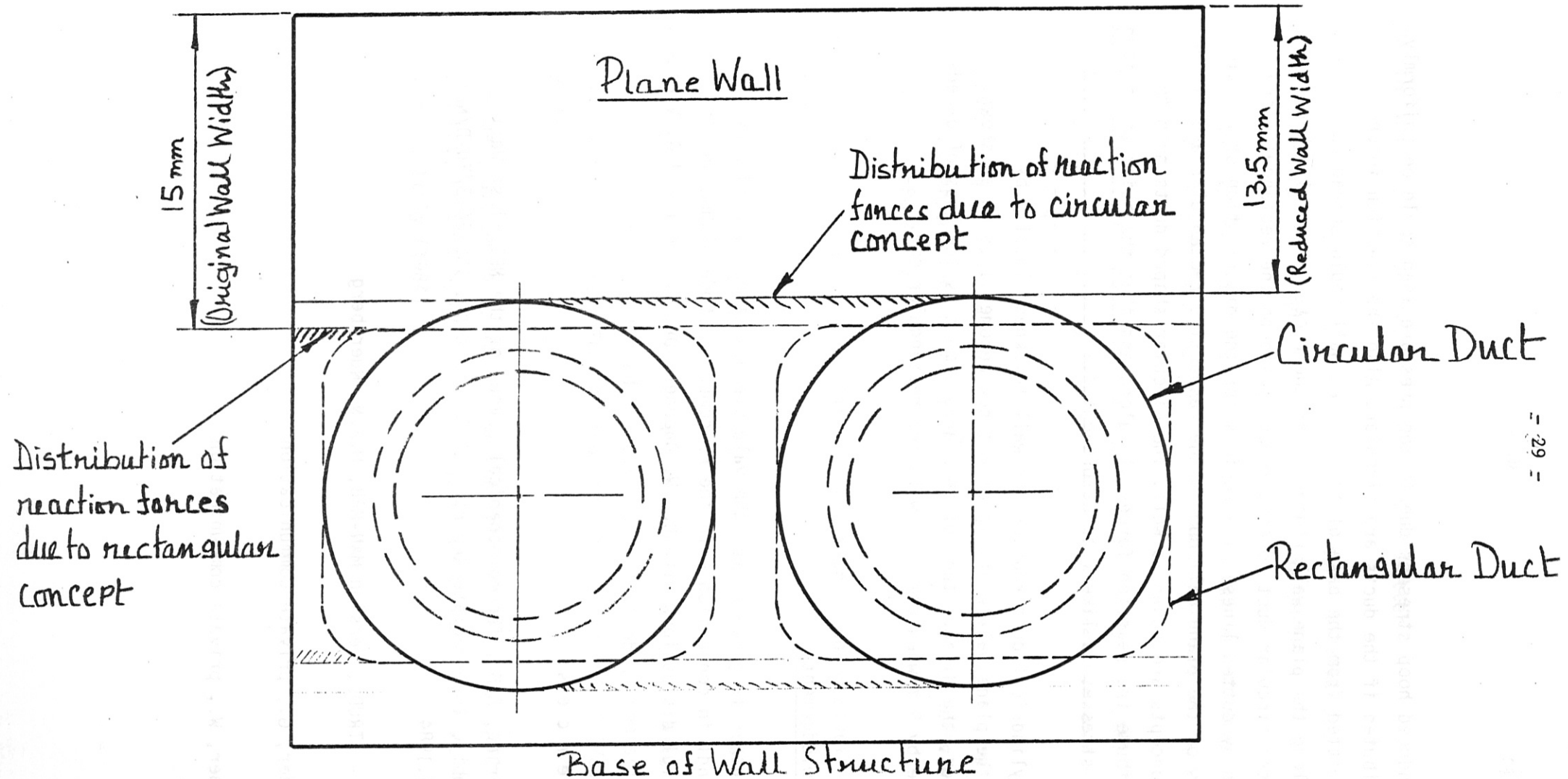
Plane Wall
15 mm (Original Wall Width)
13.5 mm (Reduced Wall Width)
Distribution of reaction forces due to circular concept
Distribution of reaction forces due to rectangular concept
Circular Duct
Rectangular Duct
Base of Wall Structure

Sketch 11

The induced hoop stresses due to the pressure load could be uniformly distributed if the ducts are circular. Also the reaction forces transmitted from the base of the mounted wall could spread out better all along the plane wall regions near the ducts. Sketch 11 shows the proposed circular duct concept superimposed on the rectangular one (shown by dotted lines). The regions for the distribution of reaction forces on the plane wall due to the respective rectangular and circular concepts are shown as well. The circular shaped ducts help to distribute the reaction forces all along and thus the built up of high local stresses is likely to be prevented.

The cylindrical duct reduces the wall thickness locally by 1.5 mm. Thus the plane wall width in effect now becomes 13.5 mm as shown. However, the disadvantage of this arrangement is the loss of breeder volume by 9 % when compared with the rectangular one.

Acknowledgements

The author is grateful for the valuable assistance provided by O. Jandl in connection with the FE computing Code STRUDL and for the fruitful discussions with Dr. W. Daenner, Dr. M. Soell and G. Vieider.

References

/1/ Mukherjee, S.B., Thermomechanical Layout of the NET First Wall Assembly, Intermediate Report, NET Contract No. 150/84-3/Fu-D/NET, 30.05.1984

/2/ ICES - STRUDL, Version MAN-MBB, M.A.N. Nuernberg

/3/ Vieider, G., private communication

/4/ Daenner, W., private communication

/5/ Toulonkian, "Thermophysical properties of Matter"

/6/ Daenner, W., First Wall and Blanket Structure Performance, Max-Planck-Institut fuer Plasmaphysik, Association EURATOM-IPP, D-8046 Garching

/7/ Daenner, W., Neutronics Scoping Studies for the NET Blanket, Proceedings of the 13th Symposium on Fusion Technology, Varese, Italy (1984)

/8/ Daenner, W., Estimates for Helium cooling of a Modular DEMO First Wall, Report IPP 2/258, July 1982, Max-Planck-Institut fuer Plasmaphysik, D-8046 Garching

/9/ Daenner, W., Lifetime Considerations for the First Wall of a DEMO Reactor, Proceedings of the 12th Symposium on Fusion Technology, Juelich, FRG (1982)857

/10/ Raeder, J., et.al., Kontrollierte Kernfusion, Teubner Studienbuecher, physik.

/11/ Teller, E., Fusion vol.1, Magnetic Confinement (Part B), pp.194 to 398

/12/ Cardella, A., et.al., Preliminary 3D Thermal Stress Analysis of the First Wall for the Outboard Breeding Blanket of NET, Commission of the European Communities, Engineering Division, Ispra, PER 867/84, 25.06.1984

/13/ Vieider, G., Daenner, W., Design Concepts for NET-Frist Wall and Blanket, Proceedings of the 13th Symposium on Fusion Technology, Varese, Italy (1984)

Appendix 1

List of Cases Proposed for FE-Analyses:

Case 1 (Fig. 14):	Water Cooled Plane Wall	Side Support only	Austenitic Steel
Case 2 (Fig. 15):	" "	Side and Base Supported	"
Case 3 (Fig. 16):	" "	Point Supported Base	"
Case 4 (Fig. 17):	Water Cooled Grooved Wall	Side Support only	Austenitic Steel
Case 5 (Fig. 18):	" "	Side and Base Supported	"
Case 6 (Fig. 19):	" "	Point Supported Base	"
Case 7 (Fig. 20):	Water Cooled Plane Wall	Side Support only	Martensitic Steel
Case 8 (Fig. 21):	" "	Side and Base Supported	"
Case 9 (Fig. 22):	Water Cooled Grooved Wall	Side Support only	"
Case 10 (Fig. 23):	" "	Side and Base Supported	"
Case 11 (Fig. 37):	Helium Cooled Plane Wall	Side Support only	Austenitic Steel
Case 12 (Fig. 38):	" "	Side and Base Supported	"
Case 13 (Fig. 39):	Helium Cooled Grooved Wall	Side Support only	"
Case 14 (Fig. 40):	" "	Side and Base Supported	"
Case 15 (Fig. 41):	Helium Cooled Plane Wall	Side Support only	Martensitic Steel
Case 16 (Fig. 42):	" "	Side and Base Supported	"
Case 17 (Fig. 43):	Helium Cooled Grooved Wlall	Side Support only	"
Case 18 (Fig. 44):	" "	Side and Base Supported	"
Case 19 (Fig. 49):	Water Cooled Thin Wall	Side Support only	Austenitic Steel
Case 20 (Fig. 50):	" "	Side and Base Supported	"
Case 21 (Fig. 51):	" "	Side Support only	Martensitic Steel
Case 22 (Fig. 52):	" "	Side and Base Supported	"
Case 23 (Fig. 59):	Helium Cooled Thin Wall	Side Support only	Austenitic Steel
Case 24 (Fig. 60):	" "	Side and Base Supported	"
Case 25 (Fig. 61):	" "	Side Support only	Martensitic Steel
Case 26 (Fig. 62):	" "	Side and Base Supported	"

Note

The figures show the contours of von Mises Stresses only

Appendix 2

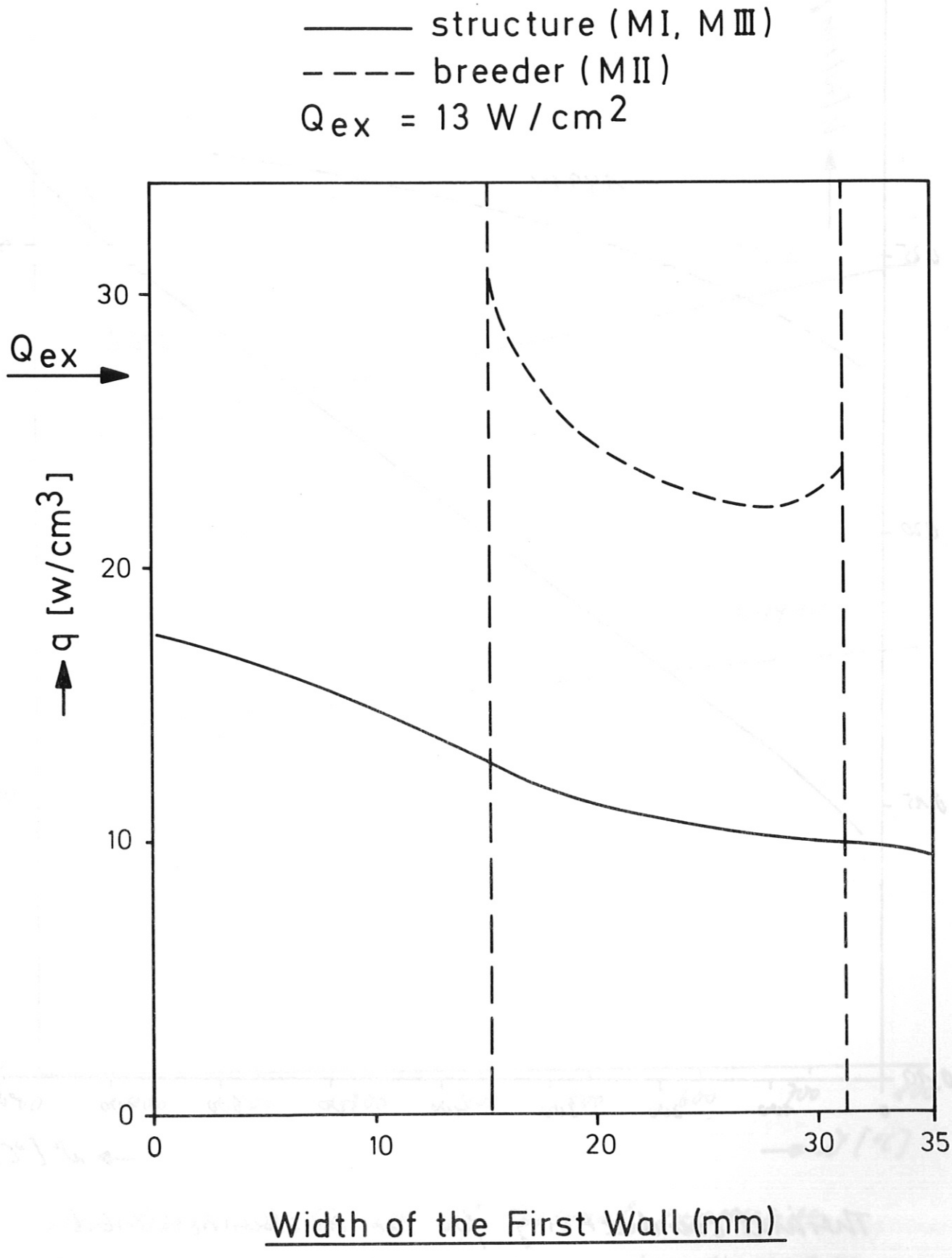
structure (MI, MIII)
breeder (MII)
Q_{ex} = 13 W / cm^2
Q_{ex}
q [W/cm^3]
30
20
10
0
0
10
20
30
35
Width of the First Wall (mm)

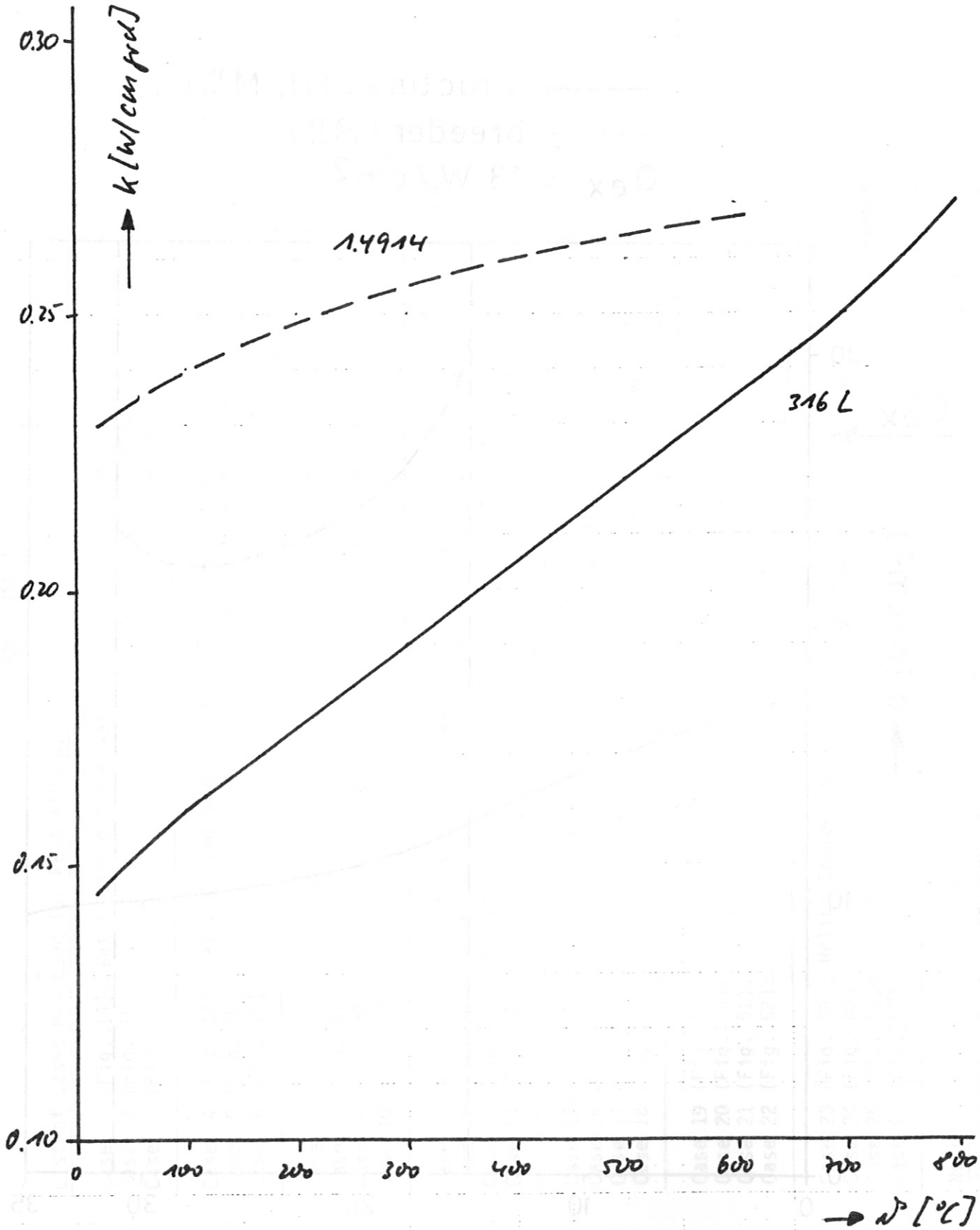

Thermal conductivity for the austenitic 316 L and the martensitic 1.4914

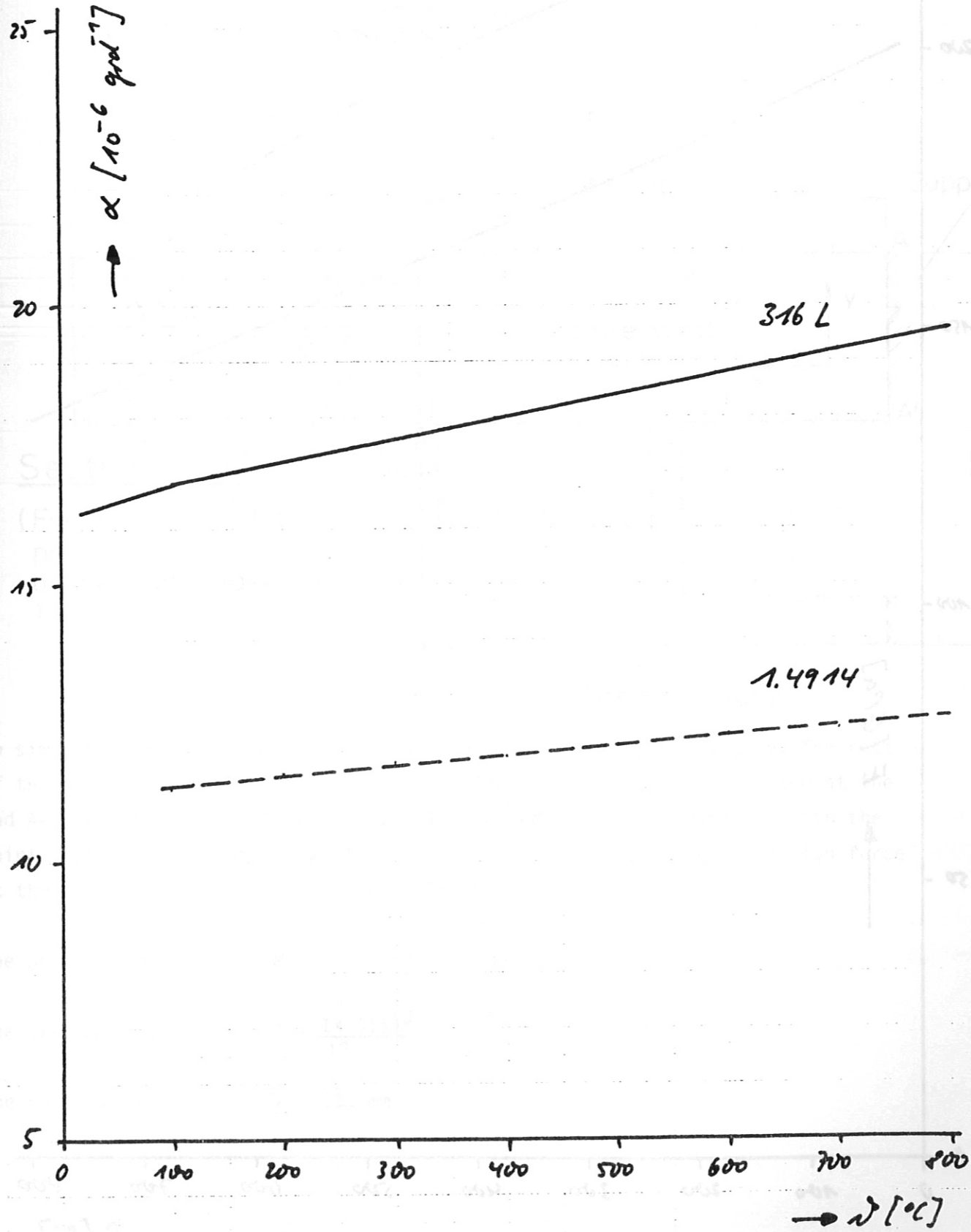

Mean linear coefficient of thermal expansion for the austenitic 316 L and the martensitic 1.4914

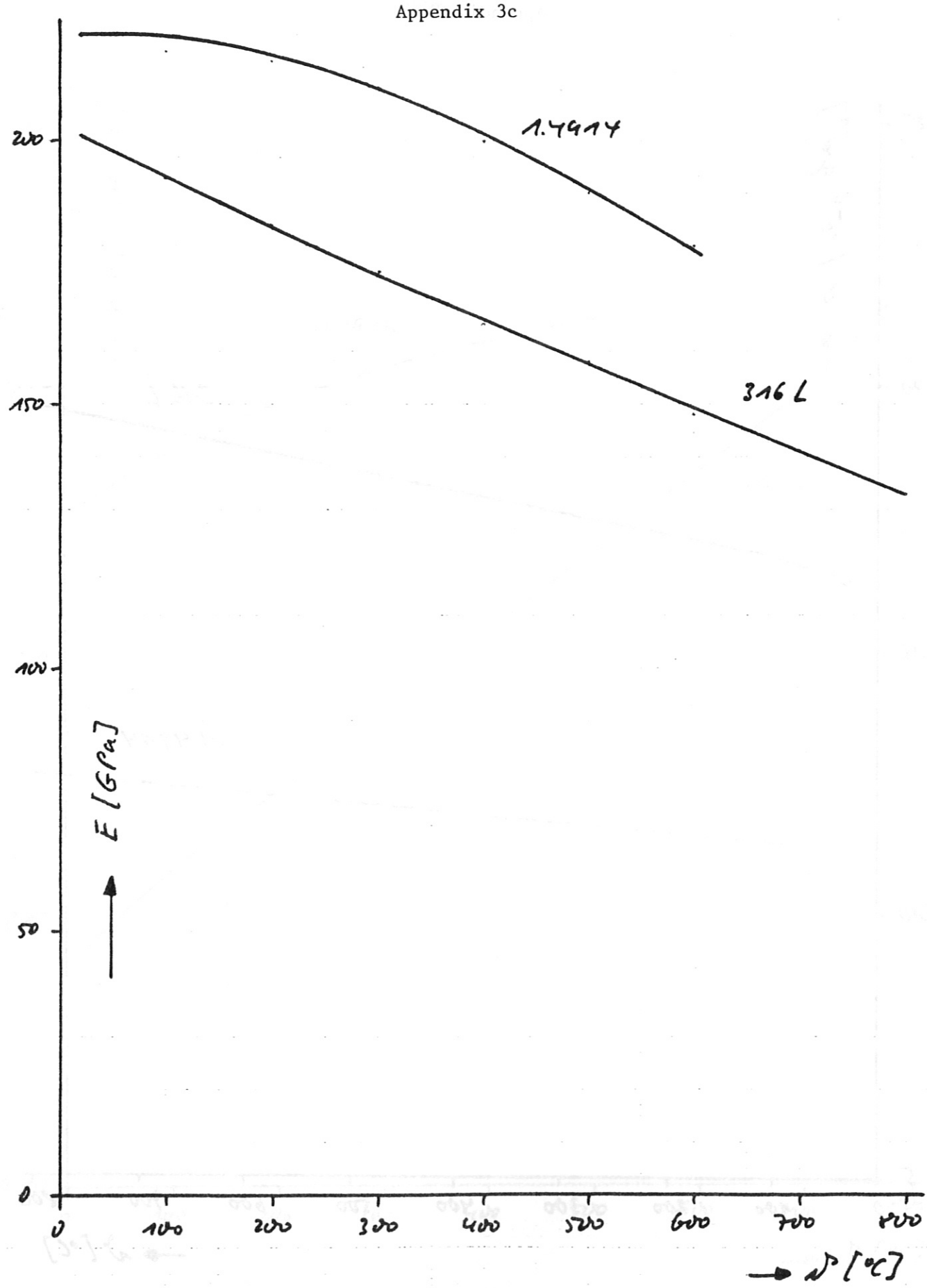

Young's modulus for the austenitic 316 L

Appendix 4a

Estimation of Bending Stresses within Plane wall

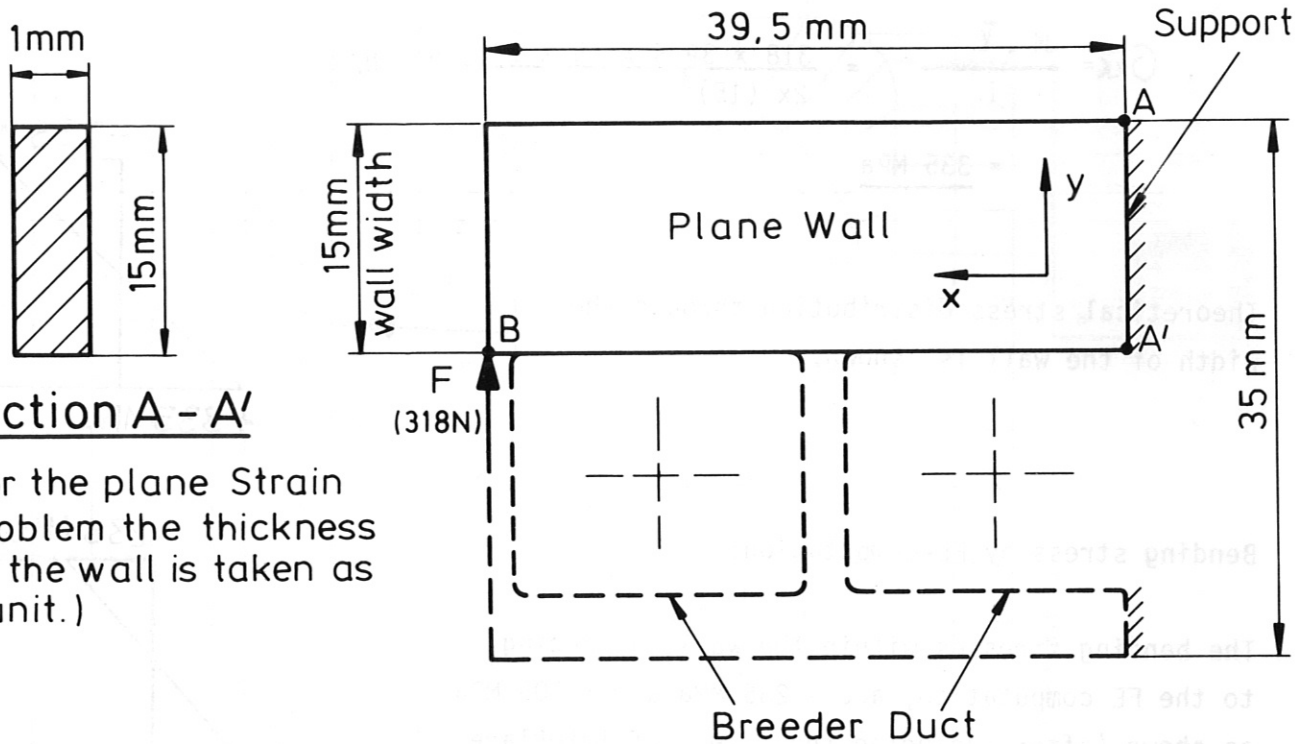

To simplify the model the width of the plane wall is only considered. The rest of the wall, shown by dotted lines, is neglected. The wall is supported at the end A-A′ and the load F at the point B is applied. The FE computation with the point supported base of the wall is carried out, Fig 15, and the reaction force at the supported point is found to be 318 N.

The bending moment $M = 318 \times 39.5$ N-mm

The area moment $I = \frac{1x\ (15)^3}{12}$ mm^4

The neutral axis $\bar{y} = \frac{15}{2}$ mm

Appendix 4b

According to the theory of bending, the stress σ_{xx} is given by

$$\sigma_{xx} = \frac{M \cdot \bar{Y}}{I} = \frac{318 \times 39.5 \times 15 \times 12}{2x\ (15)^3} = 335\ N/mm^2$$

$$= \underline{335\ MPa}$$

Theoretical stress distribution through the width of the wall is shown.

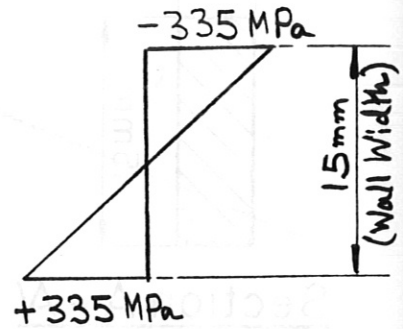

Bending stress by FE-Computation:

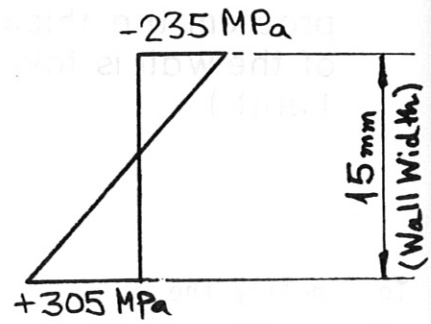

The bending stresses within the wall, according to the FE computation, are - 235 MPa and + 305 MPa as shown (after excluding the effect of interlayer thermal stresses). These values are lower than the estimated ones. In the FE computation the whole wall of 35 mm wide (including dotted regions) is considered and this has got higher structural stiffness than the wall width (15 mm) considered for estimation.

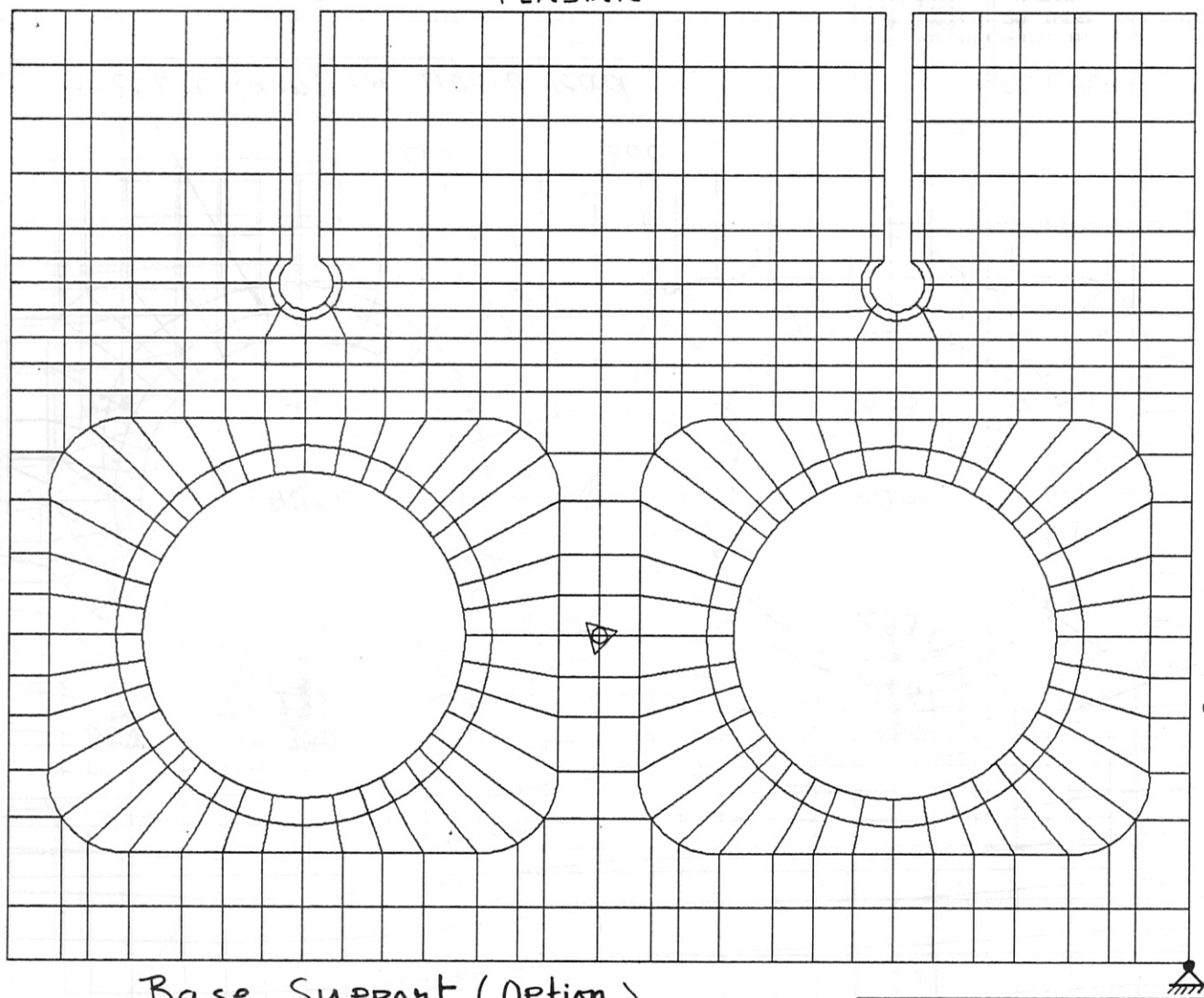
PLASMA
Side Support (Y → Free)
Base Support (Option)
(X ← Free)

Fig.1

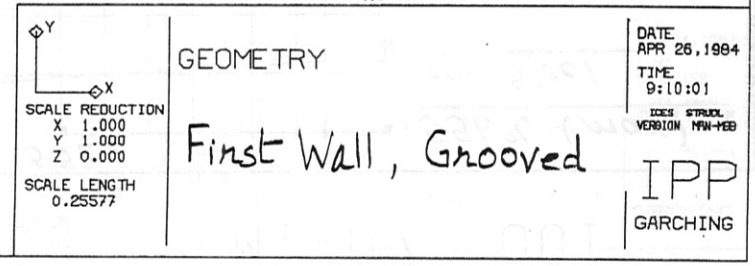
Y
X
SCALE REDUCTION
X 1.000
Y 1.000
Z 0.000
SCALE LENGTH
0.25577
GEOMETRY
First Wall, Grooved
DATE
APR 26,1984
TIME
9:10:01
ICES STRUDL
VERSION MAN-MSB
IPP
GARCHING

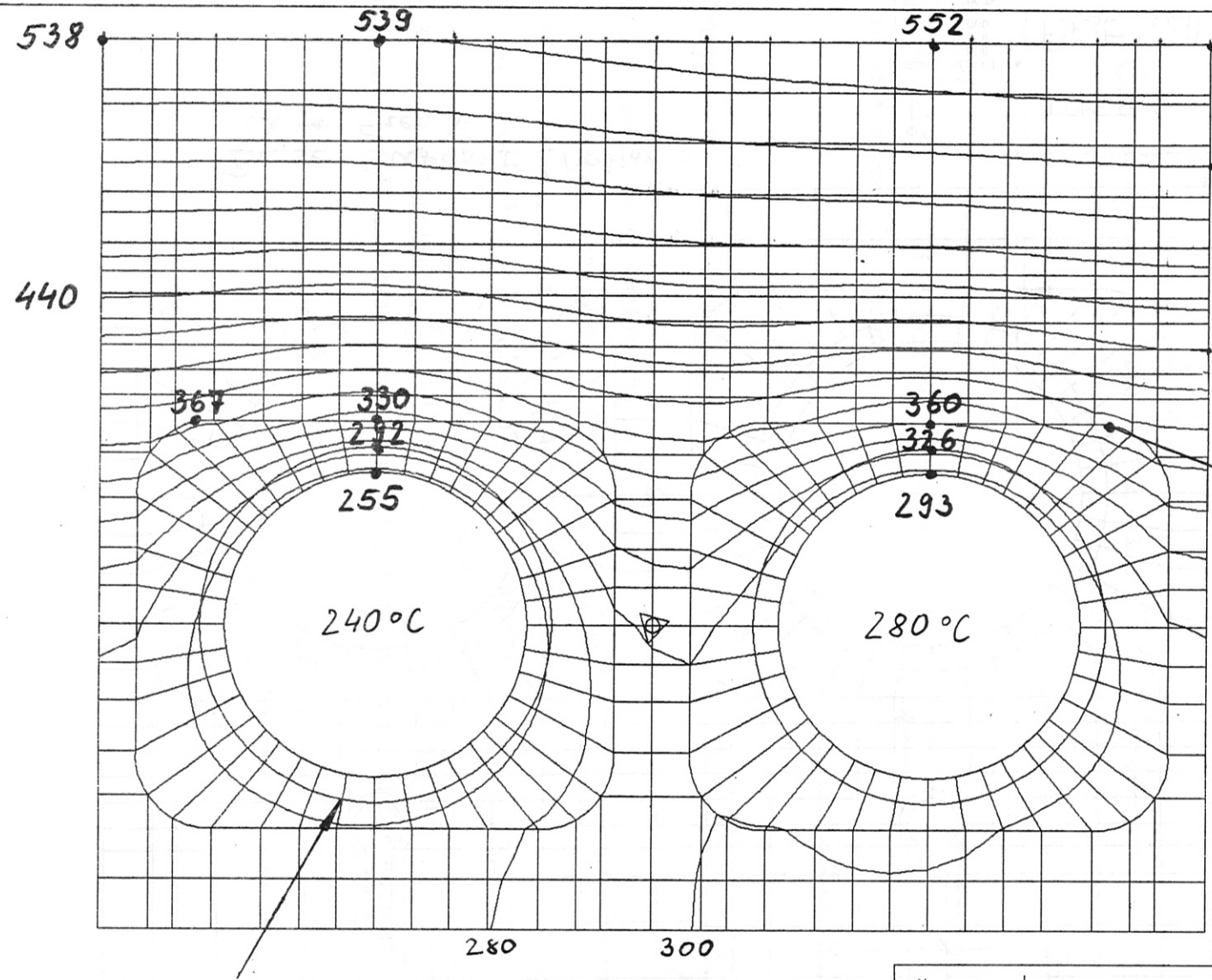

Fig. 2

Austenitic Steel (316L)

SCALE REDUCTION X 1.000 Y 1.000 Z 0.000 LEVEL SIZE 19.99999 EXPONENT 1	CONTOURS TEMPERATURE UNITS: MM NEW DEG C SEC J -- 2D THER. ANALYSIS OF FIRST WALL, BLWPSPL LOADING 1 TEMP. DISTRIBUTION	DATE JUL 19,1984 TIME 1:02:22 ICES STRUDL VERSION MAN-MSB IPP GARCHING

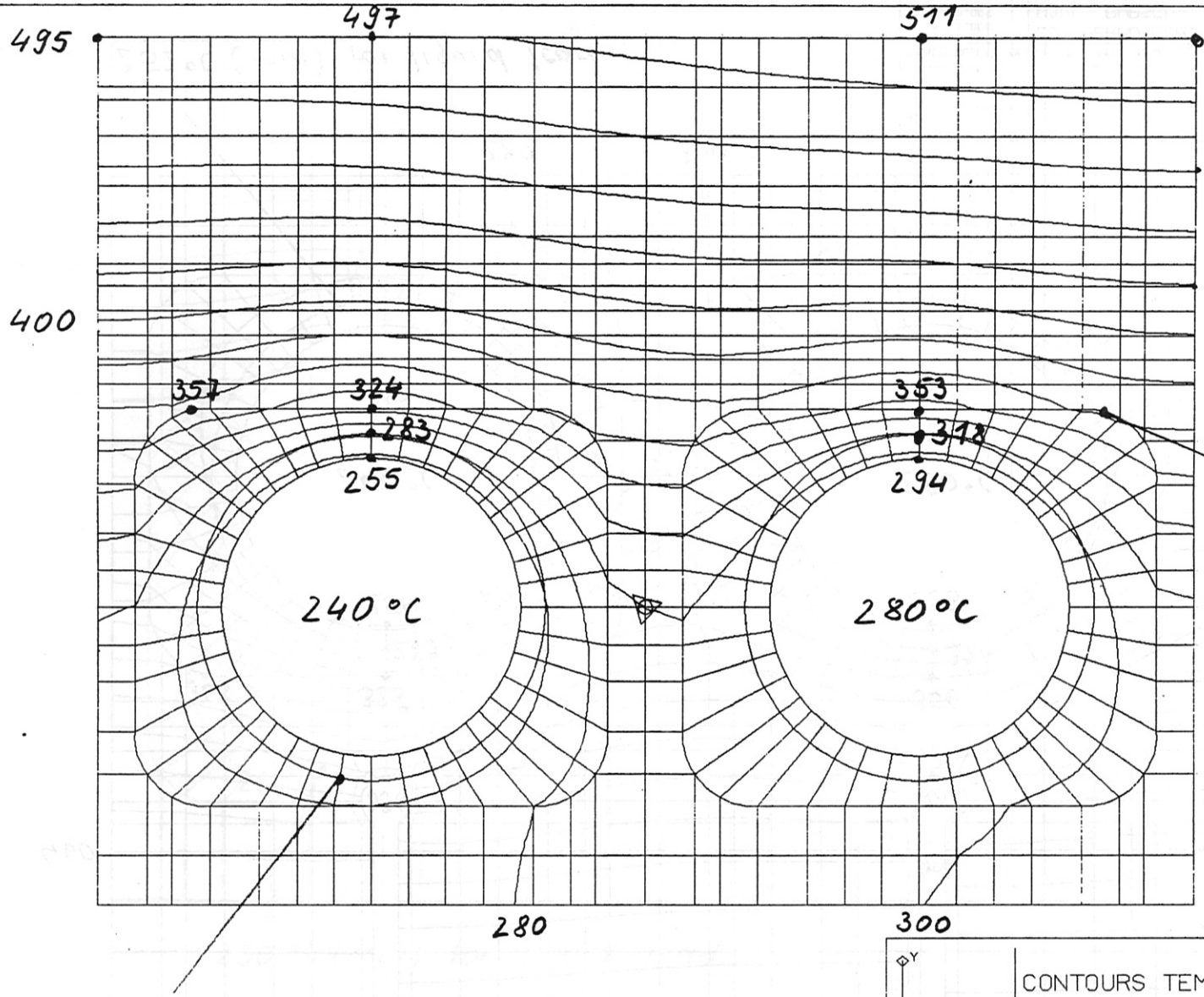
495
497
511
515°C (max)
for Steel (1.4914)
480
440
400
357
324
283
255
353
312
294
385°C (max)
for liquid lead
240 °C
280 °C
280
300
250 °C (min) for liquid lead
Martensitic Steel (1.4914)

Fig. 3

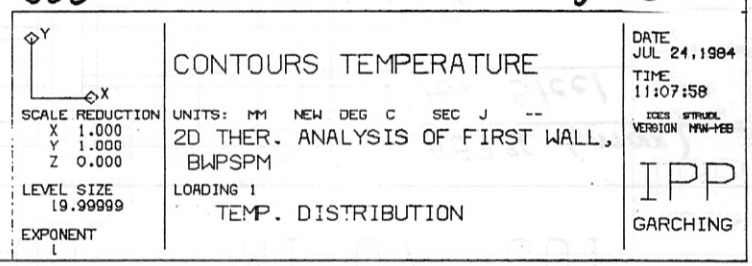
Y
X
SCALE REDUCTION
X 1.000
Y 1.000
Z 0.000
LEVEL SIZE
19.99999
EXPONENT
1
CONTOURS TEMPERATURE
UNITS: MM NEW DEG C SEC J --
2D THER. ANALYSIS OF FIRST WALL,
BWPSPM
LOADING 1
TEMP. DISTRIBUTION
DATE
JUL 24,1984
TIME
11:07:58
ICES STRUDL
VERSION MAY-MEB
IPP
GARCHING

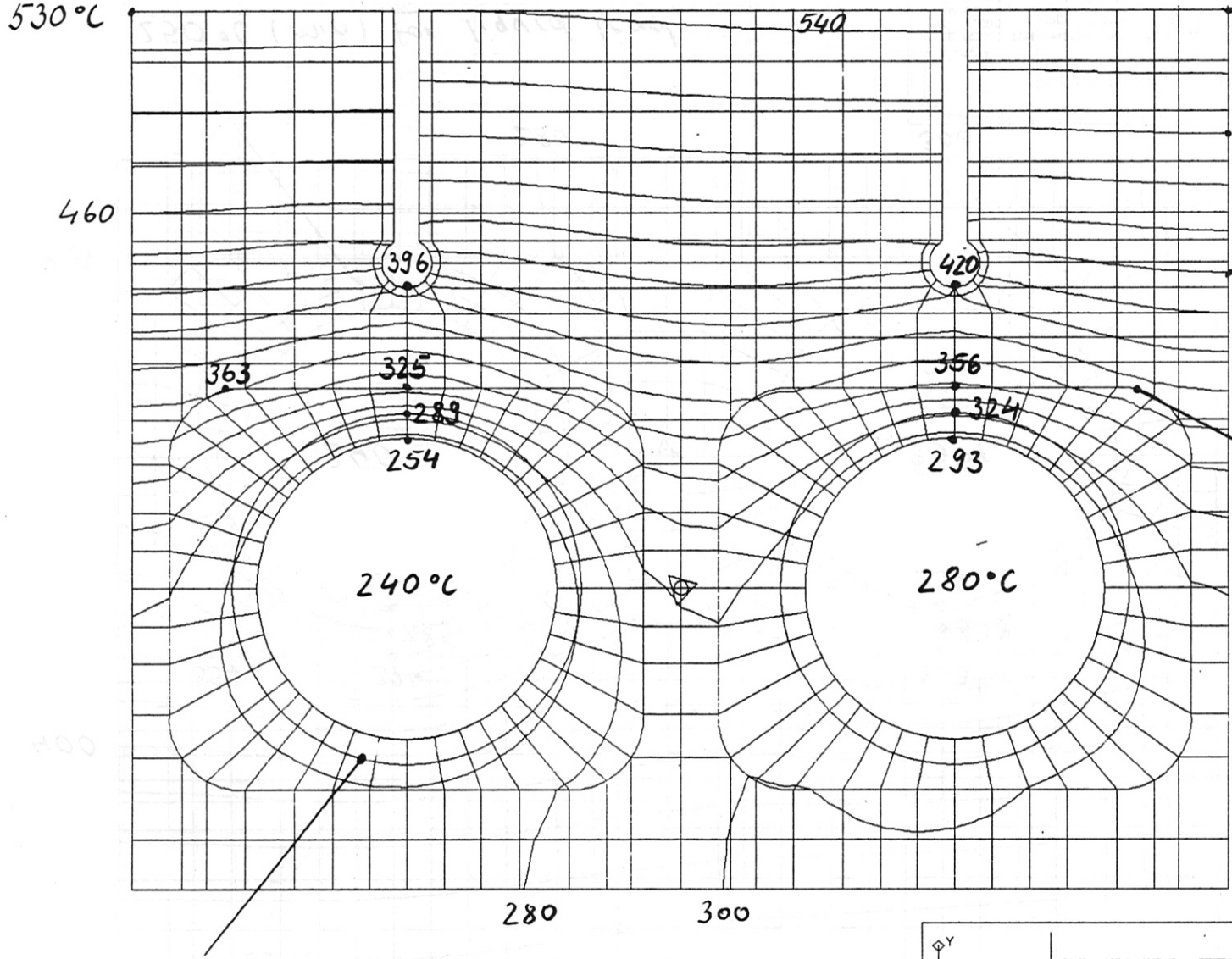

Fig. 4

Austenitic Steel (316L)

SCALE REDUCTION X 1.000 Y 1.000 Z 0.000 LEVEL SIZE 19.99999 EXPONENT 1	CONTOURS TEMPERATURE UNITS: MM NEW DEG C SEC J -- 2D THERMOMECH. ANALYSIS OF 1ST WALL, BWPSGL LOADING 1 TEMP. DISTRIBUTION
DATE JUL 19,1984 TIME 2:25:45 ICES STRUDL VERSION MAN-MEB IPP GARCHING	

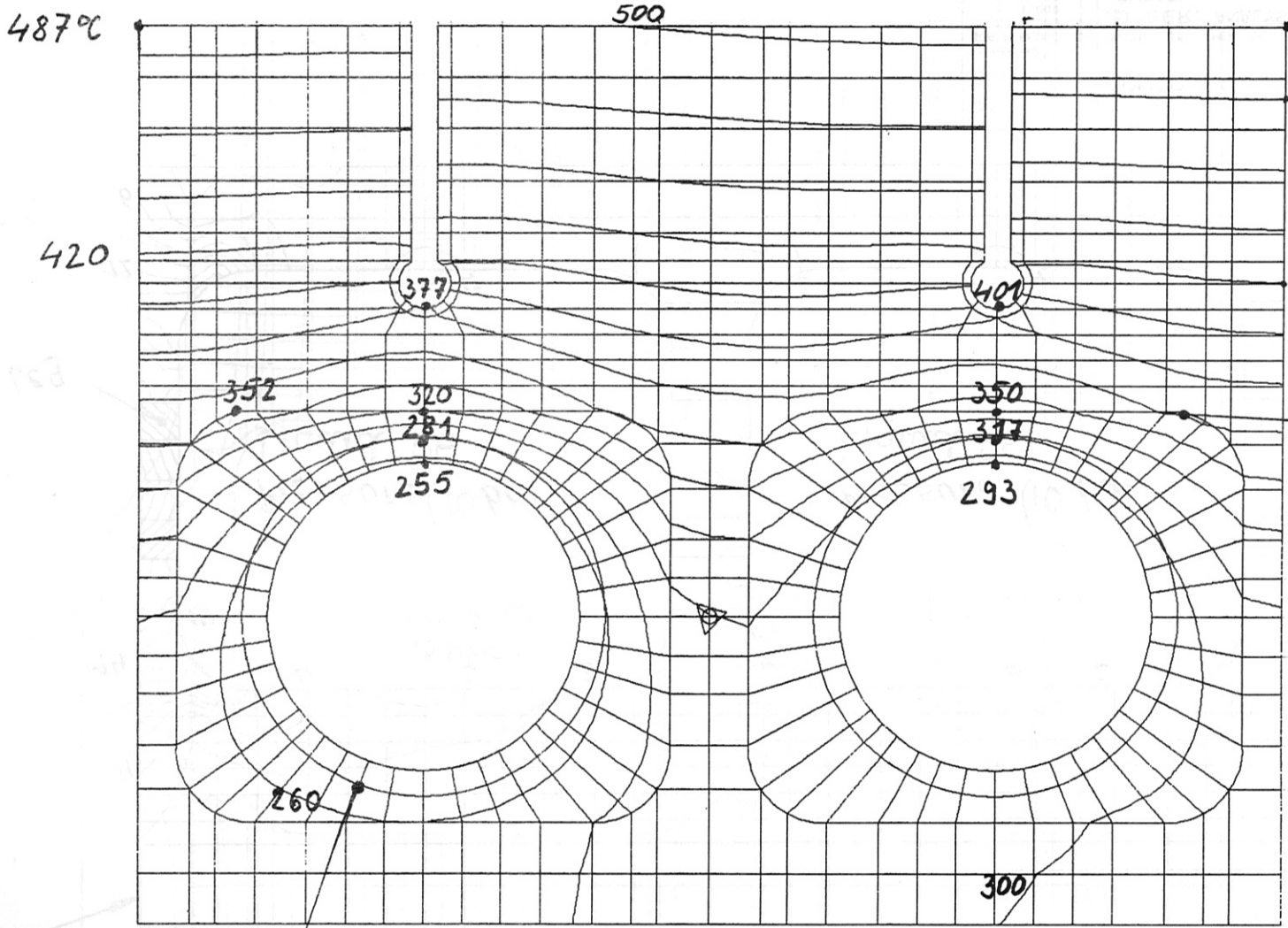

Martensitic Steel (1.4914)

Fig. 5

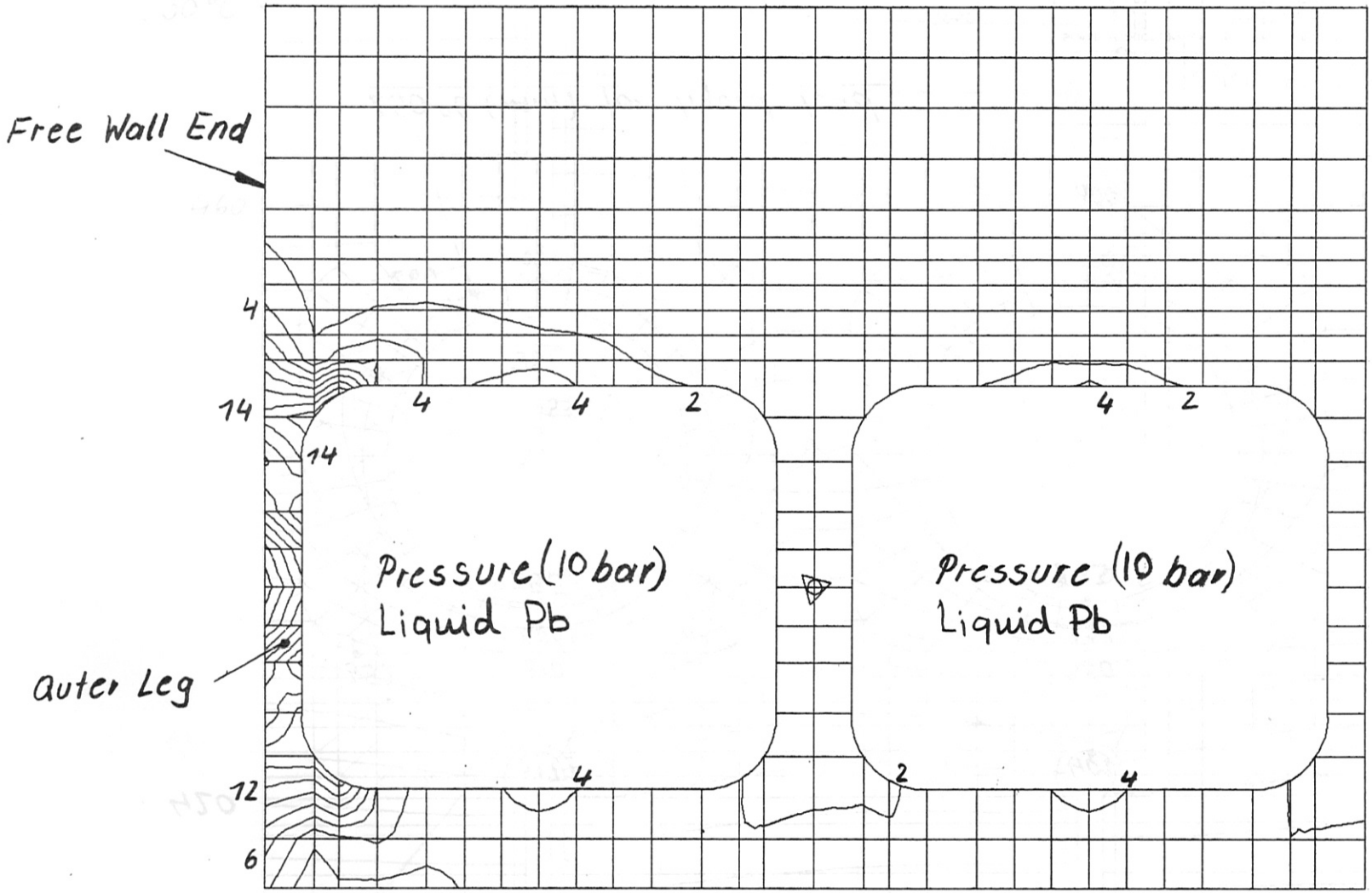

Fig. 6

CONTOURS MISES (MPa)

SCALE REDUCTION
X 1.000
Y 1.000
Z 0.000

LEVEL SIZE
2.00000

EXPONENT
0

UNITS: MM NEW DEG C SEC J --
2D THER. ANALYSIS OF FIRST WALL, BWFSPL
LOADING 2
FLUID LEAD PRESSURE (N/MM**2)

DATE
JUL 16,1984
TIME
21:49:29

IPP
GARCHING

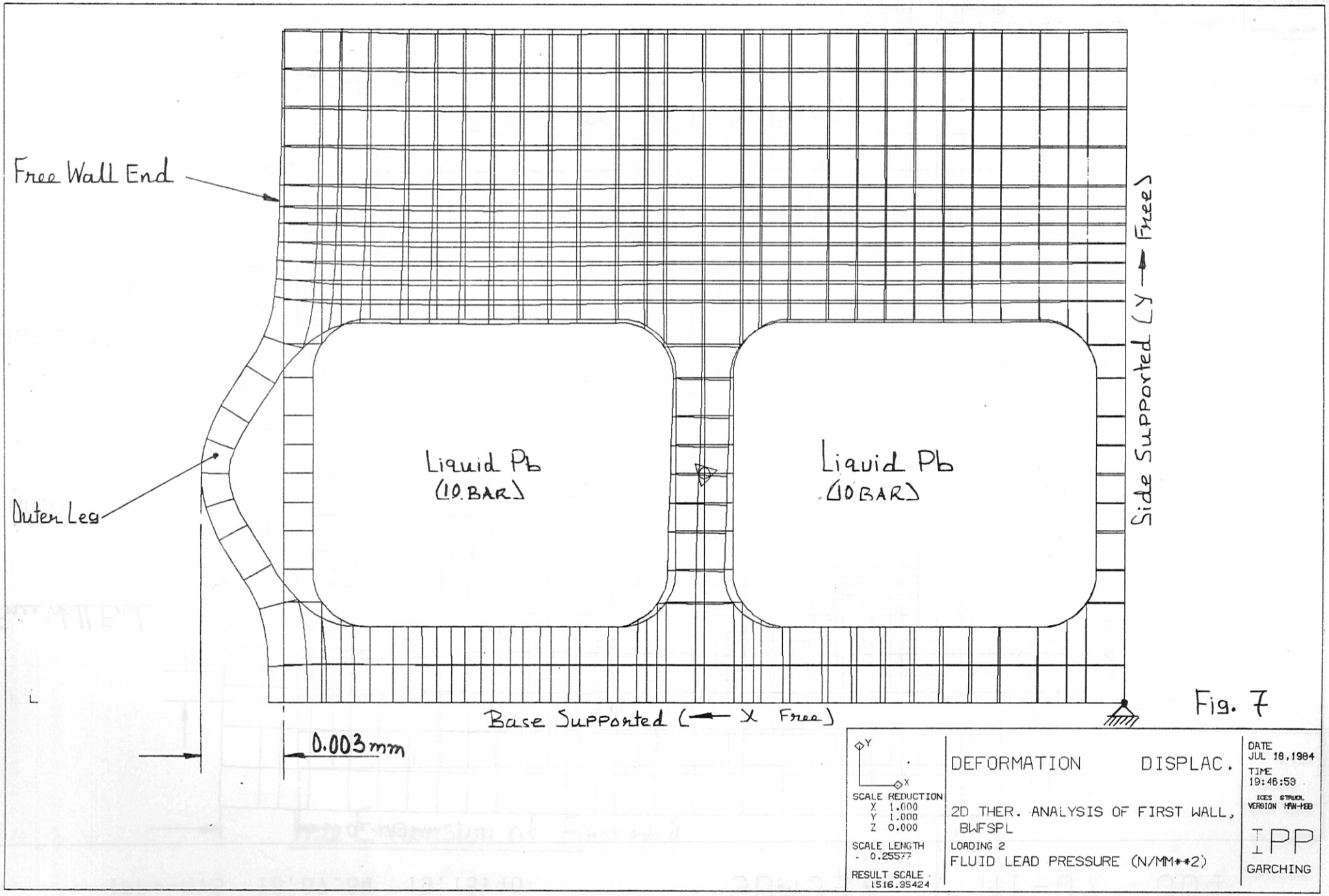
Free Wall End
Outer Leg
Liquid Pb
(10 BAR)
Liquid Pb
(0 BAR)
Side Supported (Y → Free)
Base Supported (← X Free)
0.003mm
Y
X
SCALE REDUCTION
X 1.000
Y 1.000
Z 0.000
SCALE LENGTH
0.25577
RESULT SCALE
1516.95424
DEFORMATION DISPLAC.
2D THER. ANALYSIS OF FIRST WALL, BWFSPL
LOADING 2
FLUID LEAD PRESSURE (N/MM**2)
DATE
JUL 18,1984
TIME
19:46:59
ICES STRUDL
VERSION MAN-MSB
IPP
GARCHING

Fig. 7

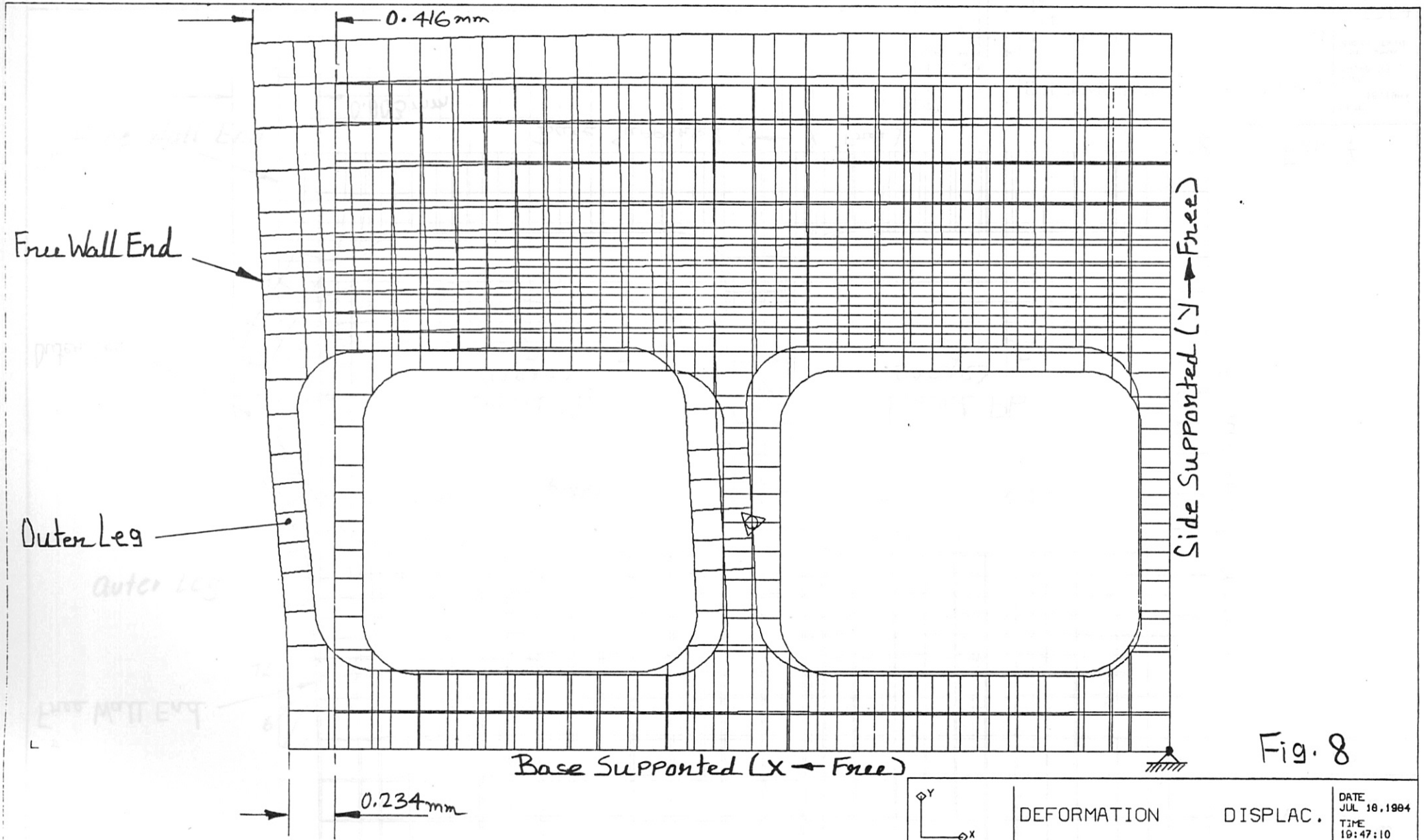
0.416mm
Free Wall End
Outer Leg
Side Supported (Y → Free)
Base Supported (X ← Free)
0.234mm
Y
X
SCALE REDUCTION
X 1.000
Y 1.000
Z 0.000
SCALE LENGTH
0.27598
RESULT SCALE
10.61565
DEFORMATION DISPLAC.
2D THER. ANALYSIS OF FIRST WALL, BWFSPL
LOADING 3
TEMP. + PRESSURE
DATE
JUL 18,1984
TIME
19:47:10
ICES STRUDL
VERSION MAR-VEB
IPP
GARCHING

Fig. 8

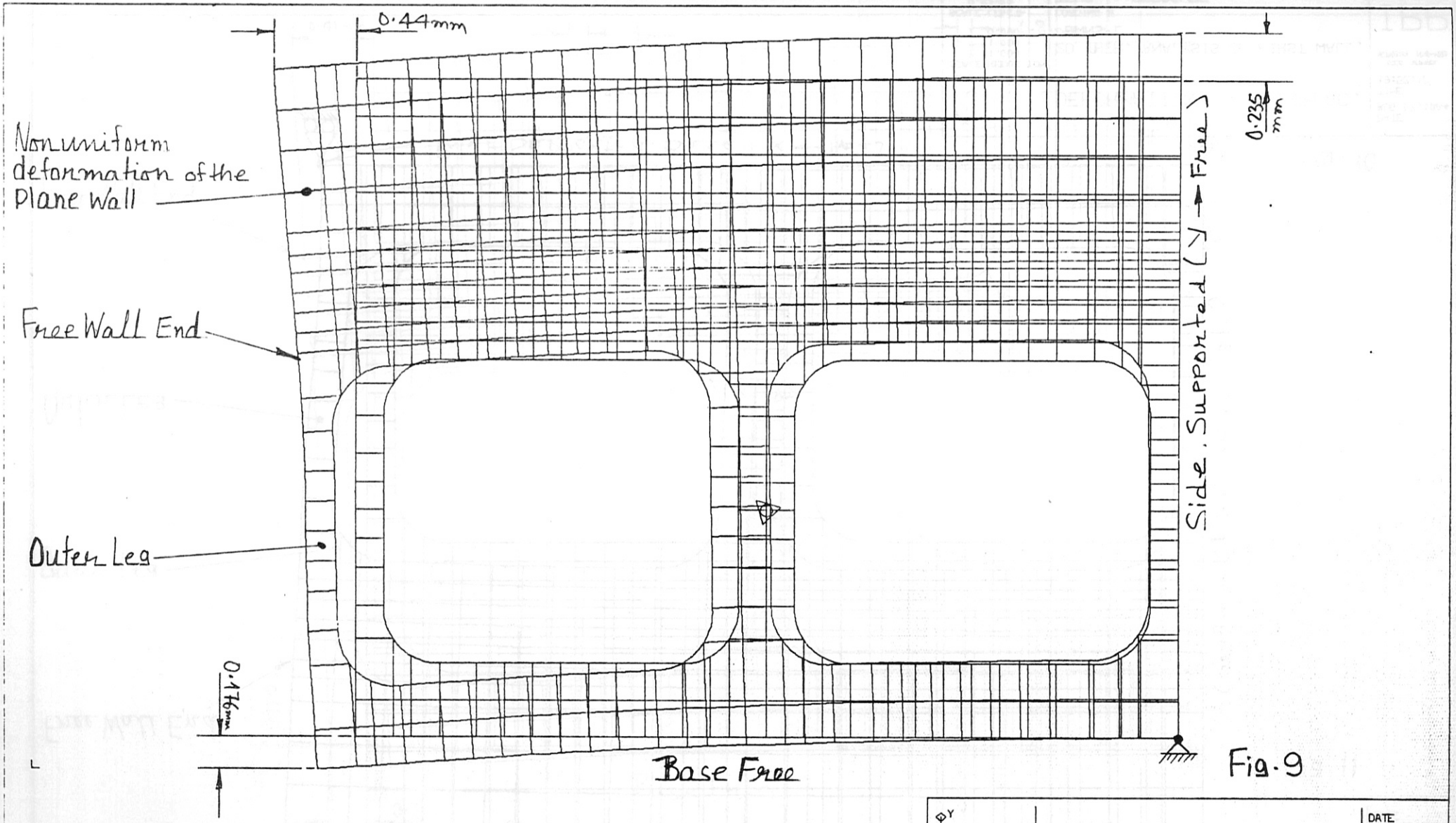
0·44mm
0·235 mm
Nonuniform deformation of the Plane Wall
Free Wall End
Outer Leg
Side, Supported (Y → Free)
0·176mm
Base Free
Fig·9
Free Expansion of First Wall
Y
X
SCALE REDUCTION
X 1.000
Y 1.000
Z 0.000
SCALE LENGTH
0.28642
RESULT SCALE
9.73823
DEFORMATION DISPLAC.
2D THER. ANALYSIS OF FIRST WALL, BWPSPL
LOADING 3
TEMP. + PRESSURE
DATE
JUL 19,1984
TIME
1:24:03
ICES STRUDL
VERSION MAN-MSB
IPP
GARCHING

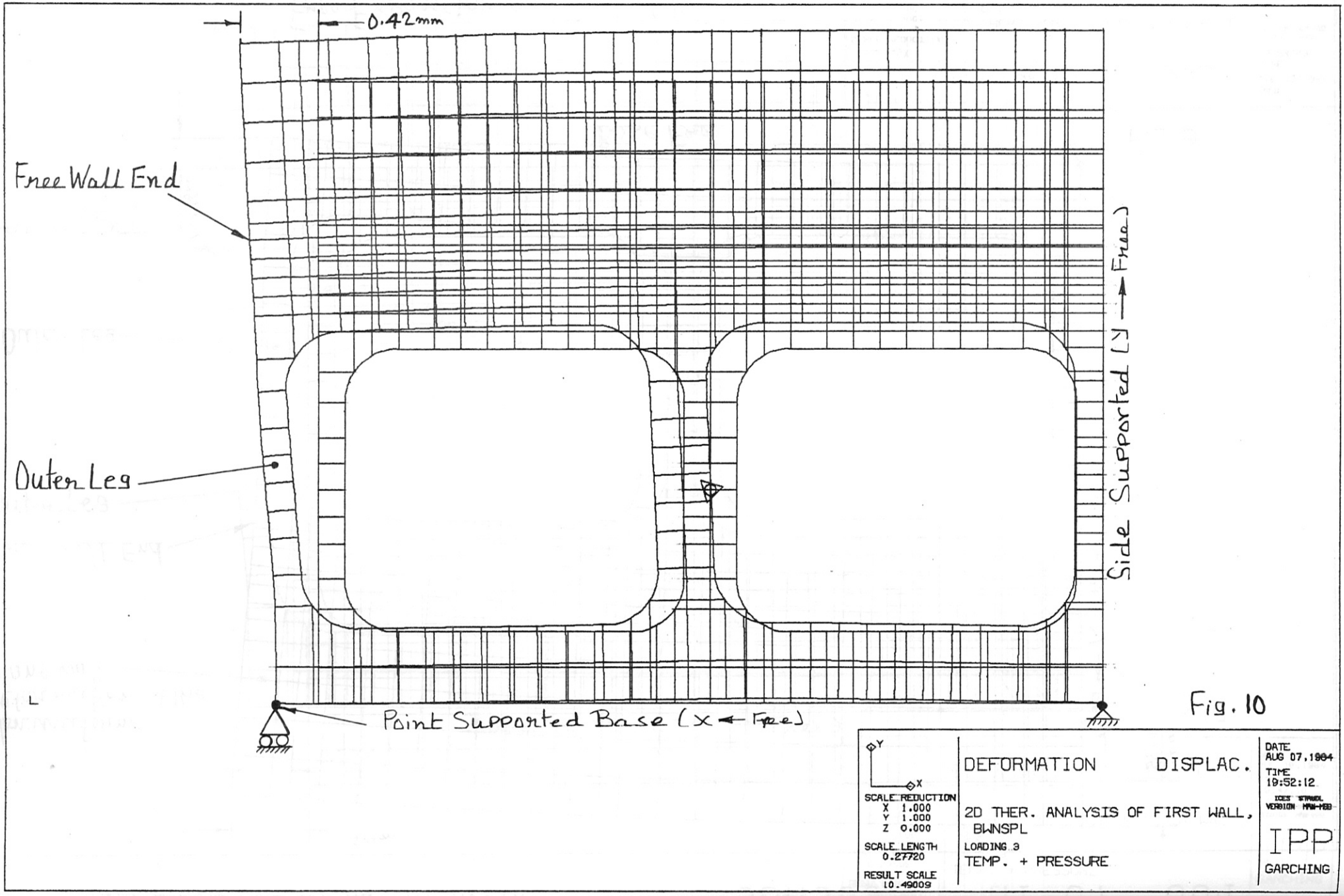
0.42mm
Free Wall End
Outer Leg
Side Supported (Y → Free)
Point Supported Base (x ← Free)
Y
X
SCALE REDUCTION
X 1.000
Y 1.000
Z 0.000
SCALE LENGTH
0.27720
RESULT SCALE
10.49009
DEFORMATION DISPLAC.
2D THER. ANALYSIS OF FIRST WALL,
BWNSPL
LOADING 3
TEMP. + PRESSURE
DATE
AUG 07,1984
TIME
19:52:12
IPP
GARCHING

Fig. 10

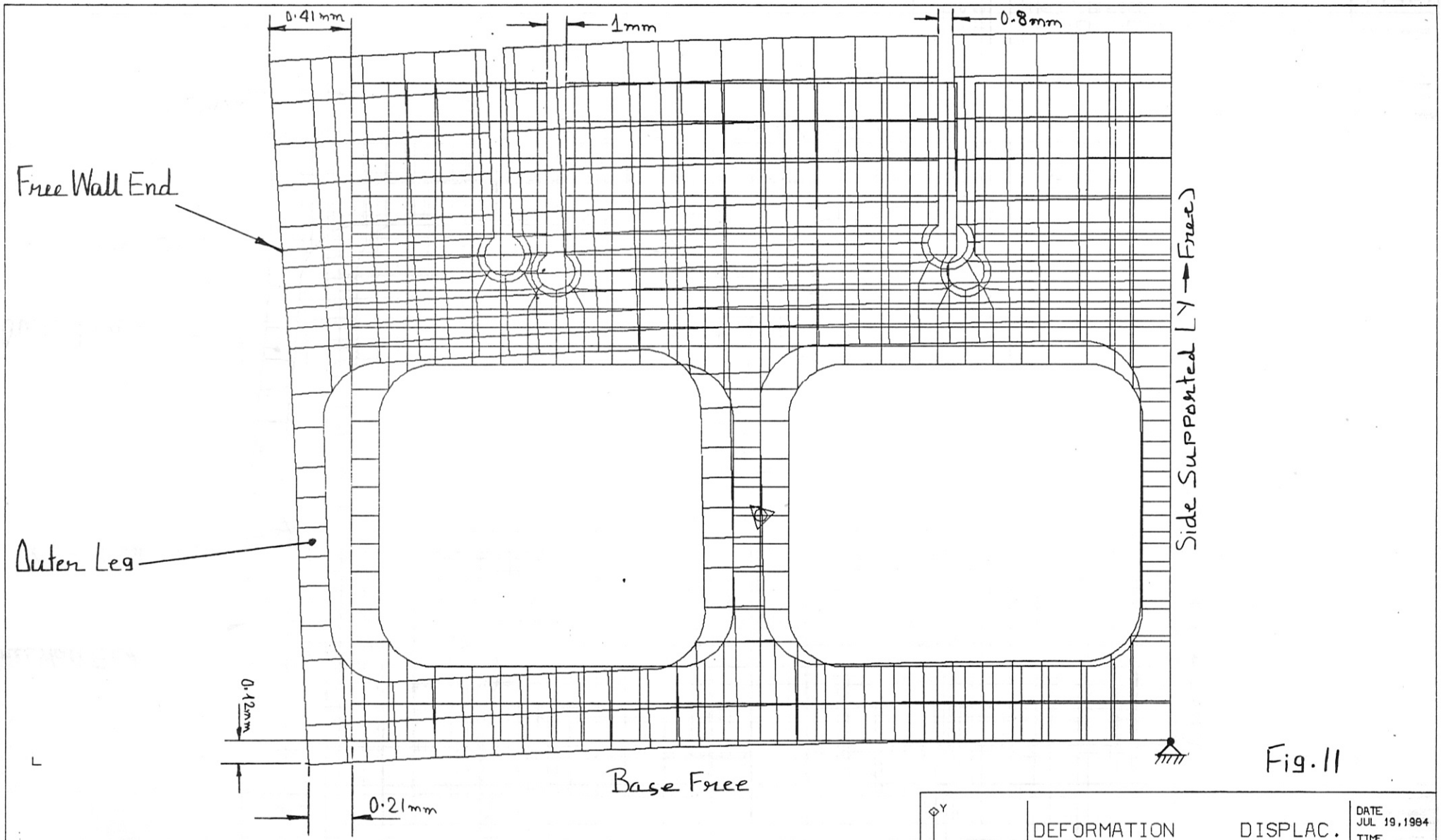

Fig. 11

Free Expansion of First Wall

SCALE REDUCTION
X 1.000
Y 1.000
Z 0.000

SCALE LENGTH
0.28482

RESULT SCALE
10.73619

DEFORMATION DISPLAC.

2D THERMOMECH. ANALYSIS OF 1ST WALL, BWPSGL

LOADING 3
TEMP. + PRESSURE

DATE
JUL 19,1984
TIME
2:57:39

IOES STRUDL VERSION MAN-MEB

IPP
GARCHING

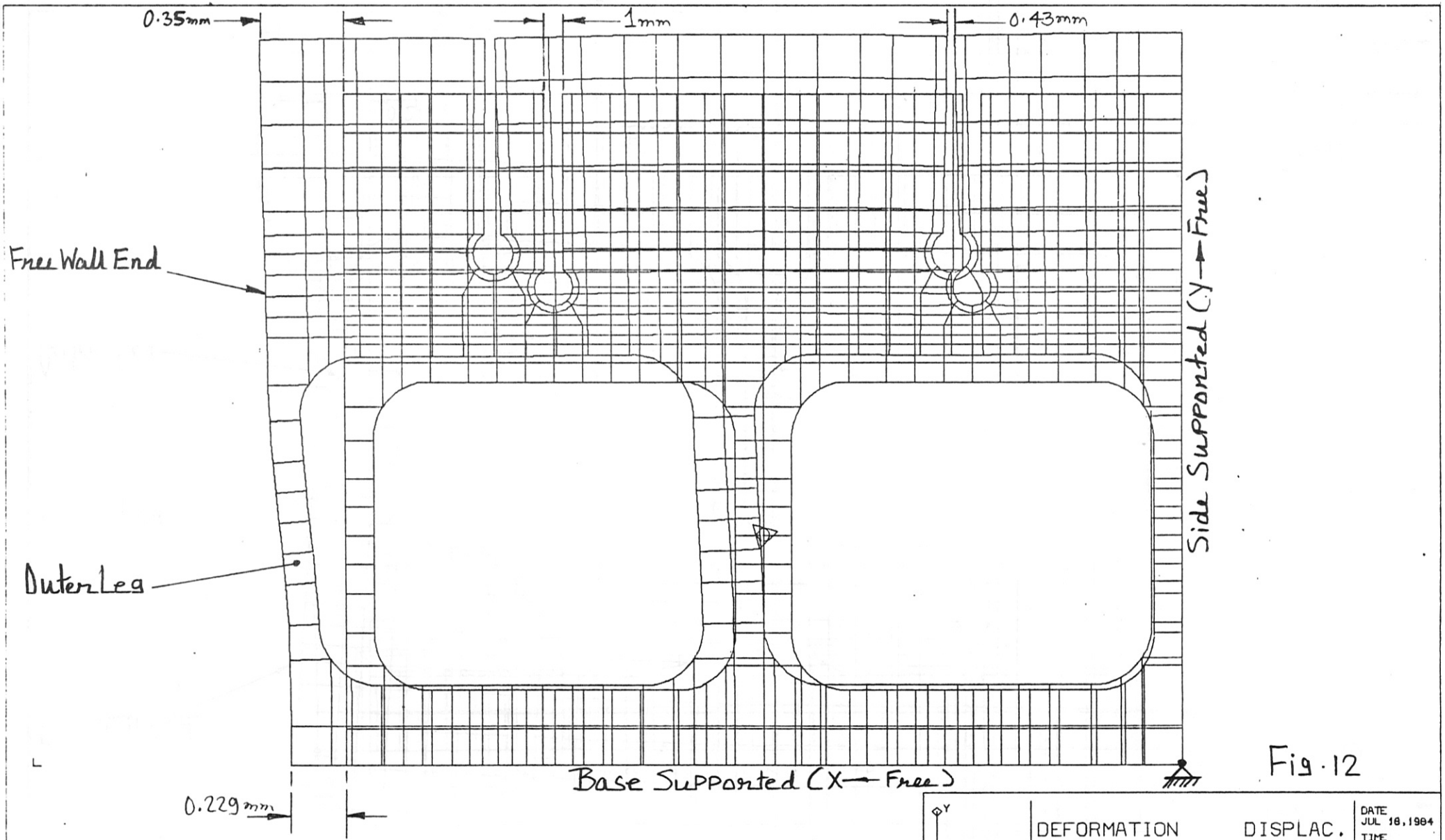
0.35mm
1mm
0.43mm
Free Wall End
Outer Leg
Side Supported (Y→Free)
Base Supported (X→Free)
0.229mm
Y
X
SCALE REDUCTION
X 1.000
Y 1.000
Z 0.000
SCALE LENGTH
0.27933
RESULT SCALE
12.83222
DEFORMATION DISPLAC.
2D THERMOMECH. ANALYSIS OF 1ST WALL, BWFSGL
LOADING 3
TEMP. + PRESSURE
DATE
JUL 18,1984
TIME
20:57:17
ICES STRUDL VERSION MAR-1988
IPP
GARCHING

Fig. 12

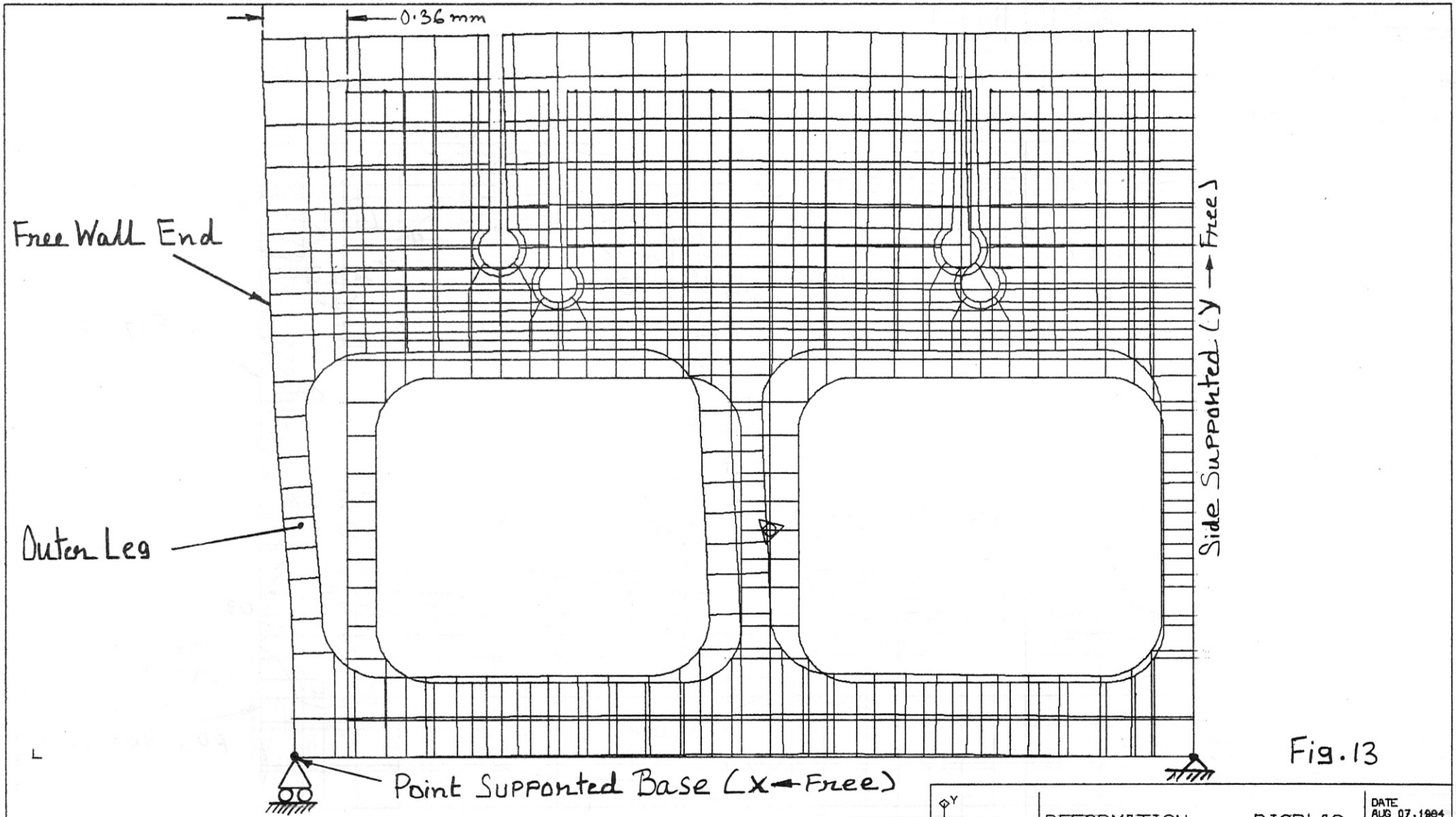
0·36 mm
Free Wall End
Outer Leg
Side Supported (Y → Free)
Point Supported Base (X ← Free)
Y
X
SCALE REDUCTION
X 1.000
Y 1.000
Z 0.000
SCALE LENGTH
0.27893
RESULT SCALE
12.36900
DEFORMATION DISPLAC.
2D THERMOMECH. ANALYSIS OF 1ST WALL, BWNSGL
LOADING 3
TEMP. + PRESSURE
DATE
AUG 07,1984
TIME
20:38:10
IPP
GARCHING

Fig.13

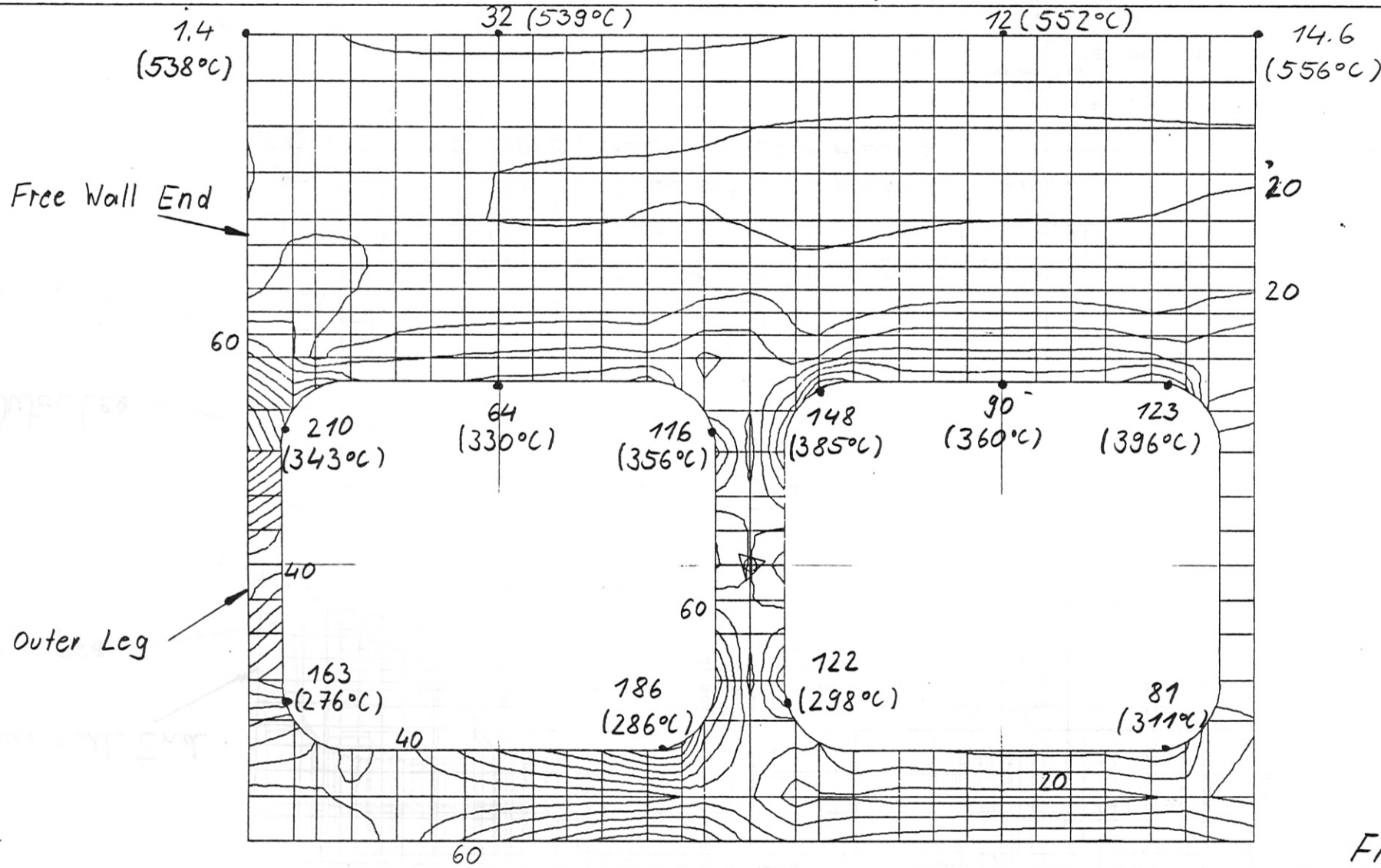

Fig. 14

SCALE REDUCTION X 1.000 Y 1.000 Z 0.000 LEVEL SIZE 19.99999 EXPONENT 1	CONTOURS MISES (MPa) UNITS: MM NEW DEG C SEC J -- 2D THER. ANALYSIS OF FIRST WALL. BWPSPL LOADING 3 TEMP. + PRESSURE	DATE JUL 19,1984 TIME 1:48:16 IKES STRUDL VERSION MAR-MSB IPP GARCHING

Case 1 Water cooled plane wall, side supported. Austenitic steel.

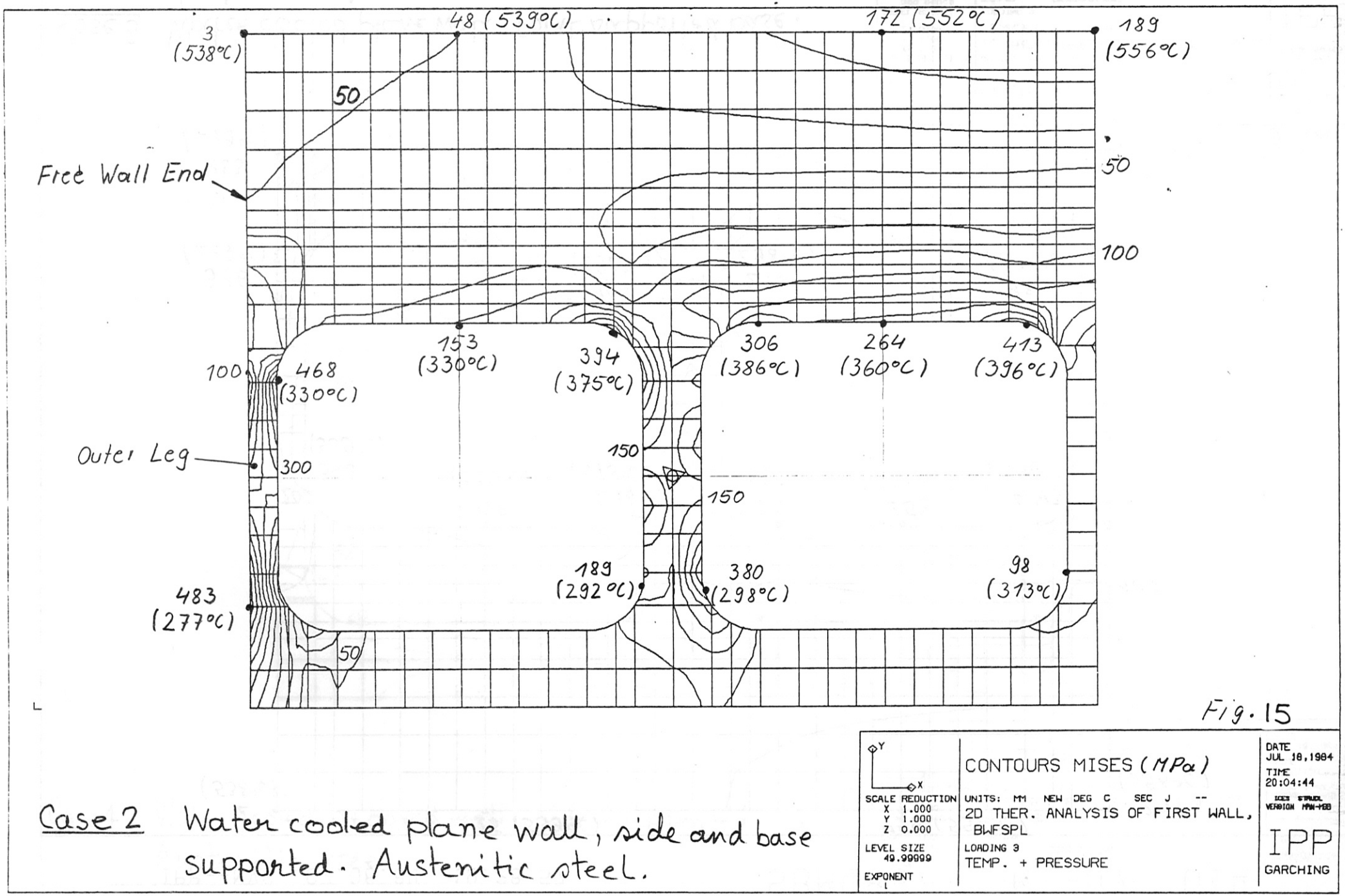

Fig. 15

Case 2 Water cooled plane wall, side and base supported. Austenitic steel.

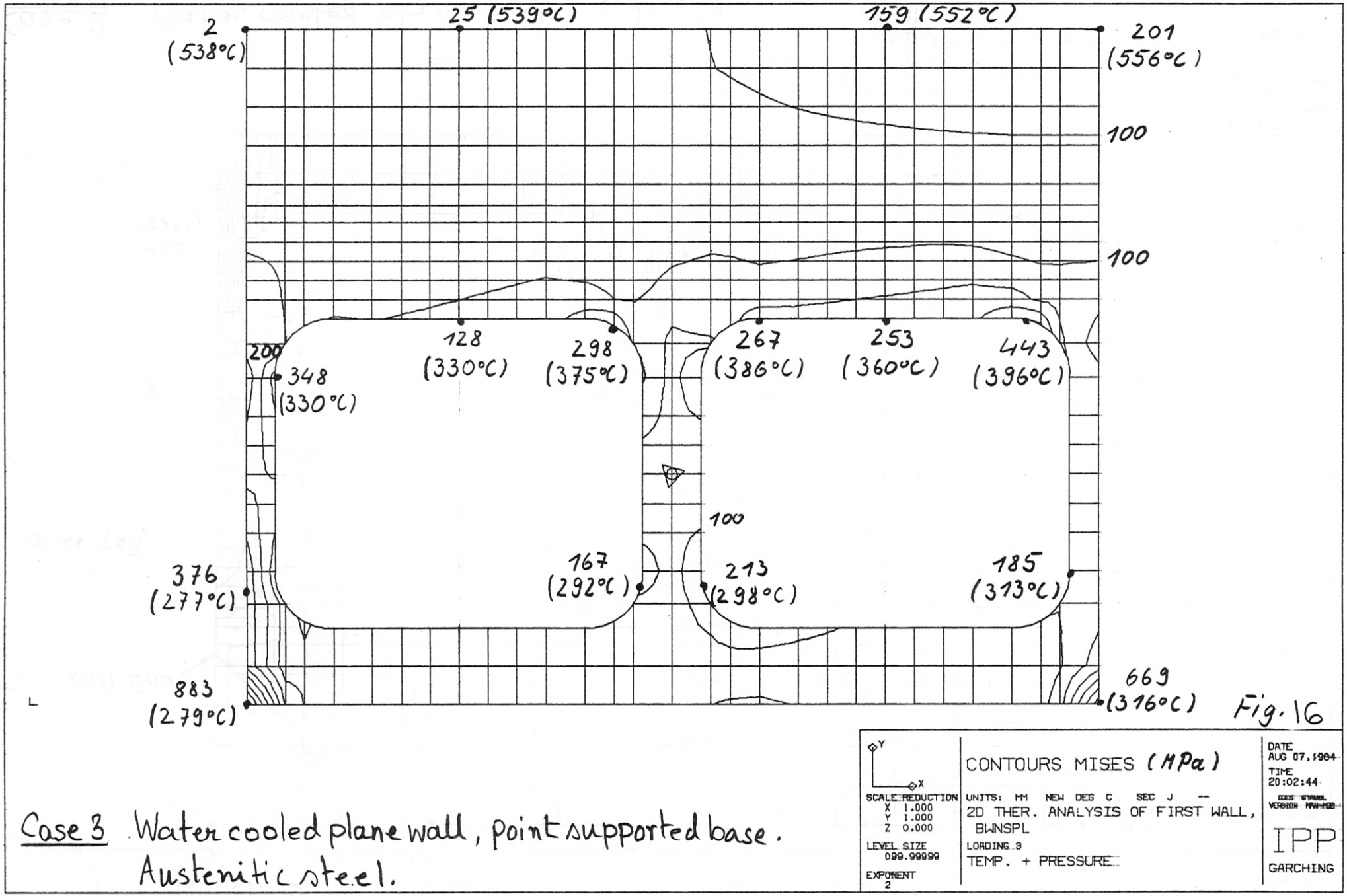

Fig. 16

Case 3 Water cooled plane wall, point supported base.
Austenitic steel.

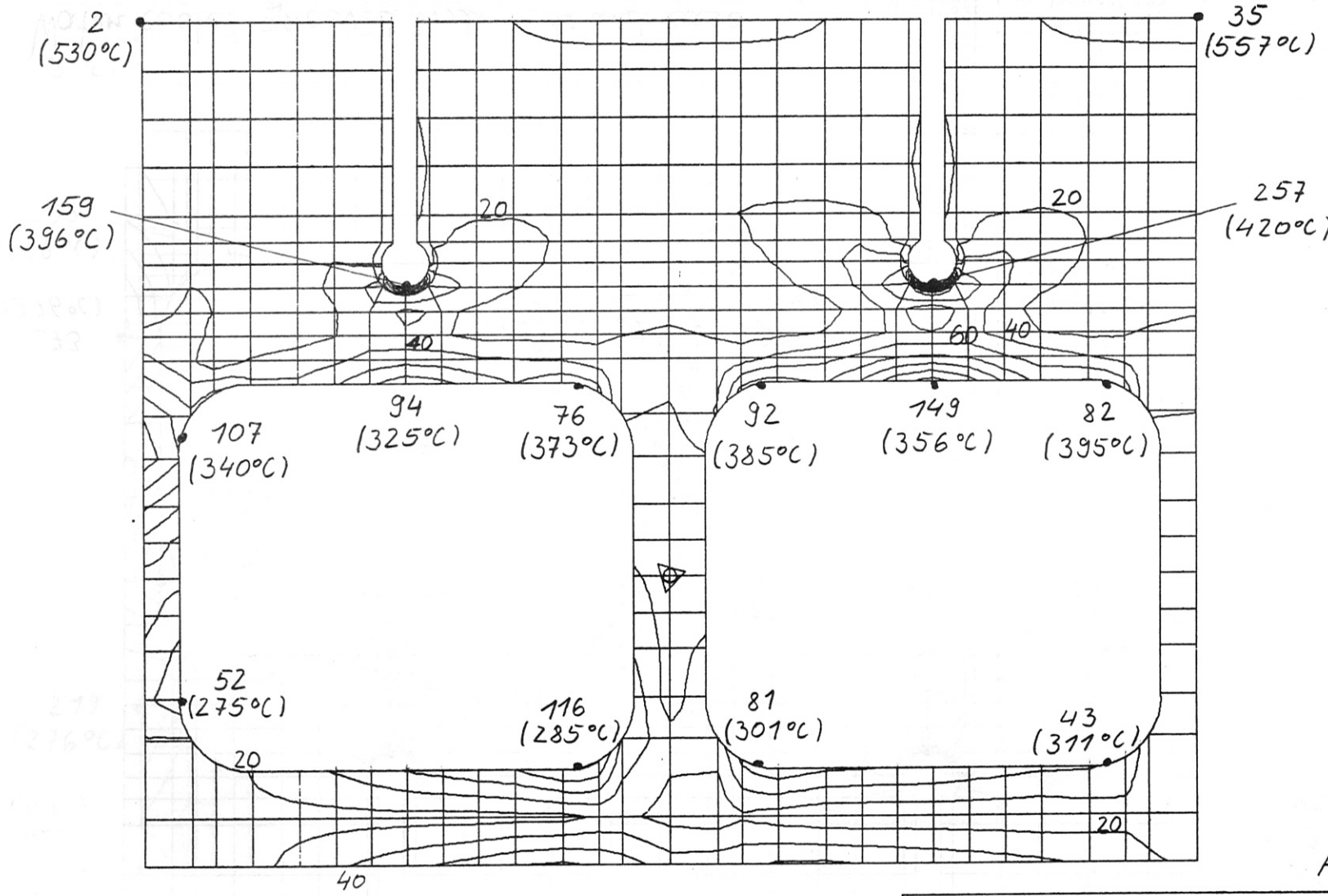

Fig. 17

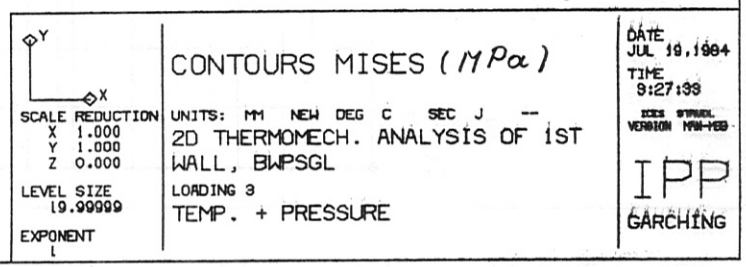

Case4 Water cooled grooved wall, side supported.
Austenitic steel.

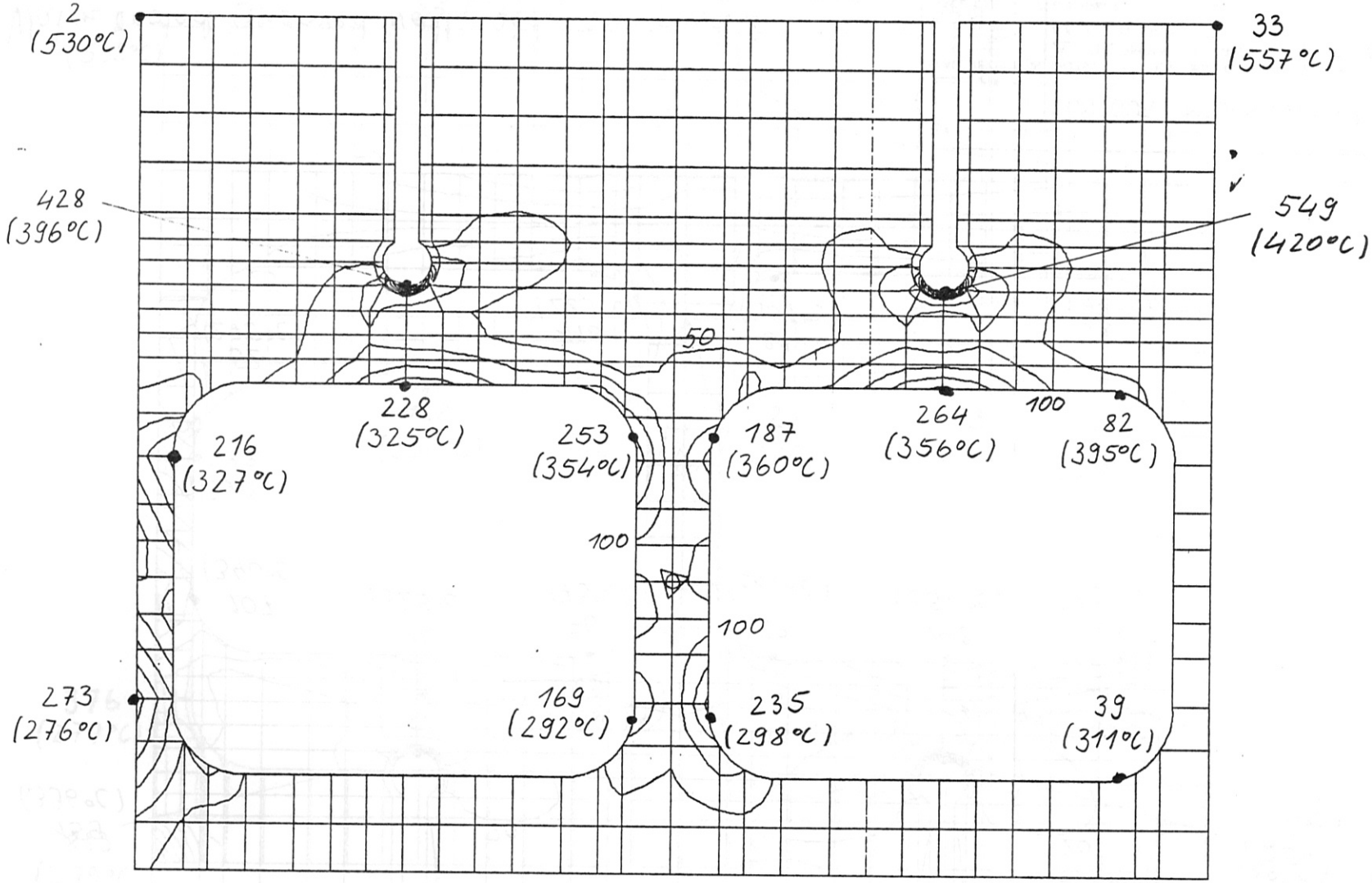

Fig. 18

Case 5 Water cooled grooved wall, side and base supported. Austenitic steel.

SCALE REDUCTION
X 1.000
Y 1.000
Z 0.000
LEVEL SIZE
49.99999
EXPONENT
0

CONTOURS MISES (MPa)

UNITS: MM NEW DEG C SEC J --
2D THERMOMECH. ANALYSIS OF 1ST WALL, BWFSGL
LOADING 3
TEMP. + PRESSURE

DATE
JUL 18,1984
TIME
21:17:47
ICES STRUDL VERSION MAR-1983

IPP
GARCHING

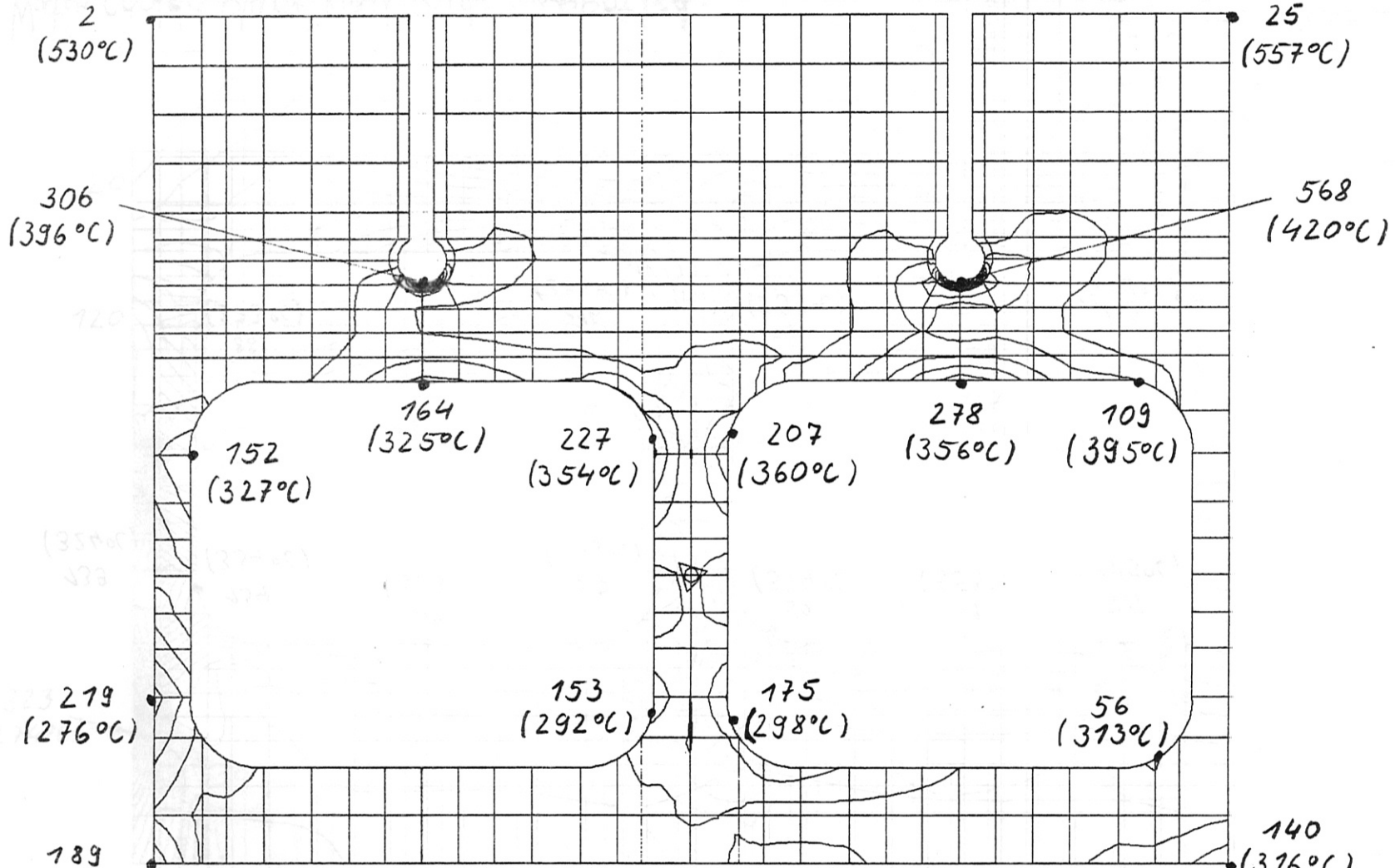

Fig. 19

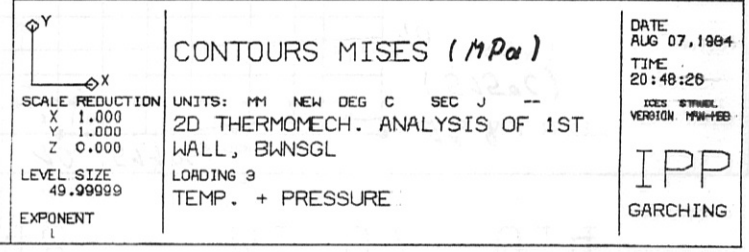

Case 6 Water cooled grooved wall, point supported base. Austenitic steel.

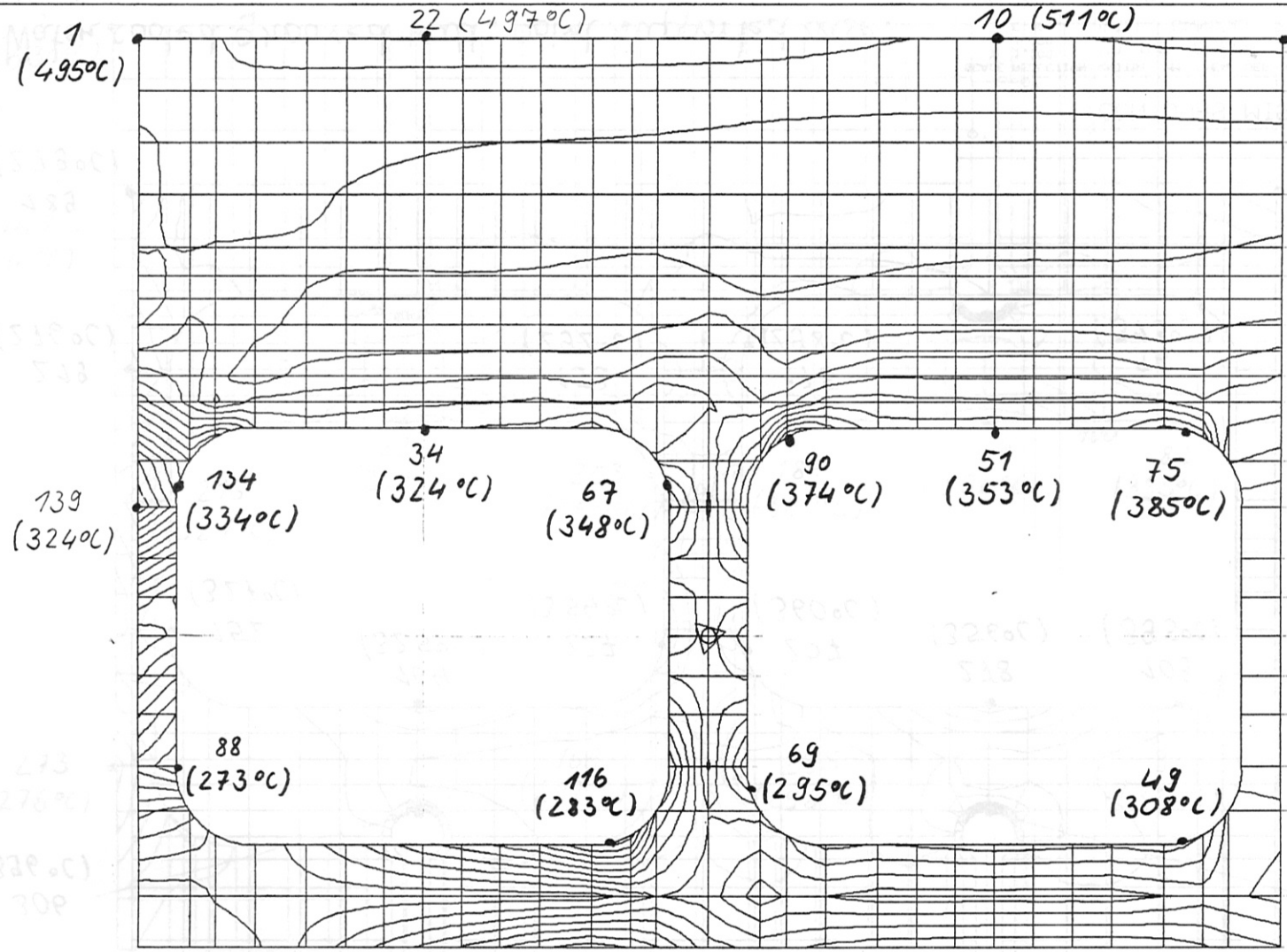

Fig. 20

Case 7 Water cooled plane wall, side supported.
Martensitic steel.

SCALE REDUCTION
X 1.000
Y 1.000
Z 0.000
LEVEL SIZE
10.00000
EXPONENT
1

CONTOURS MISES (MPa)
UNITS: MM NEW DEG C SEC J --
2D THER. ANALYSIS OF FIRST WALL.
BWPSPM
LOADING 3
TEMP. + PRESSURE

DATE
JUL 24,1984
TIME
12:14:57
DOES STRMDL VERSION MAR-MSB
IPP
GARCHING

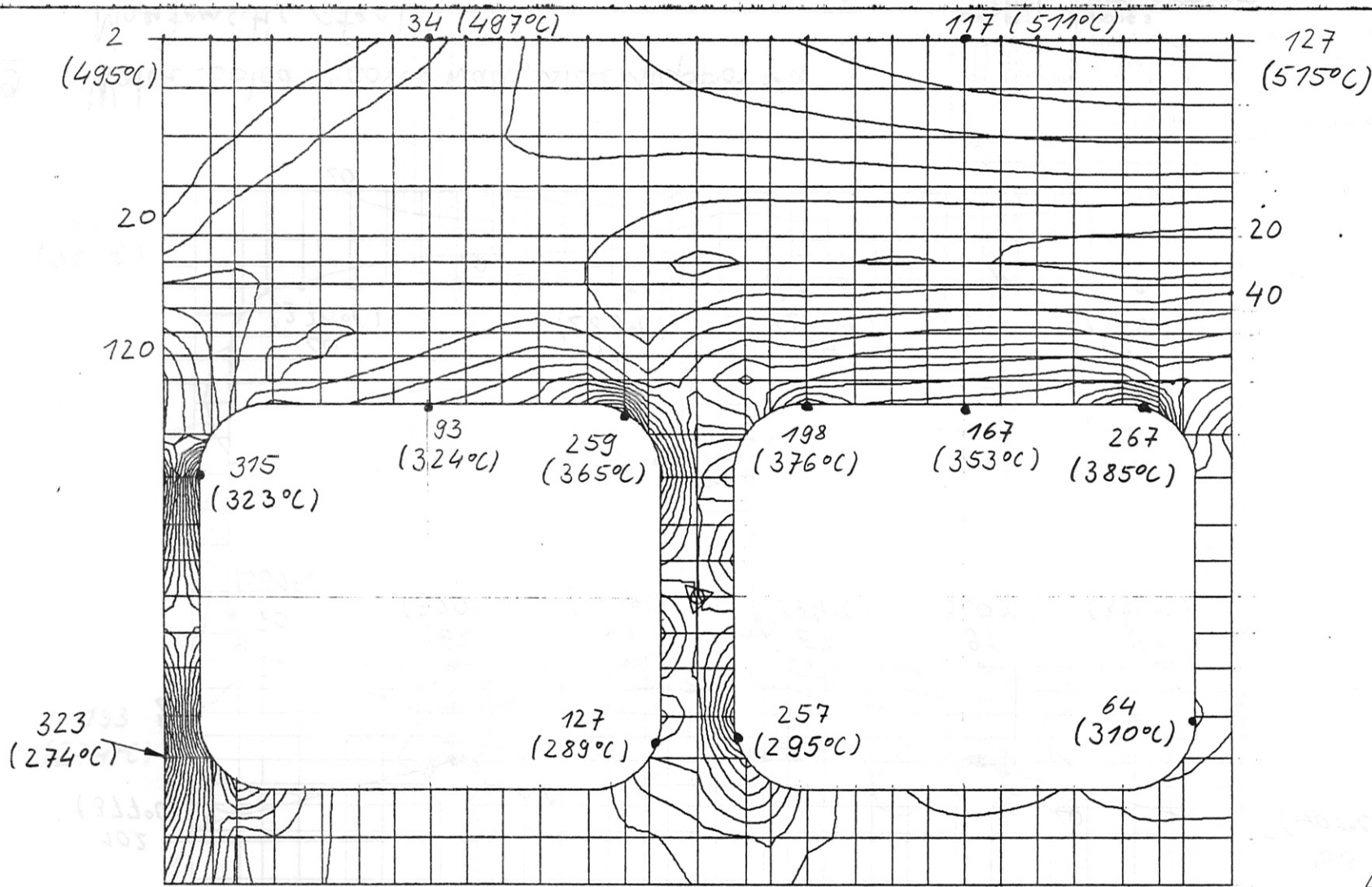

Fig. 21

Case 8 Water cooled plane wall, side and base supported.
Martensitic steel.

SCALE REDUCTION X 1.000 Y 1.000 Z 0.000 LEVEL SIZE (0.00000 EXPONENT	CONTOURS MISES (MPa) UNITS: MM NEW DEG C SEC J -- 2D THER. ANALYSIS OF FIRST WALL. BWFSPM LOADING 3 TEMP. + PRESSURE	DATE JUL 24,1984 TIME 10:50:12 IPP GARCHING

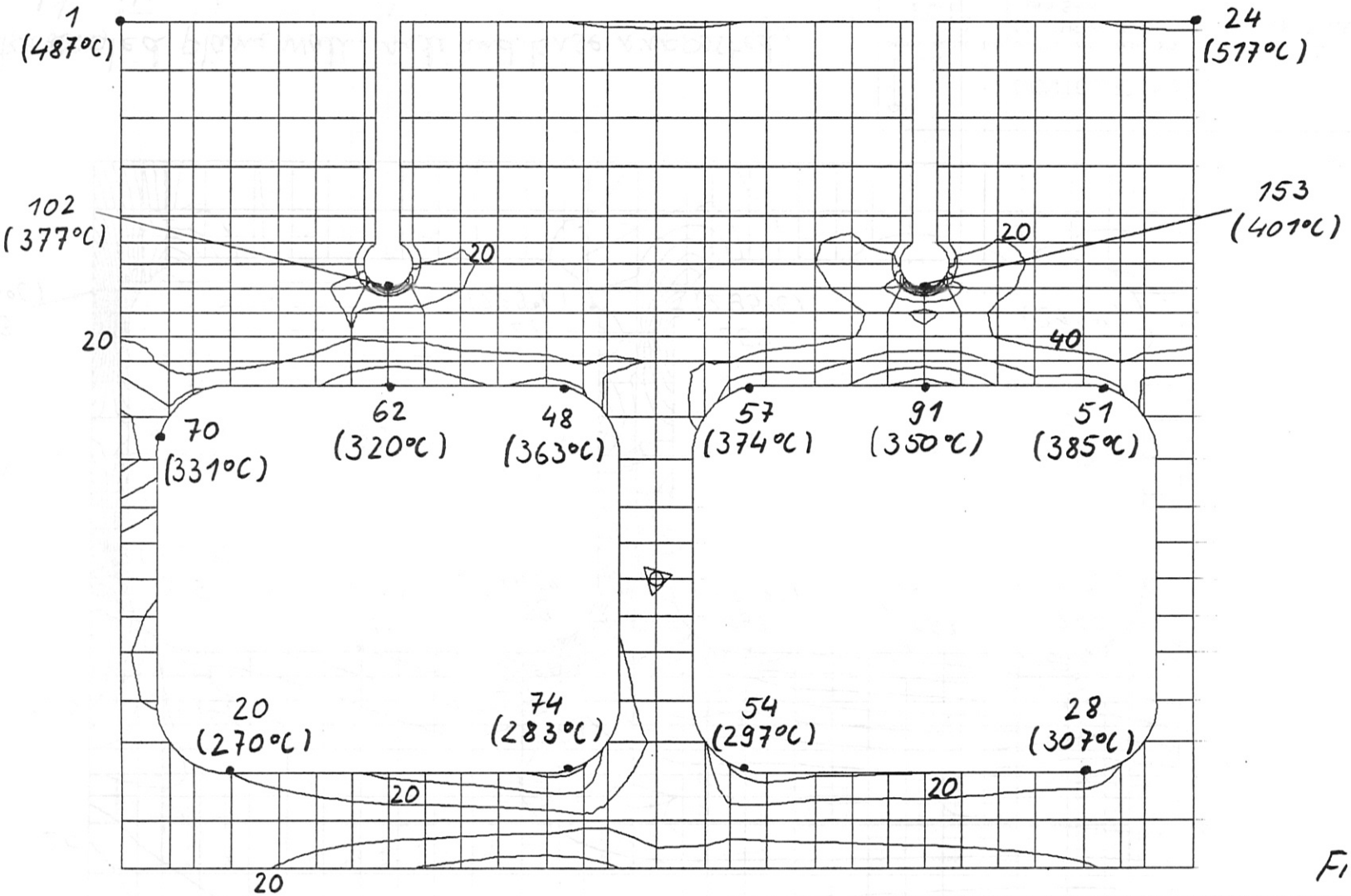

Fig. 22

Case 9 Water cooled grooved wall, side supported.
Martensitic steel.

SCALE REDUCTION
X 1.000
Y 1.000
Z 0.000
LEVEL SIZE
19.99999
EXPONENT
1

CONTOURS MISES (MPa)
UNITS: MM NEW DEG C SEC J --
2D THERMOMECH. ANALYSIS OF 1ST WALL, BWPSGM
LOADING 3
TEMP. + PRESSURE

DATE
JUL 24,1984
TIME
14:19:11
IDEAS STRUDL VERSION MAN-MSB
IPP
GARCHING

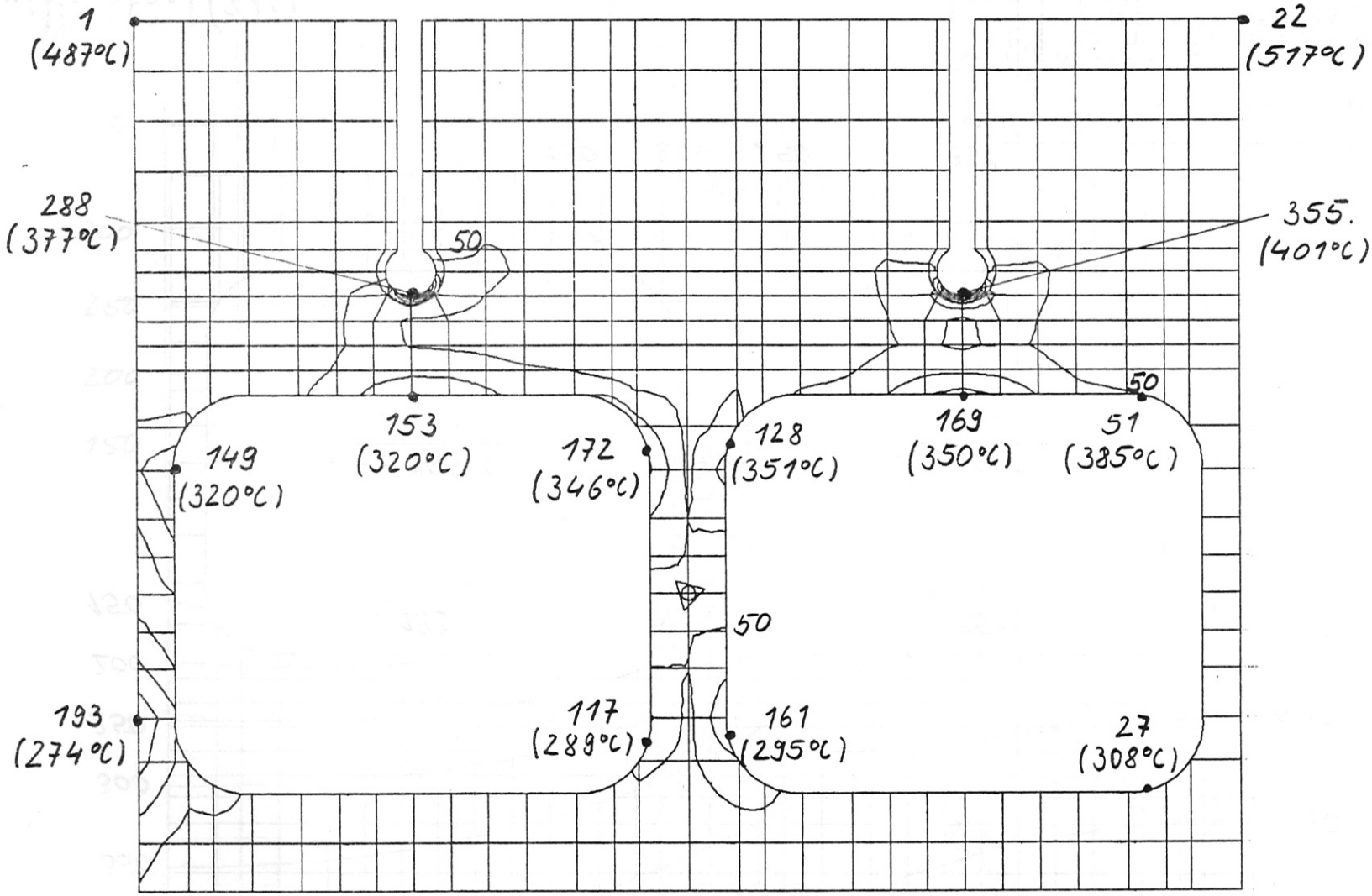

Fig. 23

Case 10 Water cooled grooved wall, side and base supported. Martensitic steel.

SCALE REDUCTION
X 1.000
Y 1.000
Z 0.000
LEVEL SIZE
49.99999
EXPONENT
1

CONTOURS MISES (MPa)
UNITS: MM NEW DEG C SEC J --
2D THERMOMECH. ANALYSIS OF 1ST WALL, BWFSGM
LOADING 3
TEMP. + PRESSURE

DATE
JUL 24.1984
TIME
19:32:39
ICES STRUDL VERSION MMM-MSB
IPP
GARCHING

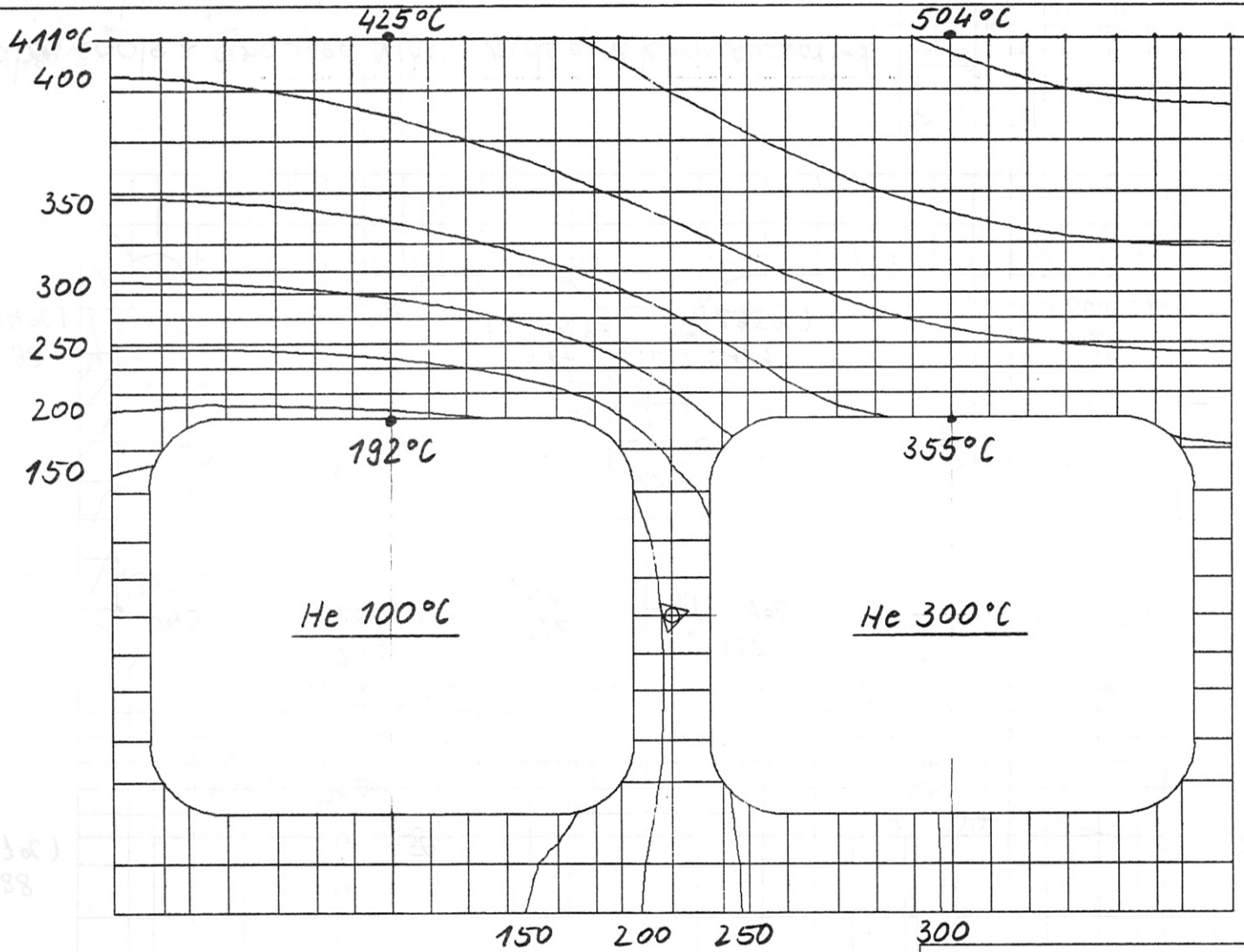

Fig. 24

Austenitic steel (316L)

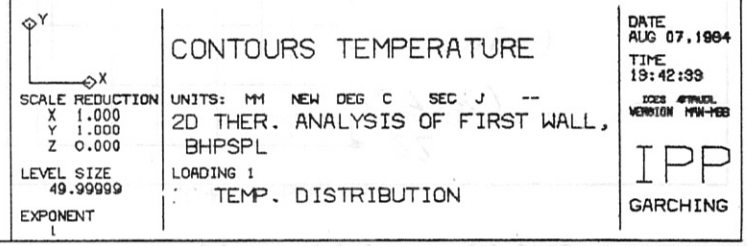

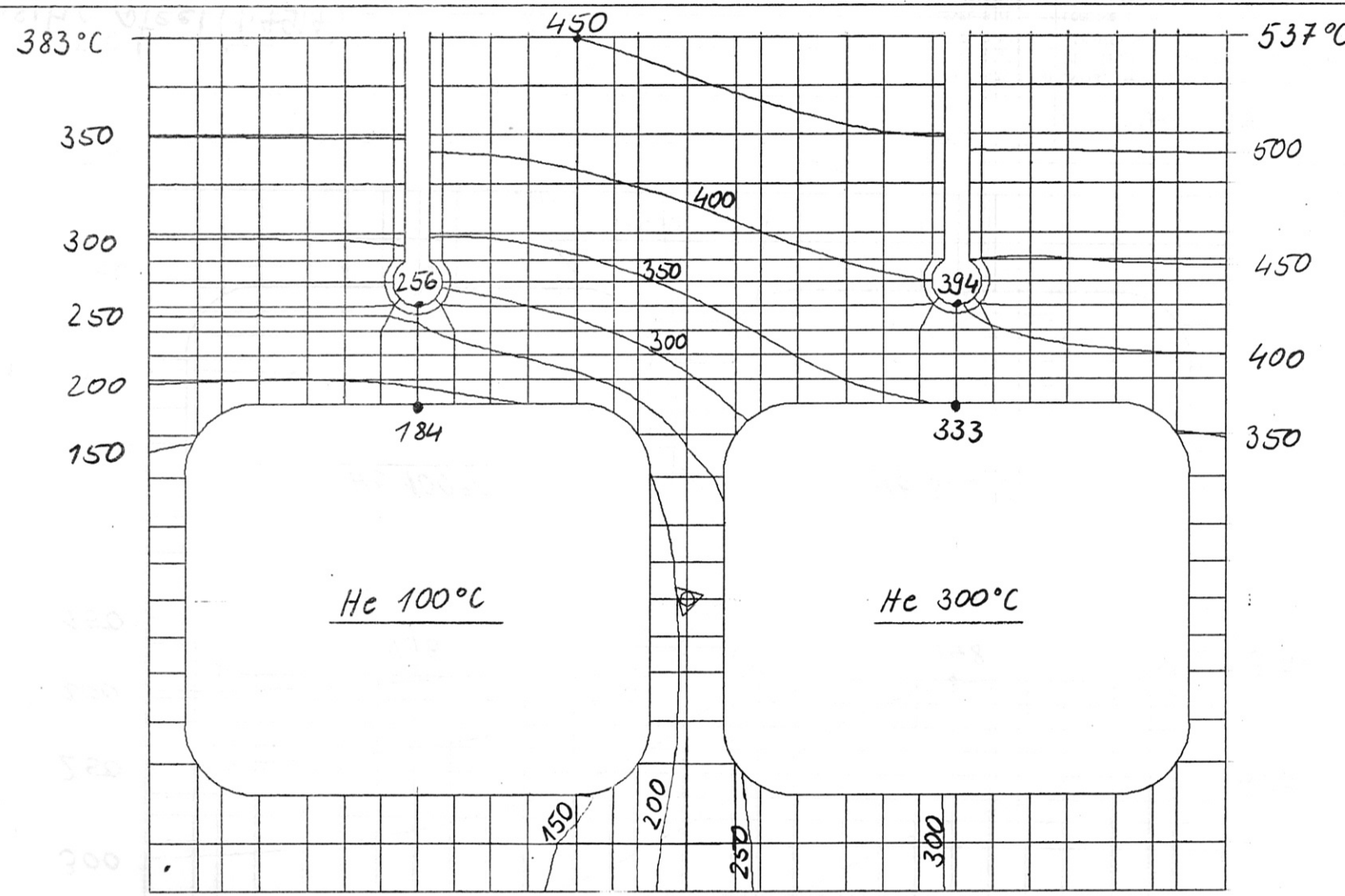

Fig. 25

Austenitic steel (316L)

SCALE REDUCTION X 1.000 Y 1.000 Z 0.000 LEVEL SIZE 49.99999 EXPONENT 1	CONTOURS TEMPERATURE UNITS: MM NEW DEG C SEC J -- 2D THERMOMECH. ANALYSIS OF 1ST WALL, BHPSGL LOADING 1 :: TEMP. DISTRIBUTION
DATE JUL 20,1984 TIME 15:09:30 IGES STRUCL VERSION MAR-FEB IPP GARCHING	

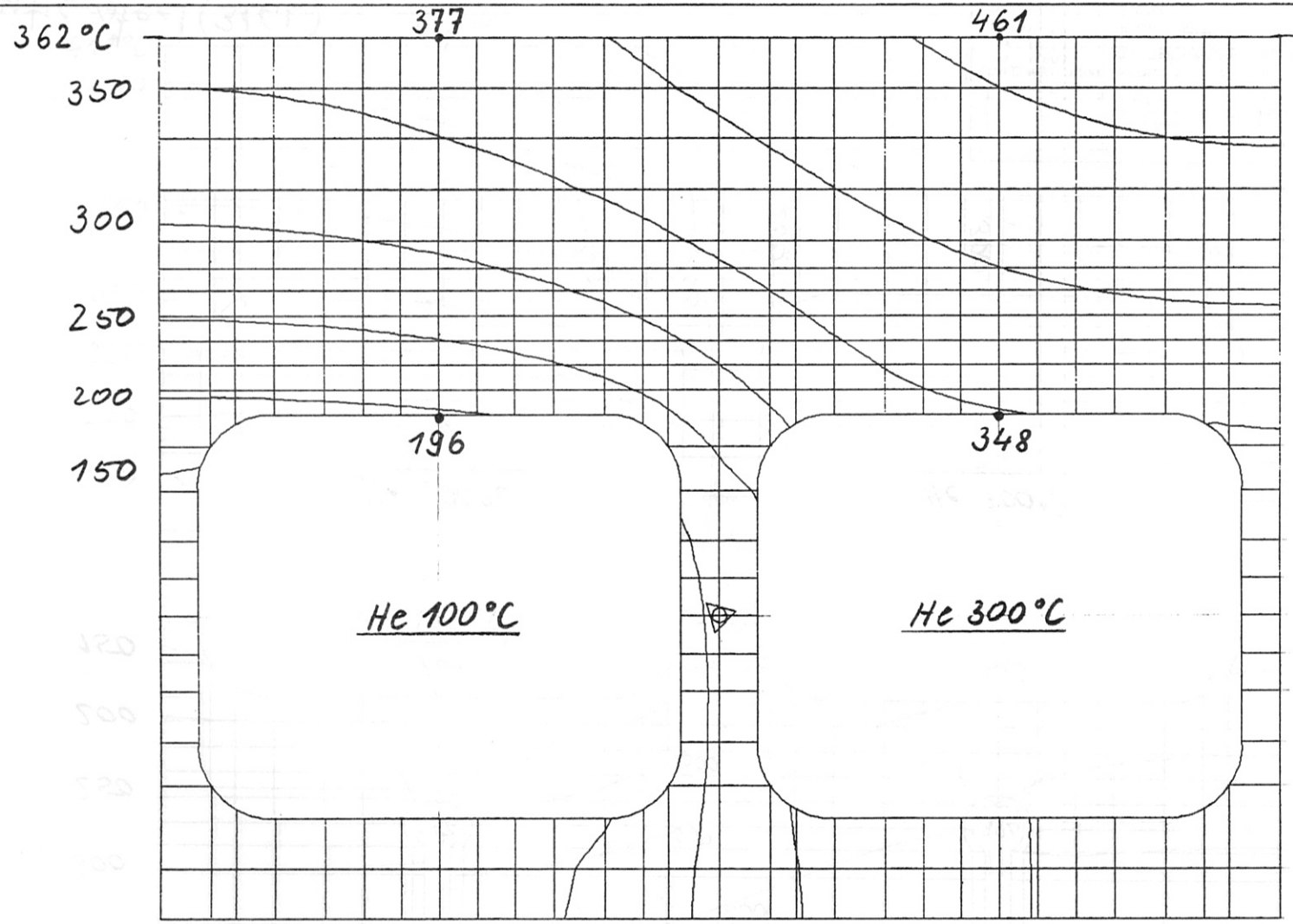

Fig. 26

Martensitic steel (1.4914)

SCALE REDUCTION
X 1.000
Y 1.000
Z 0.000
LEVEL SIZE
49.99999
EXPONENT
1

CONTOURS TEMPERATURE

UNITS: MM NEW DEG C SEC J --
2D THER. ANALYSIS OF FIRST WALL,
BHPSPM
LOADING 1
TEMP. DISTRIBUTION

DATE
JUL 23,1984
TIME
19:25:08
IDES WINDEL
VERSION MAY-MSB

IPP
GARCHING

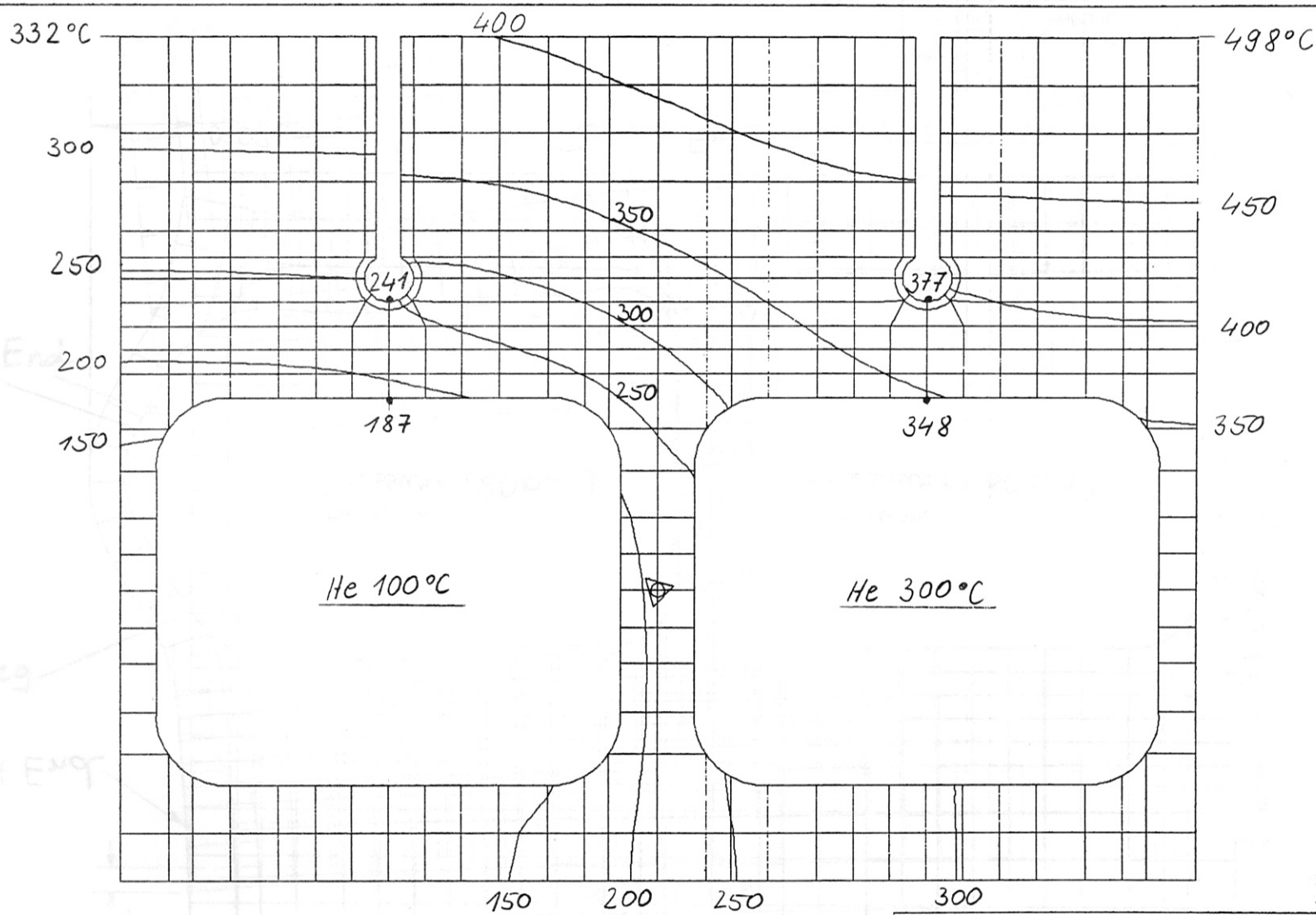

Fig. 27

Martensitic Steel (1.4914)

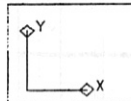

SCALE REDUCTION
X 1.000
Y 1.000
Z 0.000
LEVEL SIZE
49.99999
EXPONENT
1

CONTOURS TEMPERATURE

UNITS: MM NEW DEG C SEC J --
2D THERMOMECH. ANALYSIS OF 1ST WALL, BHPSGM
LOADING 1
TEMP. DISTRIBUTION

DATE
JUL 23,1984
TIME
20:39:15
ICES STRUDL VERSION MAN-MSB

IPP
GARCHING

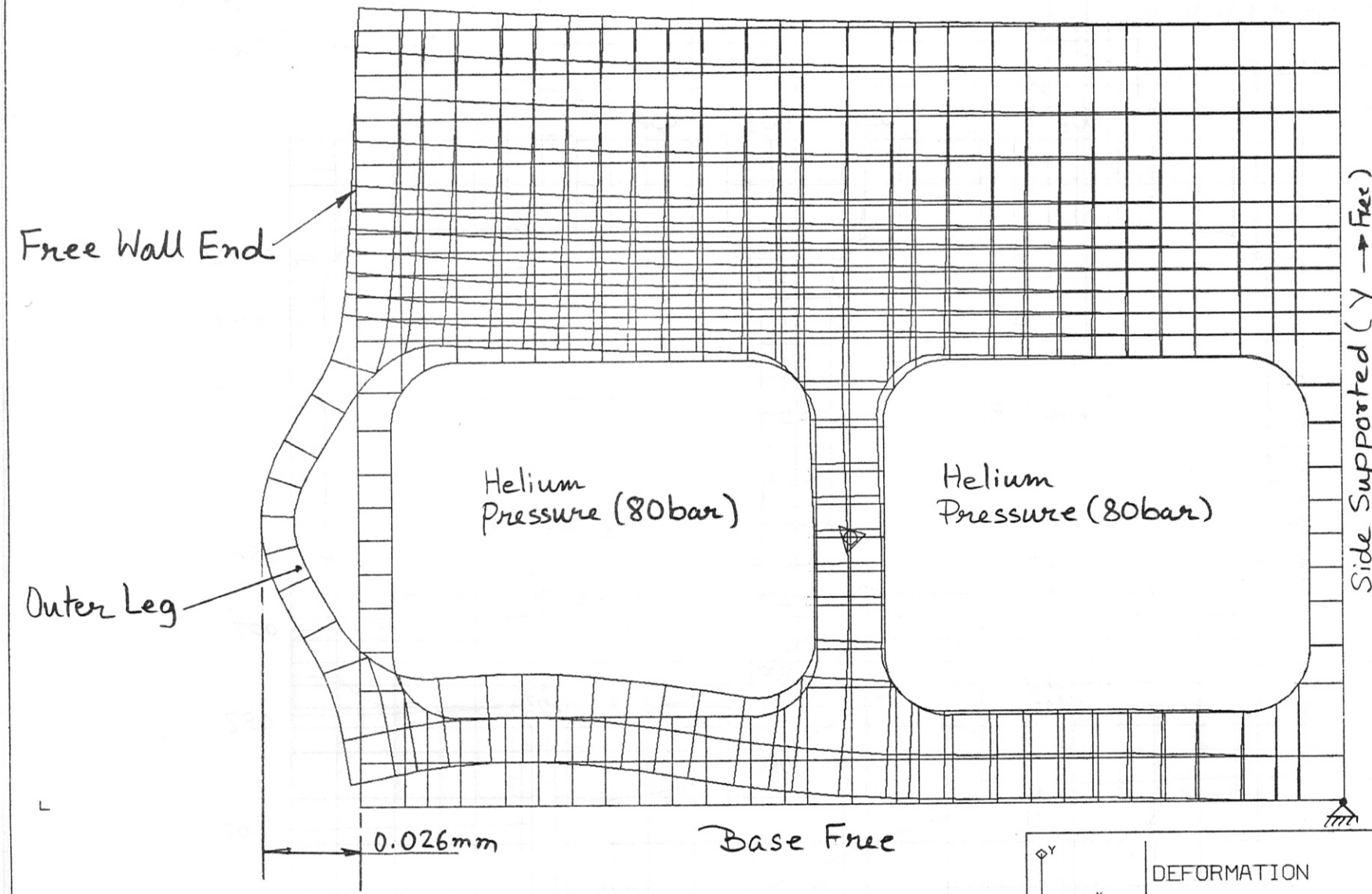
Free Wall End
Outer Leg
Helium Pressure (80bar)
Helium Pressure (80bar)
Side Supported (Y → Free)
0.026mm
Base Free
Y
X
SCALE REDUCTION
X 1.000
Y 1.000
Z 0.000
SCALE LENGTH
0.26324
RESULT SCALE
167.78483
DEFORMATION DISPLAC.
2D THER. ANALYSIS OF FIRST WALL, BHPSPL
LOADING 2
HELIUM GAS PRESSURE (N/MM**2)
DATE
JUL 23,1984
TIME
14:08:51
IPP
GARCHING

Fig. 28

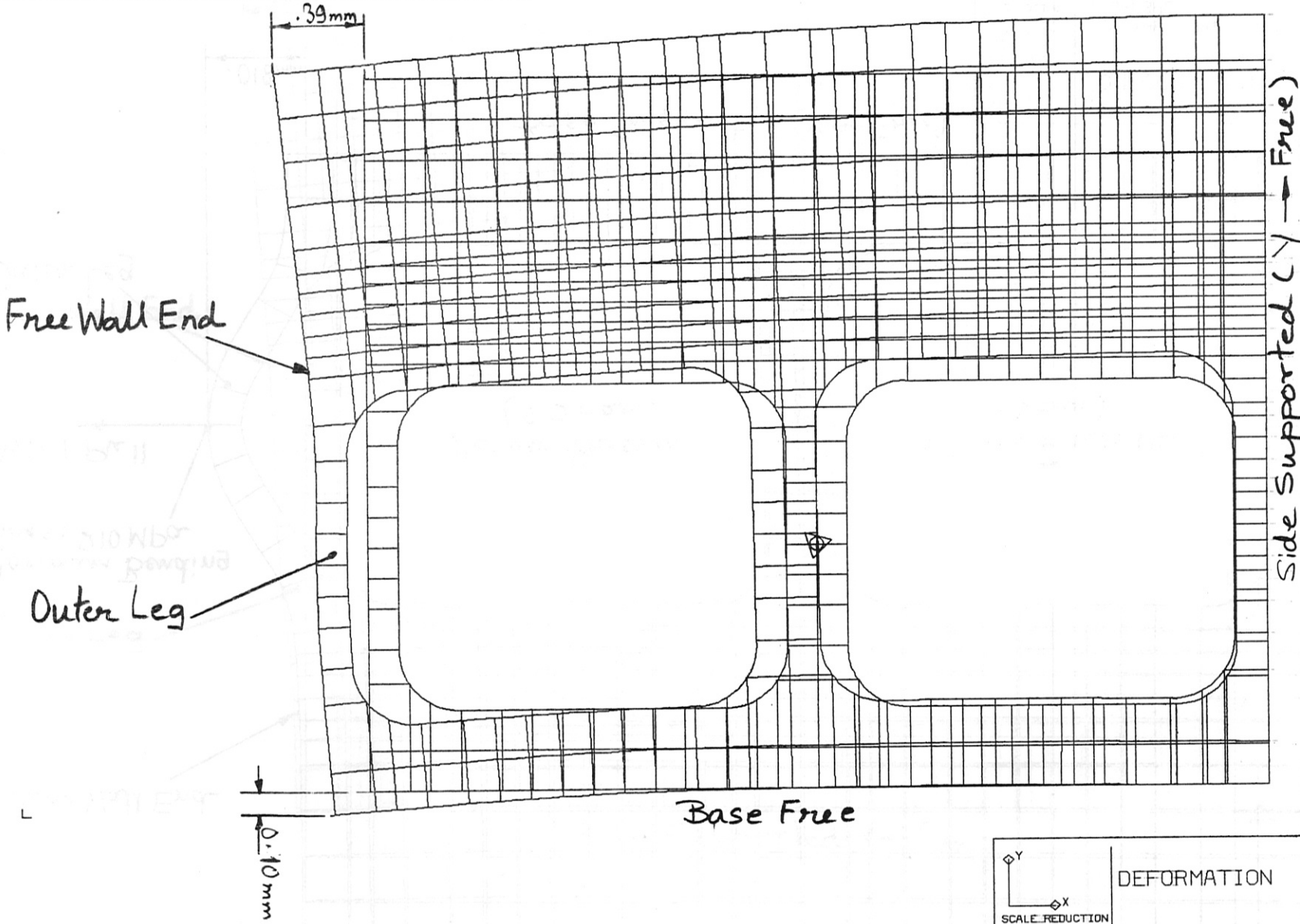

Fig. 29

Y
X

SCALE REDUCTION
X 1.000
Y 1.000
Z 0.000

SCALE LENGTH
0.28378

RESULT SCALE
11.59603

DEFORMATION DISPLAC.

2D THER. ANALYSIS OF FIRST WALL, BHPSPL

LOADING 3
TEMP. + PRESSURE

DATE
JUL 23,1984
TIME
14:08:58

ICES STRUDL
VERSION MAM-MOD

IPP
GARCHING

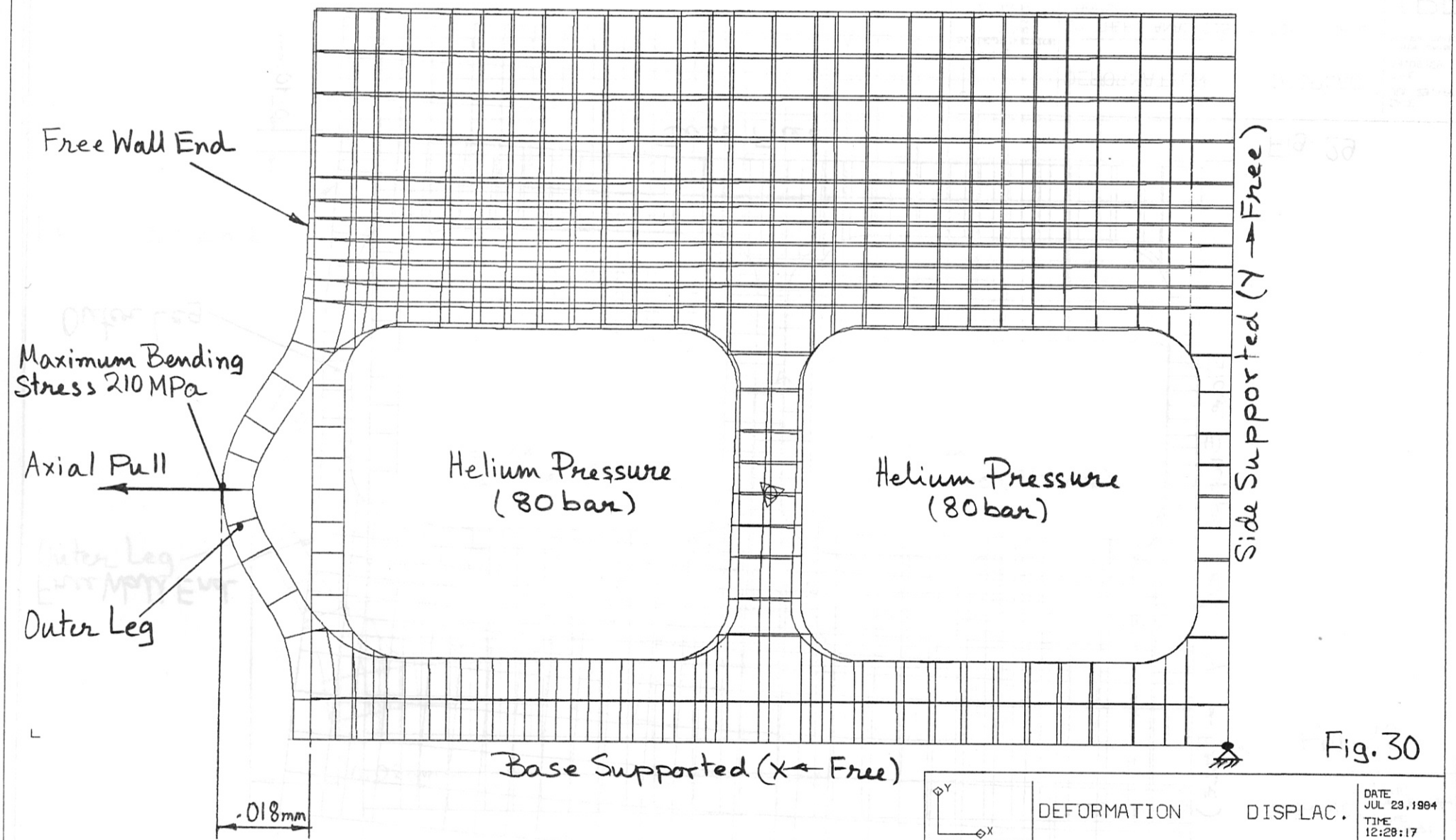
Free Wall End
Maximum Bending Stress 210 MPa
Axial Pull
Outer Leg
Helium Pressure (80 bar)
Helium Pressure (80 bar)
Side Supported (Y ← Free)
Base Supported (X ← Free)
.018mm
Y
X
SCALE REDUCTION
X 1.000
Y 1.000
Z 0.000
SCALE LENGTH
0.25577
RESULT SCALE
204.29017
DEFORMATION DISPLAC.
2D THER. ANALYSIS OF FIRST WALL, BHFSPL
LOADING 2
HELIUM GAS PRESSURE (N/MM**2)
DATE
JUL 23,1984
TIME
12:28:17
ICES STRUDL
VERSION MAY-MEB
IPP
GARCHING

Fig. 30

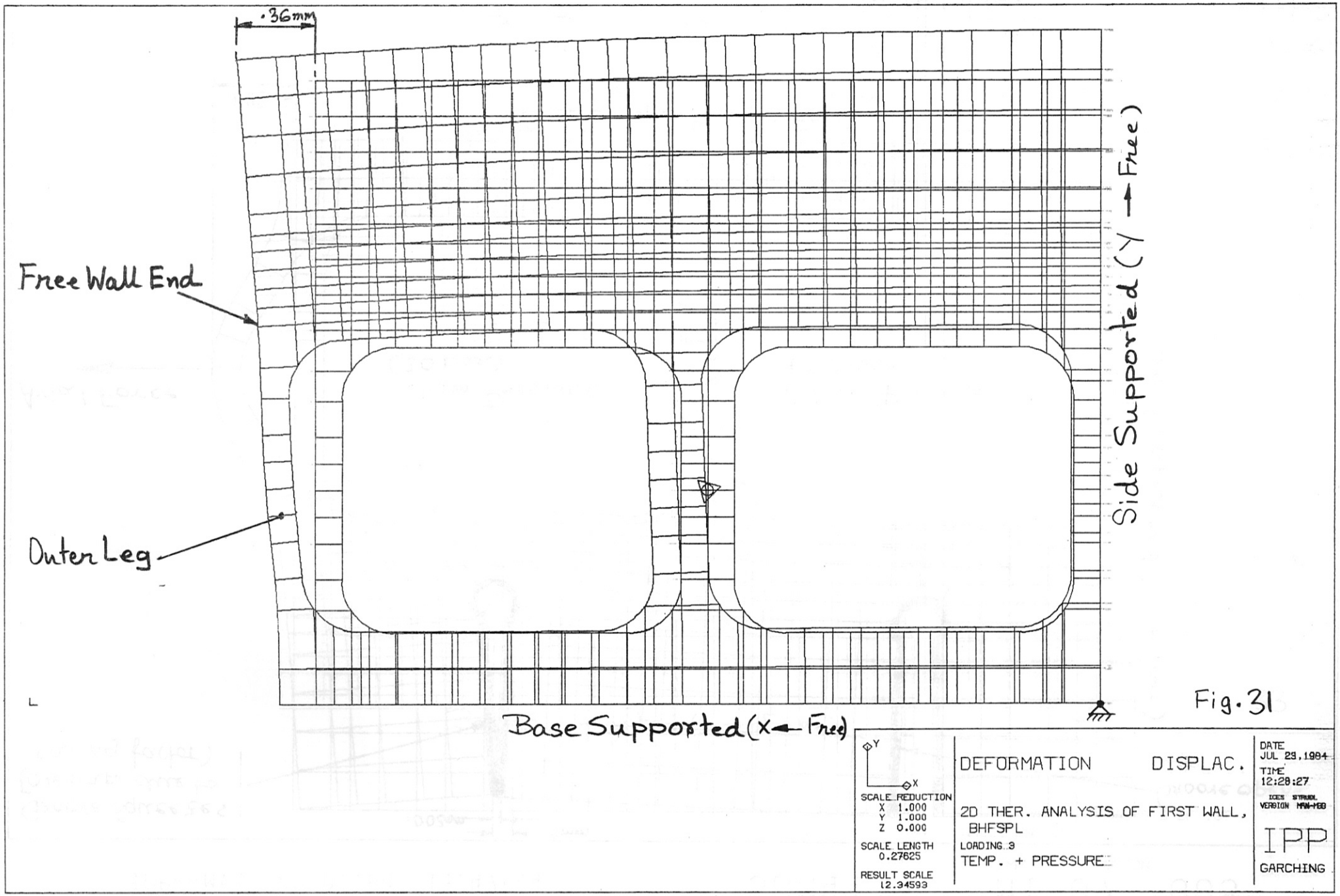
36mm
Free Wall End
Outer Leg
Side Supported (Y → Free)
Base Supported (X ← Free)
L
Y
X
SCALE REDUCTION
X 1.000
Y 1.000
Z 0.000
SCALE LENGTH
0.27625
RESULT SCALE
12.34593
DEFORMATION DISPLAC.
2D THER. ANALYSIS OF FIRST WALL, BHFSPL
LOADING 3
TEMP. + PRESSURE
DATE
JUL 23,1984
TIME
12:28:27
ICES STRUDL
VERSION MAN-MSB
IPP
GARCHING

Fig. 31

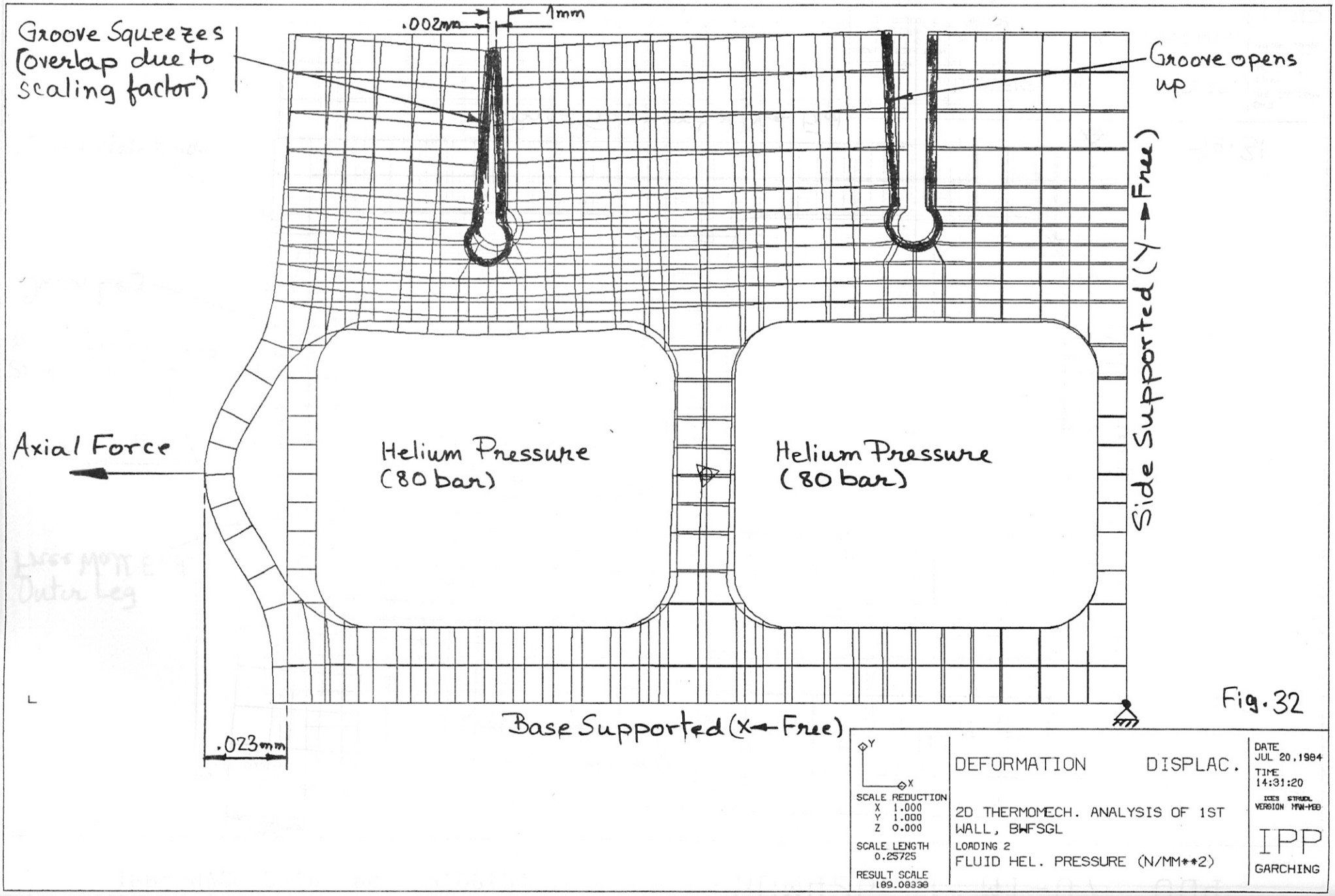
Groove Squeezes (overlap due to scaling factor)
.002mm
1mm
Groove opens up
Side Supported (Y←Free)
Axial Force
Helium Pressure (80 bar)
Helium Pressure (80 bar)
.023mm
Base Supported (X←Free)
Y
X
SCALE REDUCTION
X 1.000
Y 1.000
Z 0.000
SCALE LENGTH
0.25725
RESULT SCALE
189.08338
DEFORMATION DISPLAC.
2D THERMOMECH. ANALYSIS OF 1ST WALL, BWFSGL
LOADING 2
FLUID HEL. PRESSURE (N/MM**2)
DATE
JUL 20,1984
TIME
14:31:20
IDES STRUDL VERSION MAN-MSB
IPP
GARCHING

Fig. 32

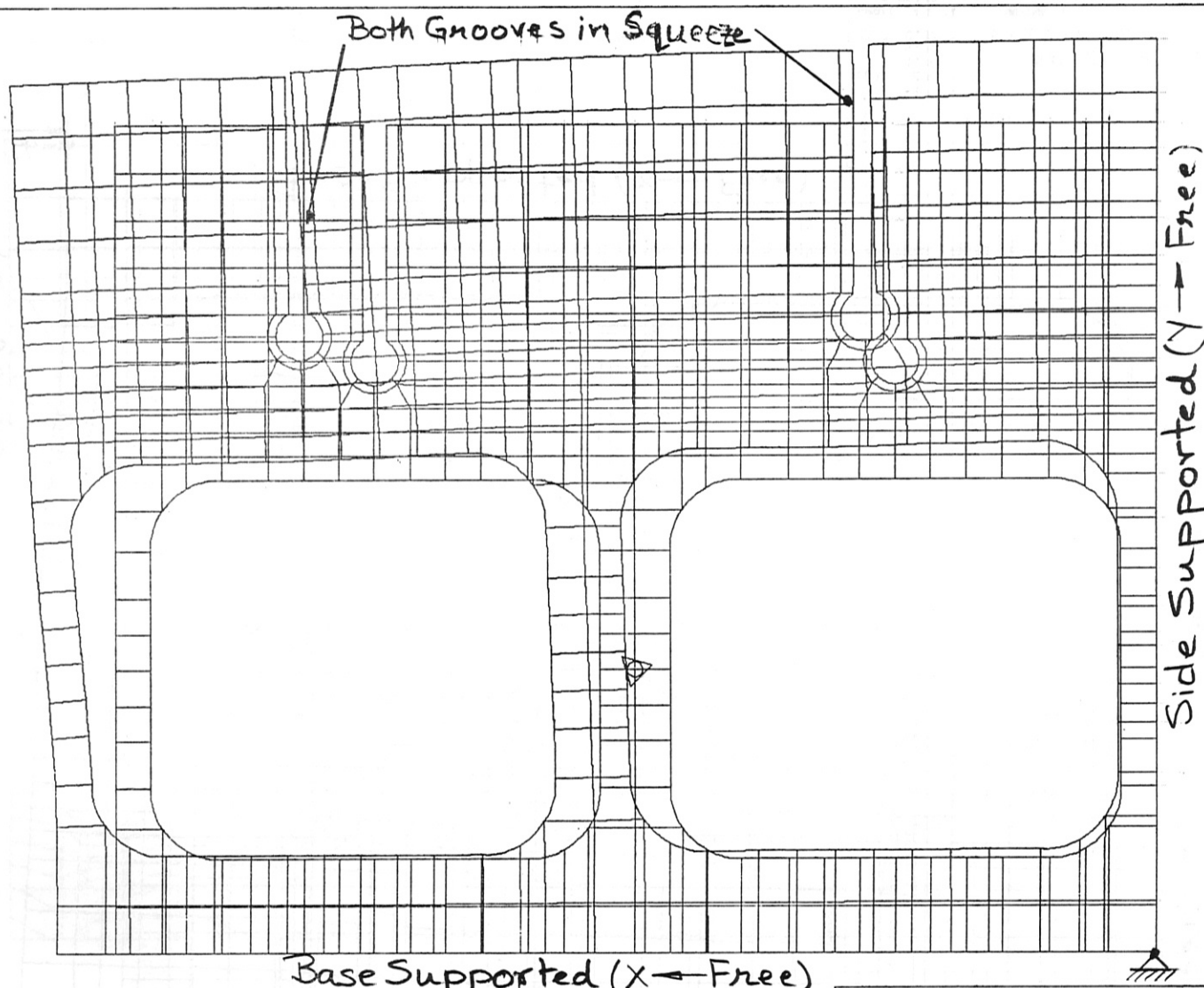

Fig. 33

Y
X
SCALE REDUCTION
X 1.000
Y 1.000
Z 0.000
SCALE LENGTH
0.28155
RESULT SCALE
15.20725

DEFORMATION DISPLAC.

2D THERMOMECH. ANALYSIS OF 1ST WALL, BWFSGL

LOADING 1
2D TEMP. DISTRIBUTION

DATE
JUL 20,1984
TIME
14:30:23
ICES STRUDL
VERSION MAN-MEB

IPP
GARCHING

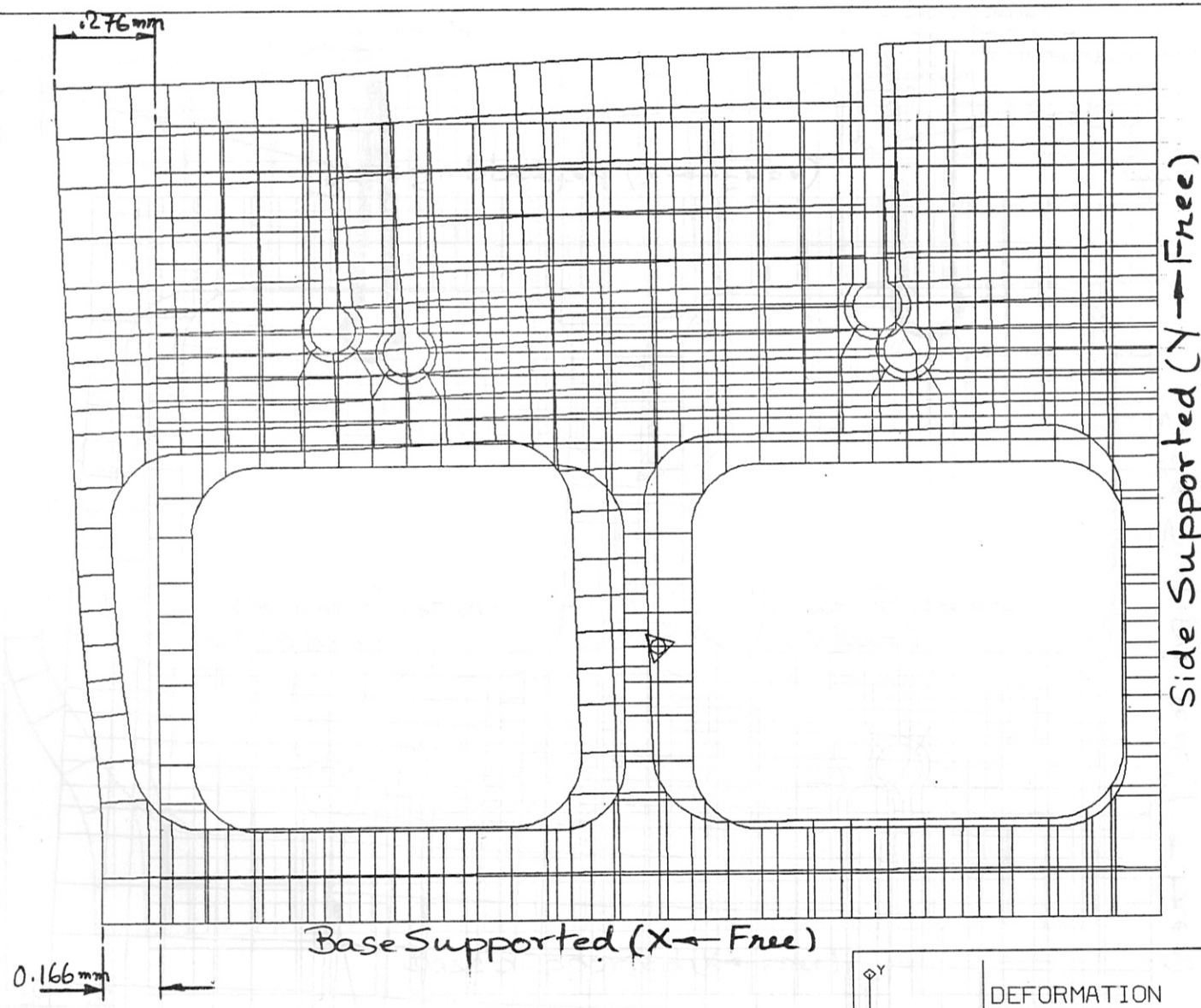

Fig. 34

Y
X
SCALE REDUCTION
X 1.000
Y 1.000
Z 0.000
SCALE LENGTH
0.28178
RESULT SCALE
15.31369

DEFORMATION DISPLAC.

2D THERMOMECH. ANALYSIS OF 1ST WALL, BWFSGL
LOADING 3
TEMP. + PRESSURE

DATE
JUL 20,1984
TIME
14:31:39
ICES STRUDL
VERSION MAR-1988

IPP
GARCHING

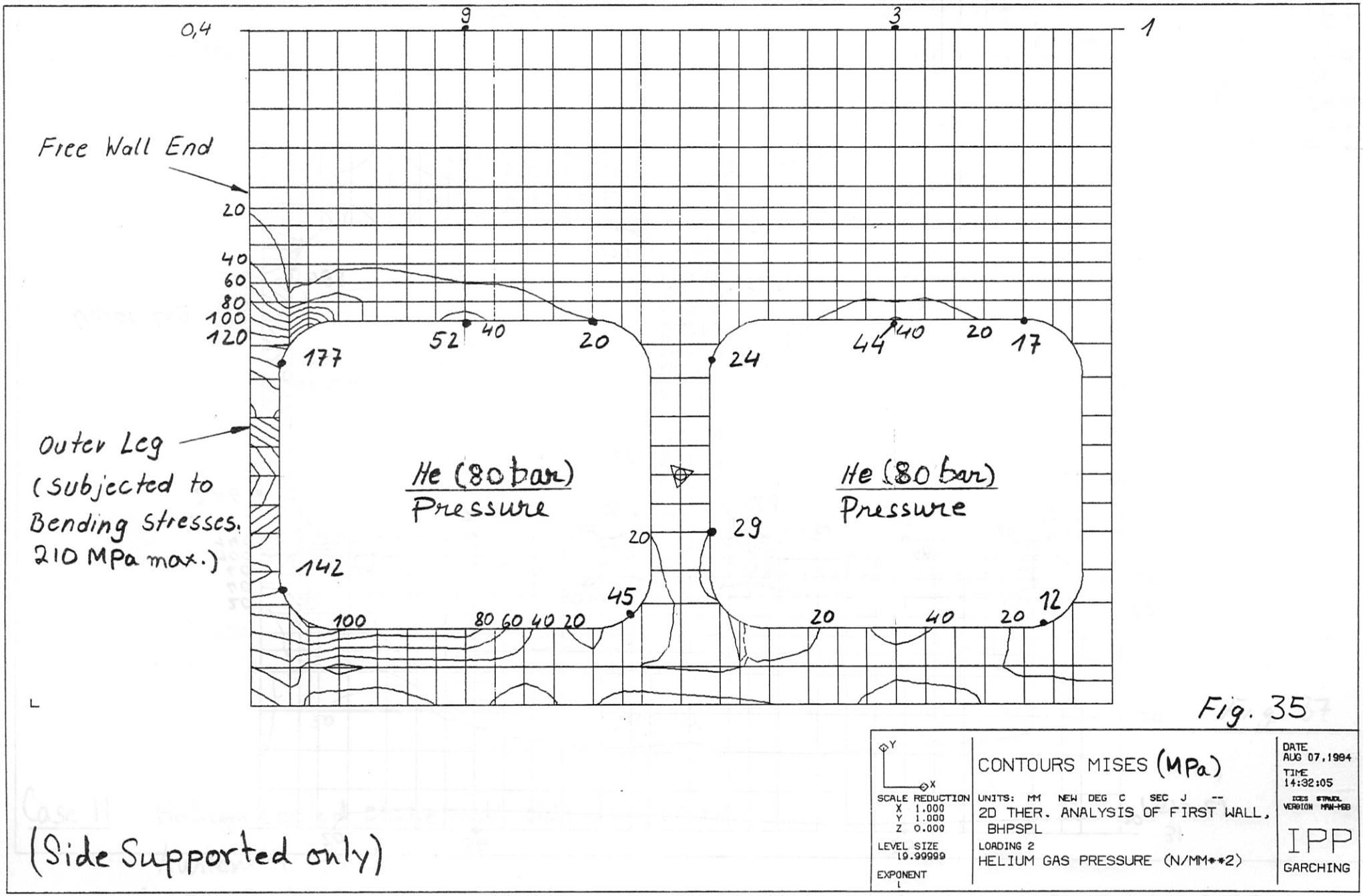
0,4
9
3
1
Free Wall End
20
40
60
80
100
120
177
52
40
20
24
44
40
20
17
Outer Leg
(subjected to
Bending Stresses.
210 MPa max.)
He (80 bar)
Pressure
He (80 bar)
Pressure
142
20
29
45
100
80 60 40 20
20
40
20
12
(Side Supported only)
CONTOURS MISES (MPa)
SCALE REDUCTION
X 1.000
Y 1.000
Z 0.000
LEVEL SIZE
19.99999
EXPONENT
UNITS: MM NEW DEG C SEC J --
2D THER. ANALYSIS OF FIRST WALL,
BHPSPL
LOADING 2
HELIUM GAS PRESSURE (N/MM**2)
DATE
AUG 07,1984
TIME
14:32:05
ICES STRUDL
VERSION MAN-MSB
IPP
GARCHING

Fig. 35

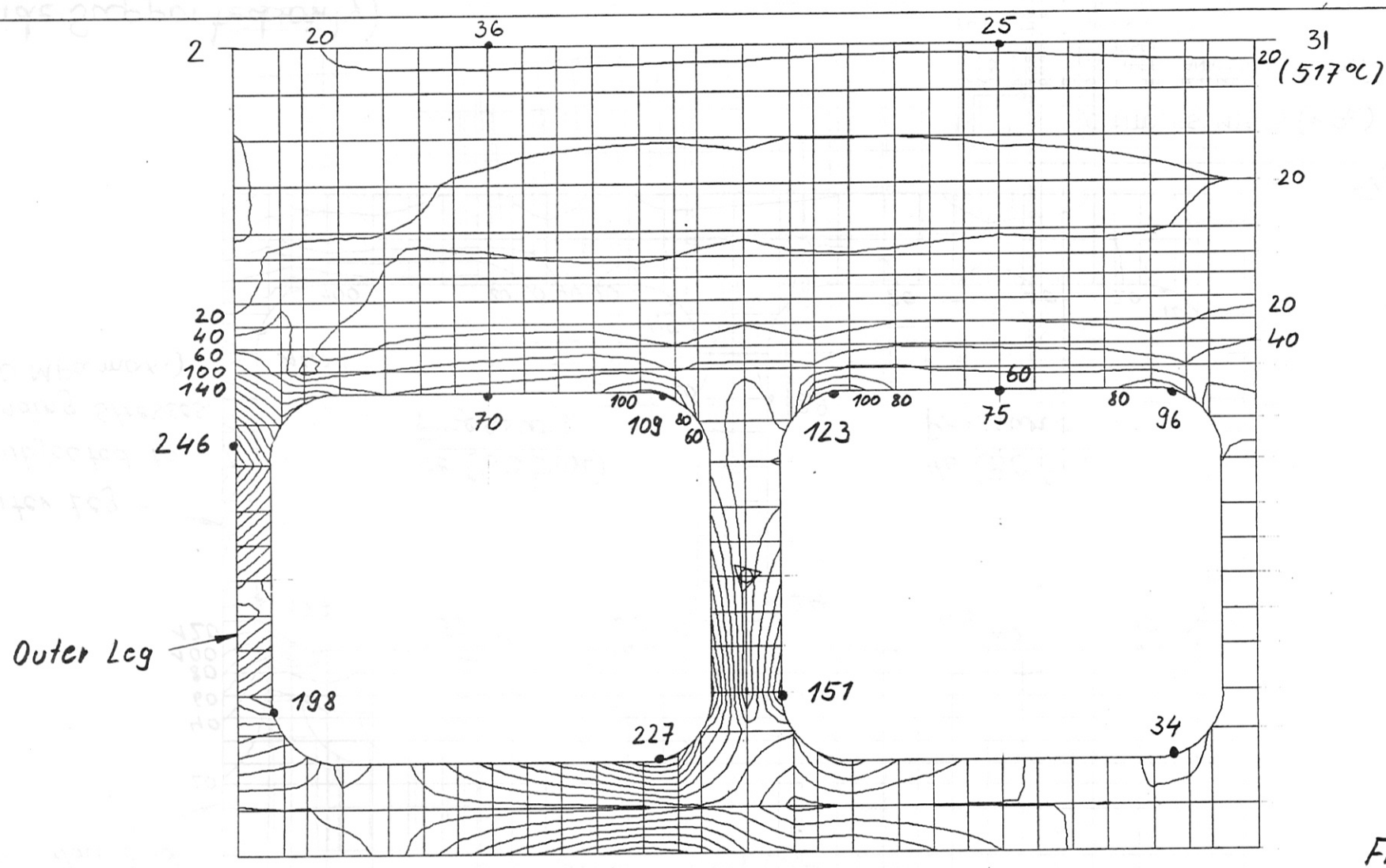

Fig. 36

(Side Supported only)

SCALE REDUCTION X 1.000 Y 1.000 Z 0.000 LEVEL SIZE 19.99999 EXPONENT 1	CONTOURS MISES (MPa) UNITS: MM NEW DEG C SEC J -- 2D THER. ANALYSIS OF FIRST WALL, BHPSPL LOADING 1 2D TEMP. DISTRIBUTION	DATE JUL 23,1984 TIME 14:16:18 IDES STRAND VERSION MARMSEB IPP GARCHING

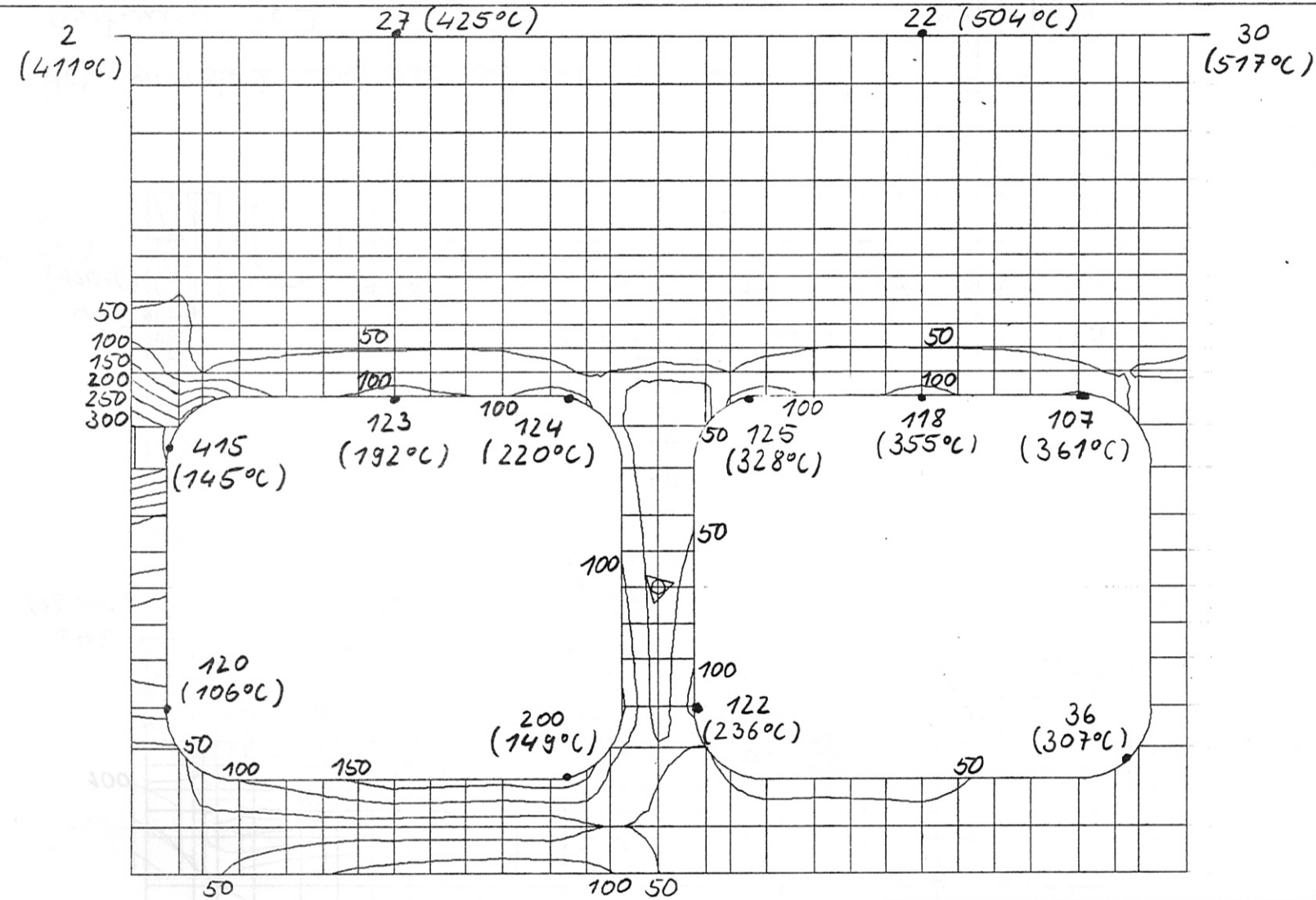

Fig. 37

SCALE REDUCTION
X 1.000
Y 1.000
Z 0.000
LEVEL SIZE
49.99999
EXPONENT
L

CONTOURS MISES (MPa)

UNITS: MM NEW DEG C SEC J --
2D THER. ANALYSIS OF FIRST WALL,
BHPSPL
LOADING 3
TEMP. + PRESSURE

DATE
JUL 23,1984
TIME
14:25:56
ICES STRUDL
VERSION MAR-MED

IPP
GARCHING

Case II Helium cooled plane wall, side supported.
Austenitic steel.

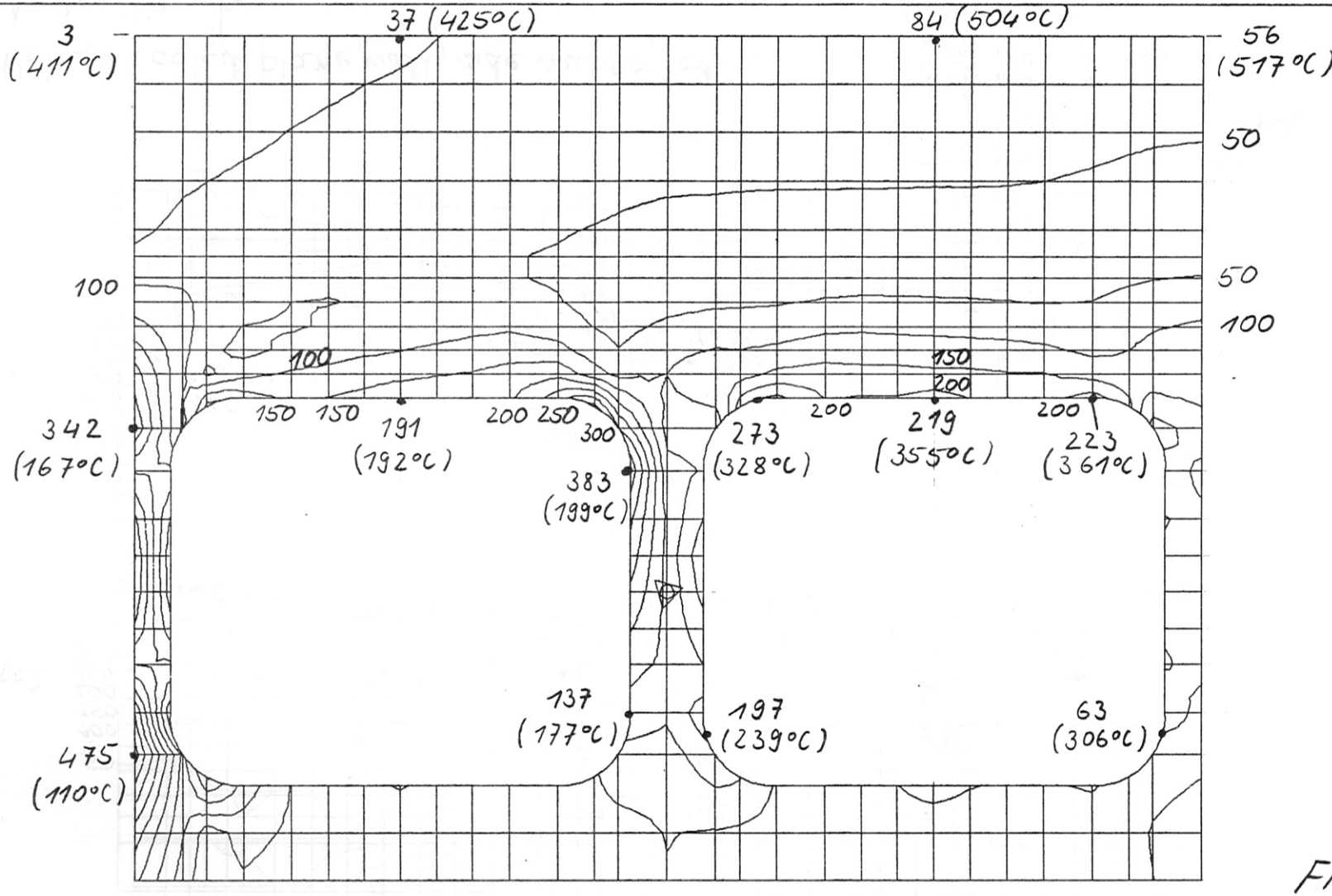

Fig. 38

Case 12 Helium cooled plane wall, side and base supported. Austenitic steel.

SCALE REDUCTION X 1.000 Y 1.000 Z 0.000 LEVEL SIZE 49.99999 EXPONENT 1	CONTOURS MISES (MPa) UNITS: MM NEW DEG C SEC J -- 2D THER. ANALYSIS OF FIRST WALL, BHFSPL LOADING 3 TEMP. + PRESSURE
	DATE JUL 23,1984 TIME 12:42:45 IDES STRUDL VERSION MAN-MSB IPP GARCHING

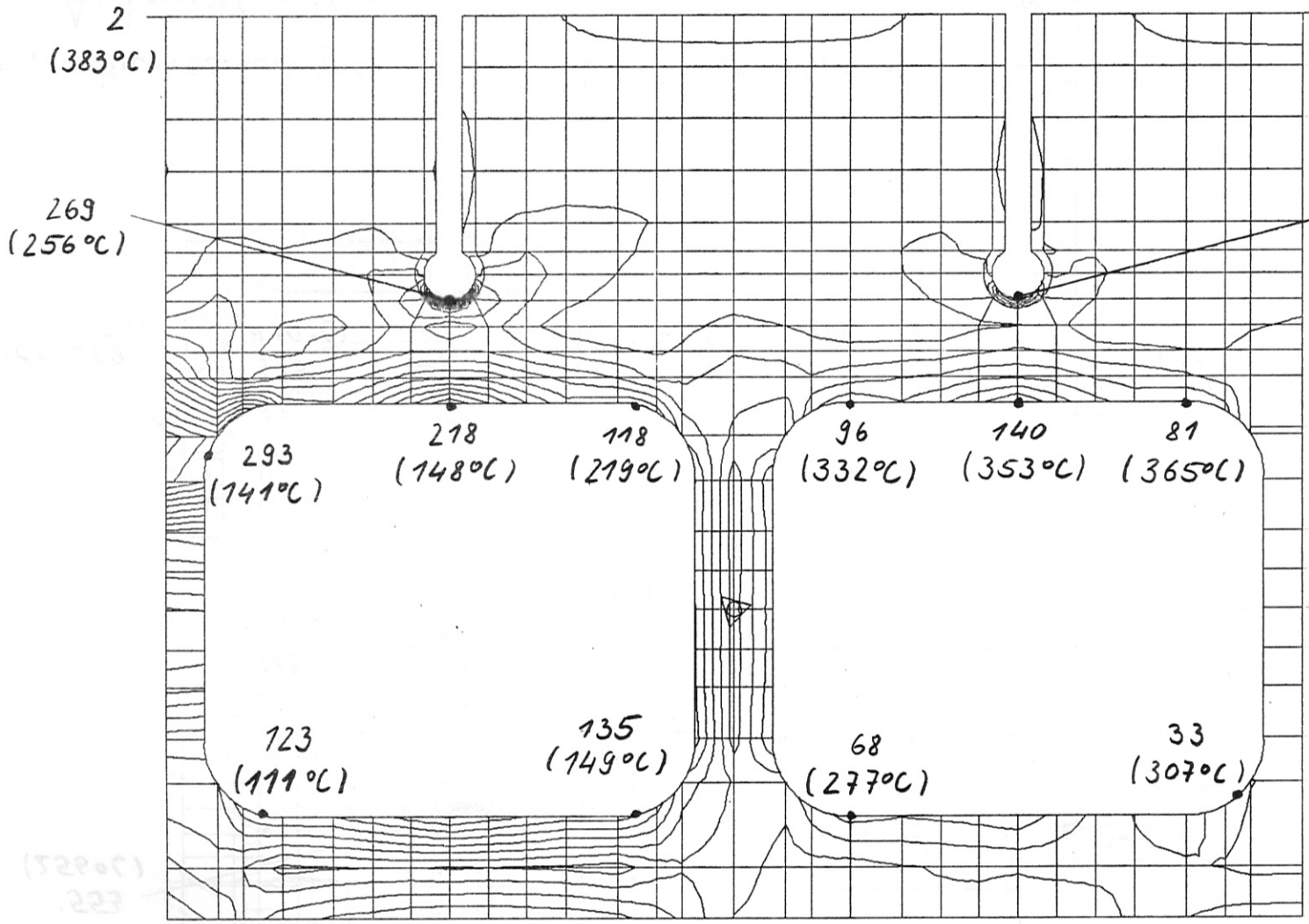

Fig. 39

Case 13 Helium cooled grooved wall, side support only.
Austenitic steel.

Y
X
SCALE REDUCTION
X 1.000
Y 1.000
Z 0.000
LEVEL SIZE
19.99999
EXPONENT
1

CONTOURS MISES (MPa)
UNITS: MM NEW DEG C SEC J --
2D THERMOMECH. ANALYSIS OF 1ST WALL, BHPSGL
LOADING 3
TEMP. + PRESSURE

DATE
JUL 20,1984
TIME
16:00:42
IGES STRUDL VERSION MAY-FEB
IPP
GARCHING

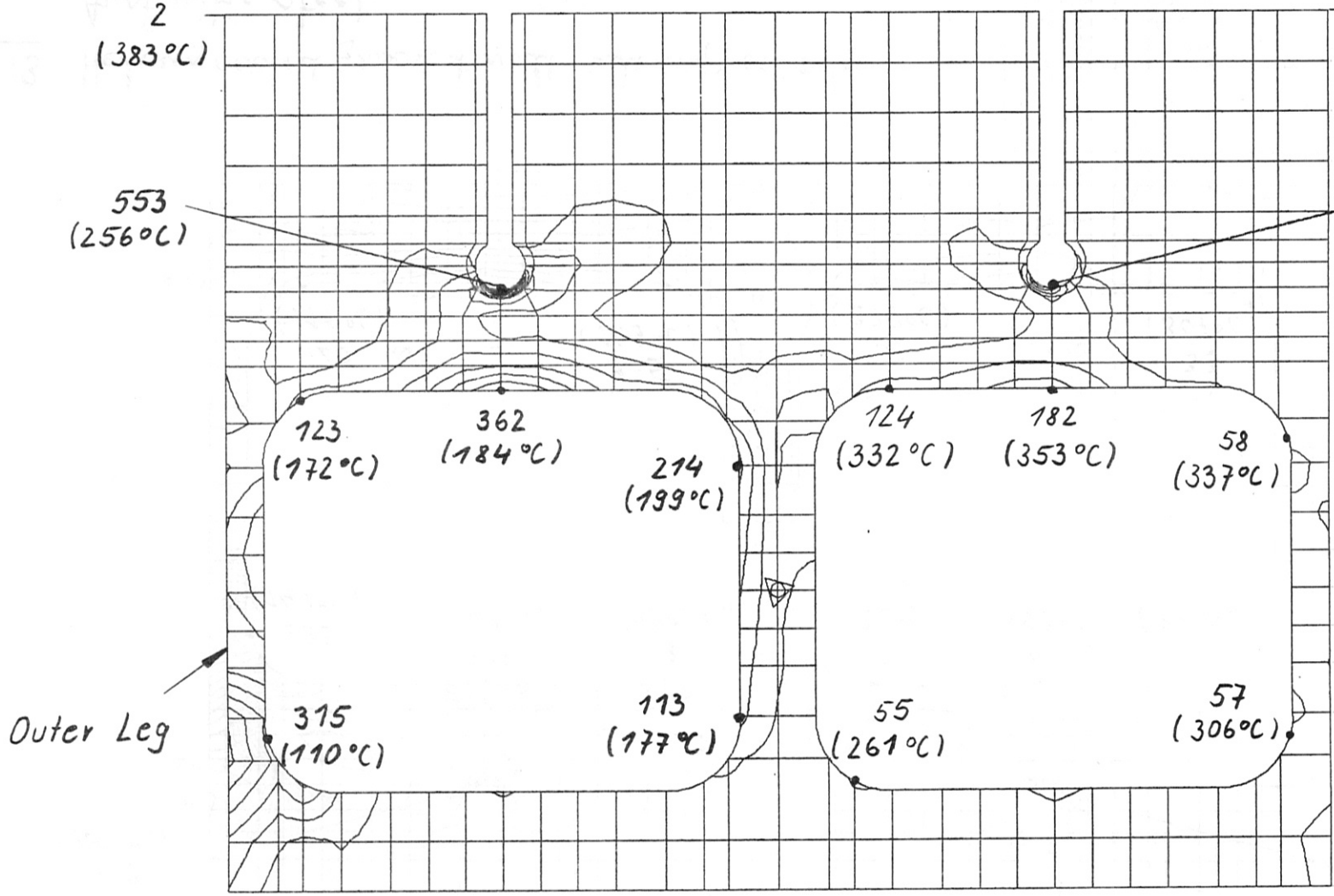

Fig. 40

Case 14 Helium cooled grooved wall, side and base supported. Austenitic steel.

SCALE REDUCTION
X 1.000
Y 1.000
Z 0.000
LEVEL SIZE
49.99999
EXPONENT
1

CONTOURS MISES (MPa)

UNITS: MM NEW DEG C SEC J --
2D THERMOMECH. ANALYSIS OF 1ST WALL, BWFSGL
LOADING 3
TEMP. + PRESSURE

DATE
JUL 20,1984
TIME
14:54:48
ICES STRUDL VERSION MAN-MEB
IPP
GARCHING

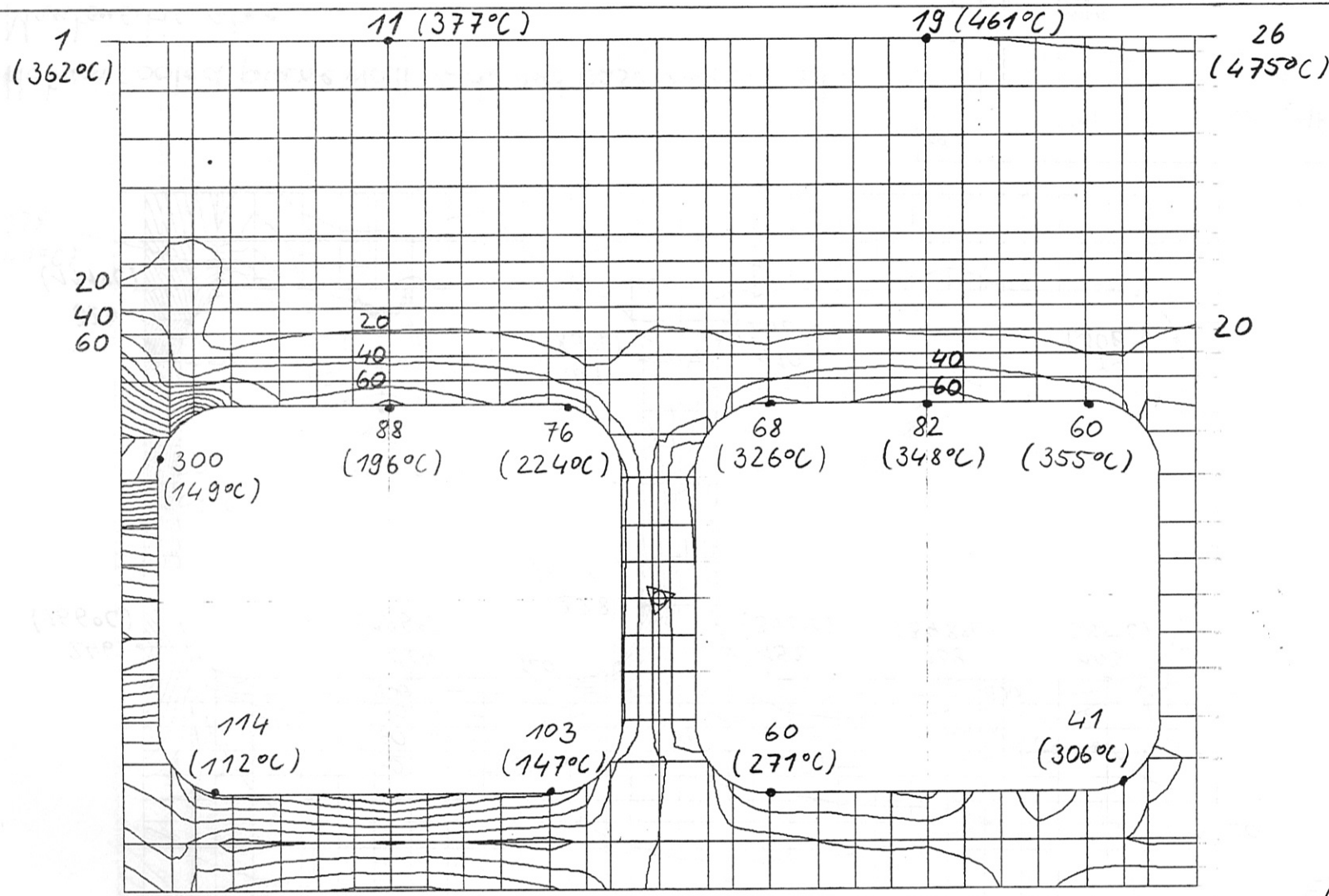

Fig. 41

Case 15 Helium cooled plane wall, side supported.
Martensitic steel.

SCALE REDUCTION
X 1.000
Y 1.000
Z 0.000
LEVEL SIZE
19.99999
EXPONENT
1

CONTOURS MISES (MPa)
UNITS: MM NEW DEG C SEC J --
2D THER. ANALYSIS OF FIRST WALL,
BHPSPM
LOADING 3
TEMP. + PRESSURE

DATE
JUL 23,1984
TIME
19:48:55
ICES STRUDL
VERSION MAN-MEB

IPP
GARCHING

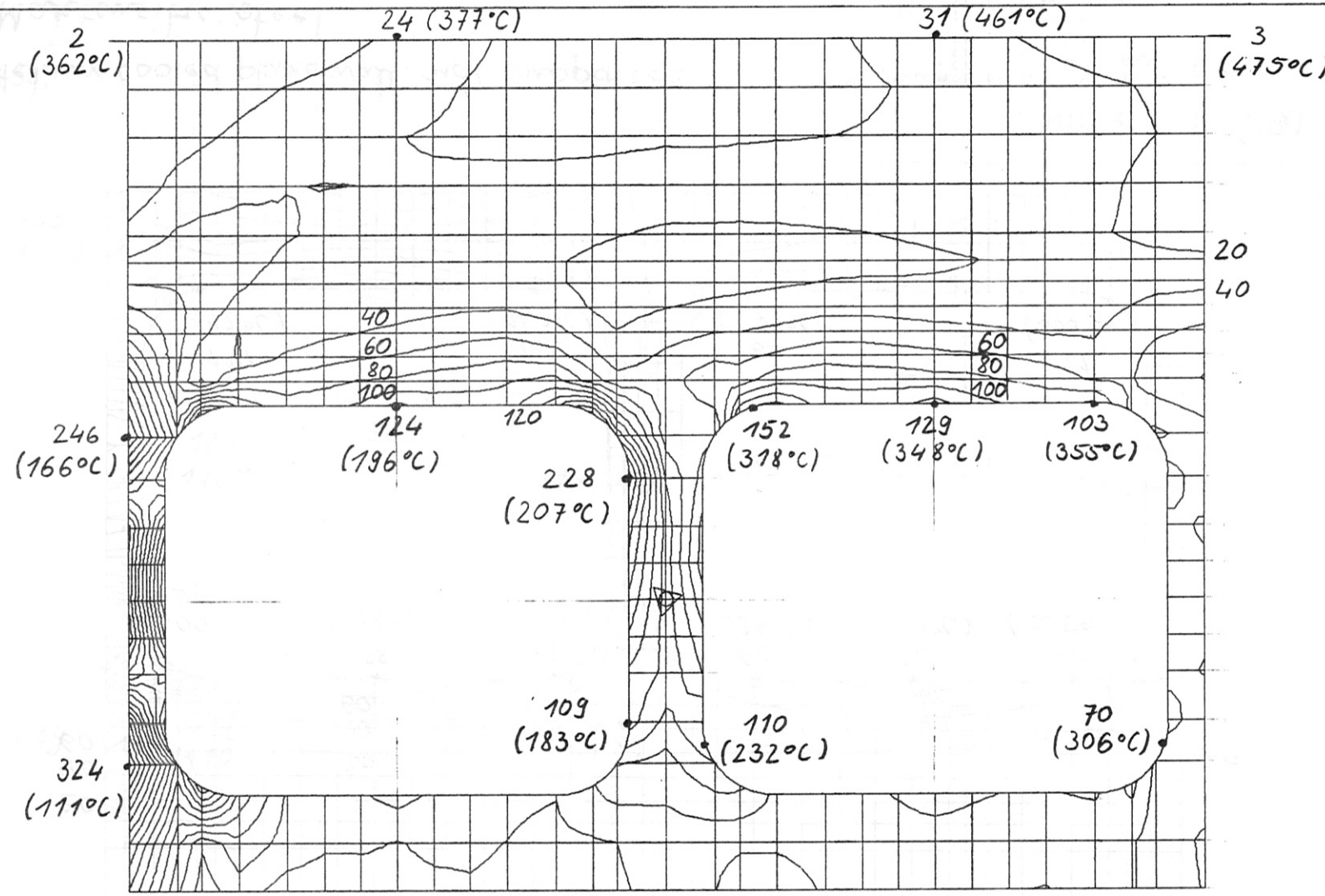

Fig. 42

Case 16 Helium cooled plane wall, side and base supported. Martensitic steel.

SCALE REDUCTION
X 1.000
Y 1.000
Z 0.000
LEVEL SIZE
19.99999
EXPONENT
1

CONTOURS MISES (MPa)
UNITS: MM NEW DEG C SEC J --
2D THER. ANALYSIS OF FIRST WALL, BHFSPM
LOADING 3
TEMP. + PRESSURE

DATE
JUL 23,1984
TIME
19:15:08
ICES SYMBOL VERSION MAR-MBB
IPP
GARCHING

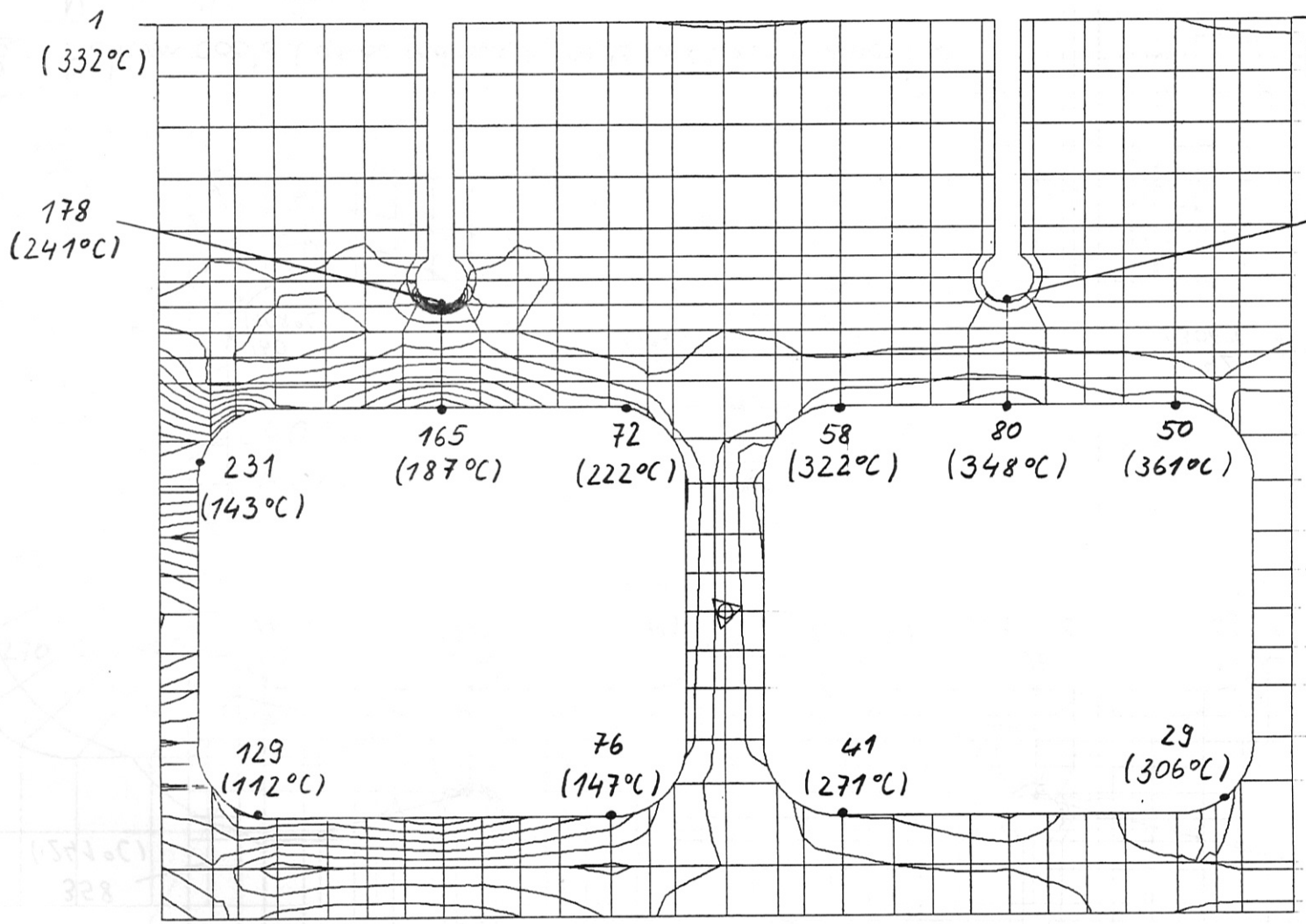

Fig. 43

Case 17 Helium cooled grooved wall, side supportd.
Martensitic steel.

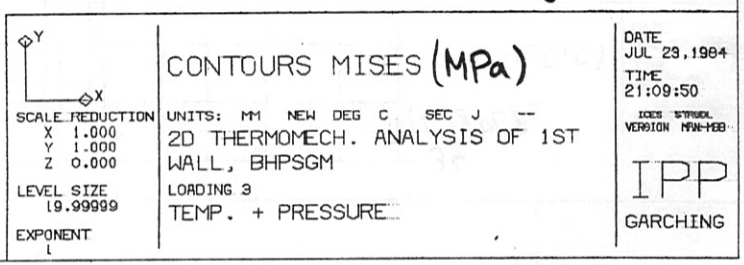

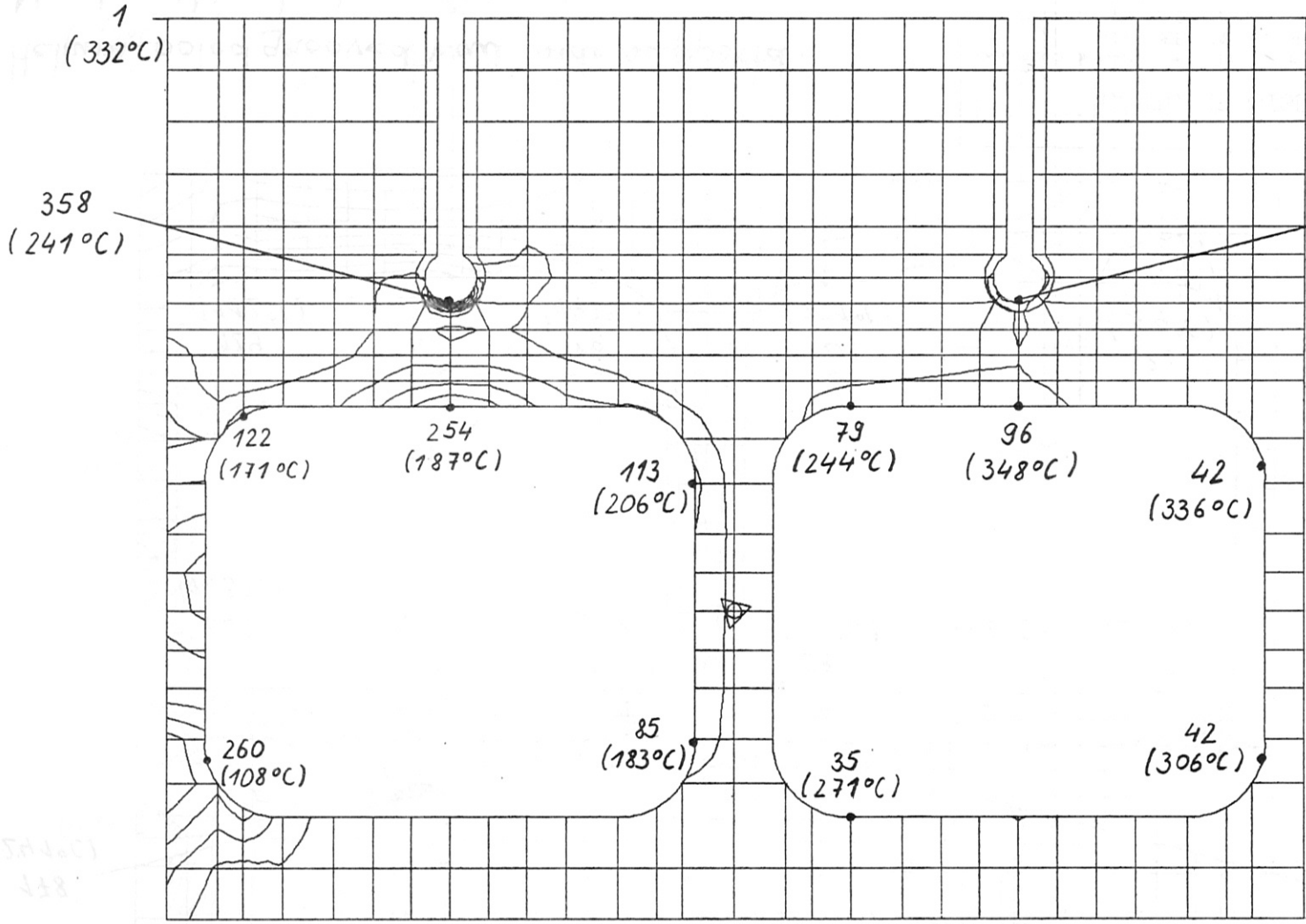

Fig. 44

Case 18 Helium cooled grooved wall, side and base supported. Martensitic steel.

SCALE REDUCTION
X 1.000
Y 1.000
Z 0.000
LEVEL SIZE
49.99999
EXPONENT
1

CONTOURS MISES (MPa)

UNITS: MM NEW DEG C SEC J —
2D THERMOMECH. ANALYSIS OF 1ST WALL, BHFSGM
LOADING 3
TEMP. + PRESSURE

DATE
JUL 23,1984
TIME
20:27:26
ICES STRUDL VERSION MAN+MEB

IPP
GARCHING

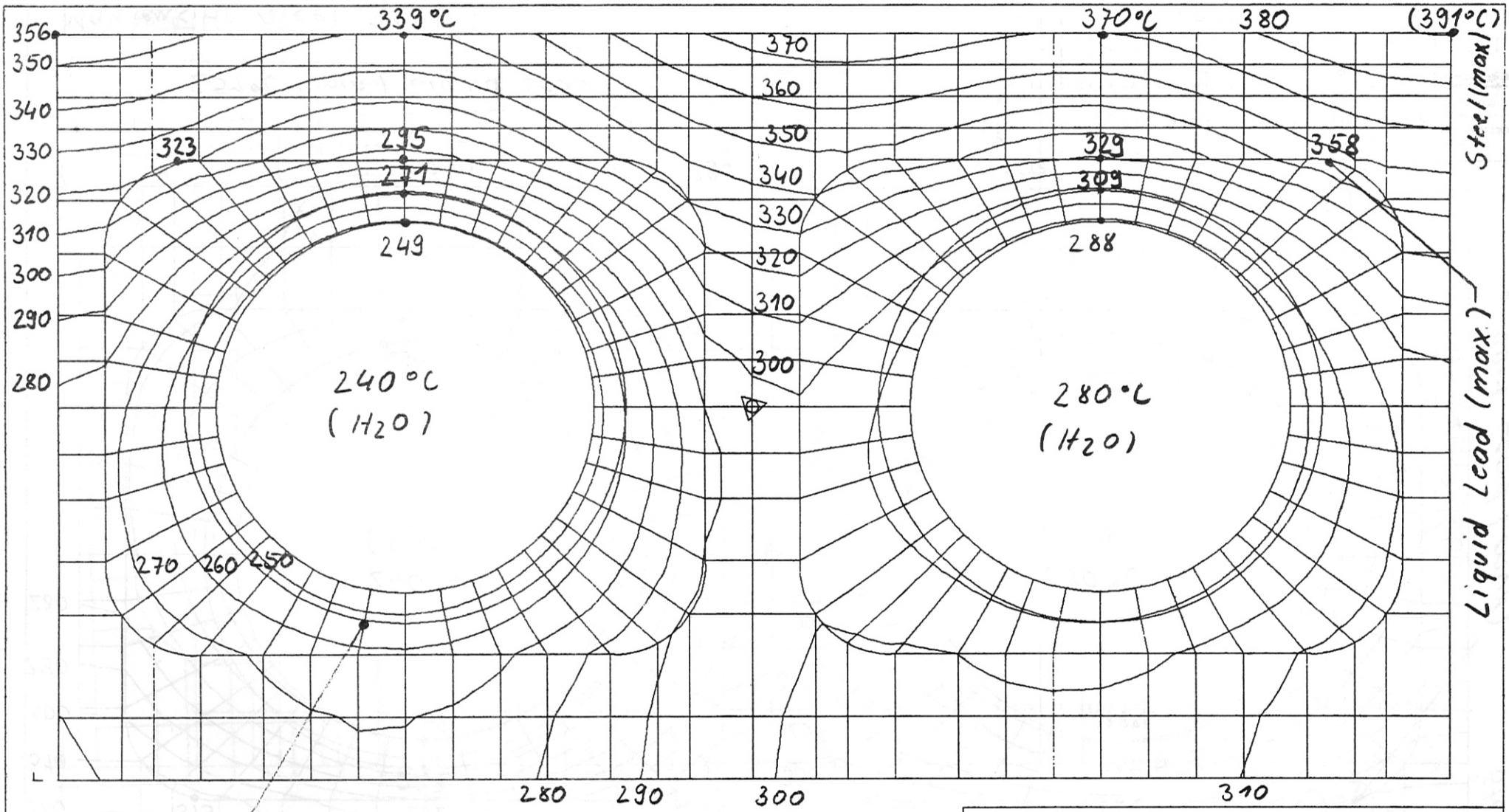
339°C
370°C
380
(391°C)
356
350
340
330
320
310
300
290
280
323
295
271
249
329
309
288
358
370
360
350
340
330
320
310
300
240°C
(H2O)
280°C
(H2O)
270 260 250
280 290 300 310
Steel (max.)
Liquid Lead (max.)
253°C (min.) Liquid Lead
Austenitic steel (316L)
CONTOURS TEMPERATURE (°C)
UNITS: MM NEW DEG C SEC J —
2D THER. ANALYSIS OF FIRST WALL, RBWFSL
LOADING 1
TEMP. DISTRIBUTION
SCALE REDUCTION
X 1.000
Y 1.000
Z 0.000
LEVEL SIZE
10.00000
EXPONENT
DATE
JUL 27.1984
TIME
10:22:39
IPP
GARCHING

Fig. 45

IPP--MVS 25.07.84 12.47:21 SBM468 M1-07 001

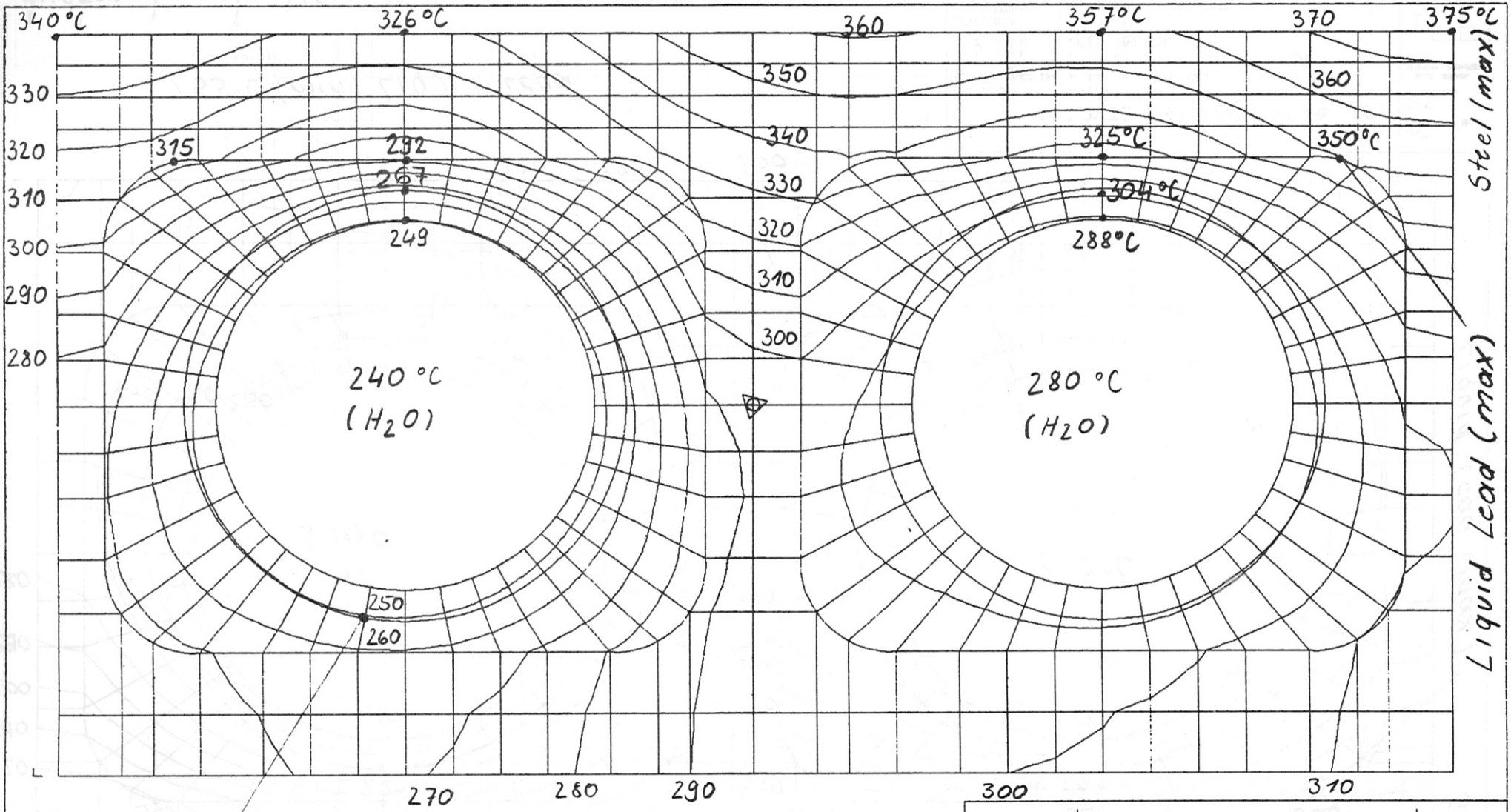

Fig. 46

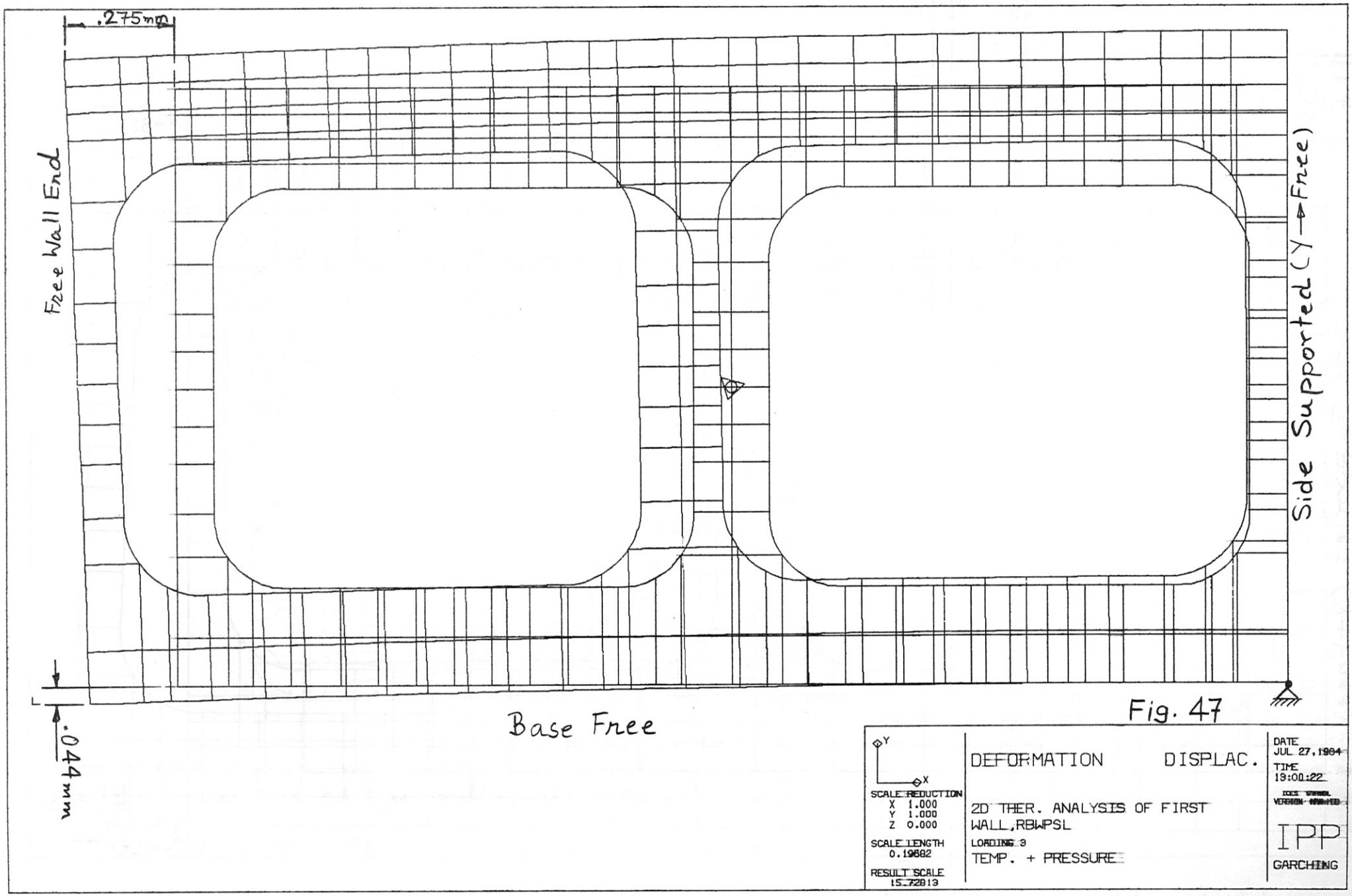
.275mm
Free Wall End
Side Supported (Y→Free)
Base Free
.044mm
Y
X
SCALE REDUCTION
X 1.000
Y 1.000
Z 0.000
SCALE LENGTH
0.19682
RESULT SCALE
15.72813
DEFORMATION DISPLAC.
2D THER. ANALYSIS OF FIRST WALL,RBWPSL
LOADING 3
TEMP. + PRESSURE
DATE
JUL 27,1984
TIME
19:00:22
IPP
GARCHING

Fig. 47

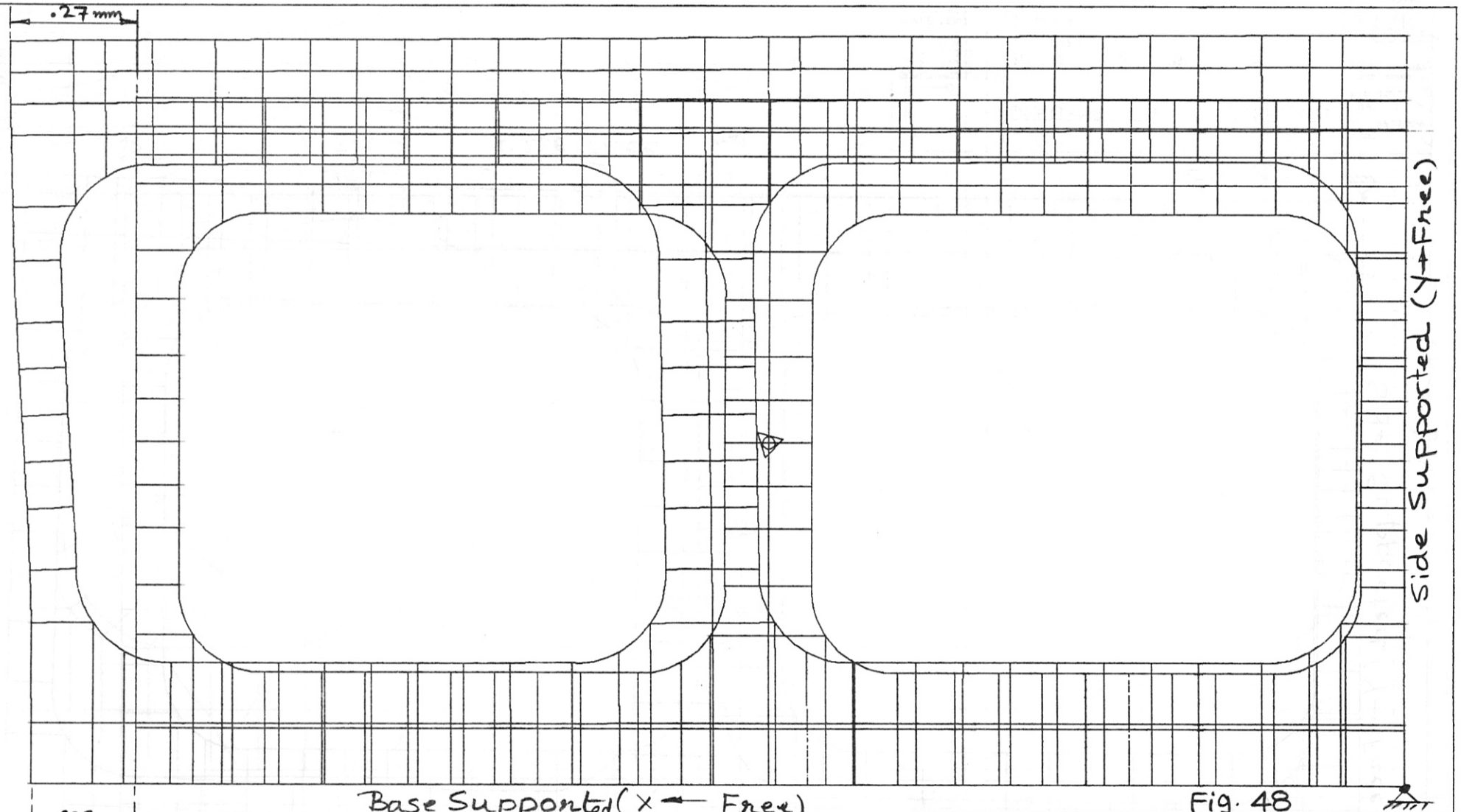

Fig. 48

SCALE REDUCTION
X 1.000
Y 1.000
Z 0.000
SCALE LENGTH
0.19190
RESULT SCALE
16.0081

DEFORMATION DISPLAC.

2D THER. ANALYSIS OF FIRST WALL,RBWFSL
LOADING 3
TEMP. + PRESSURE

DATE
JUL 27,1984
TIME
10:34:04

IPP
GARCHING

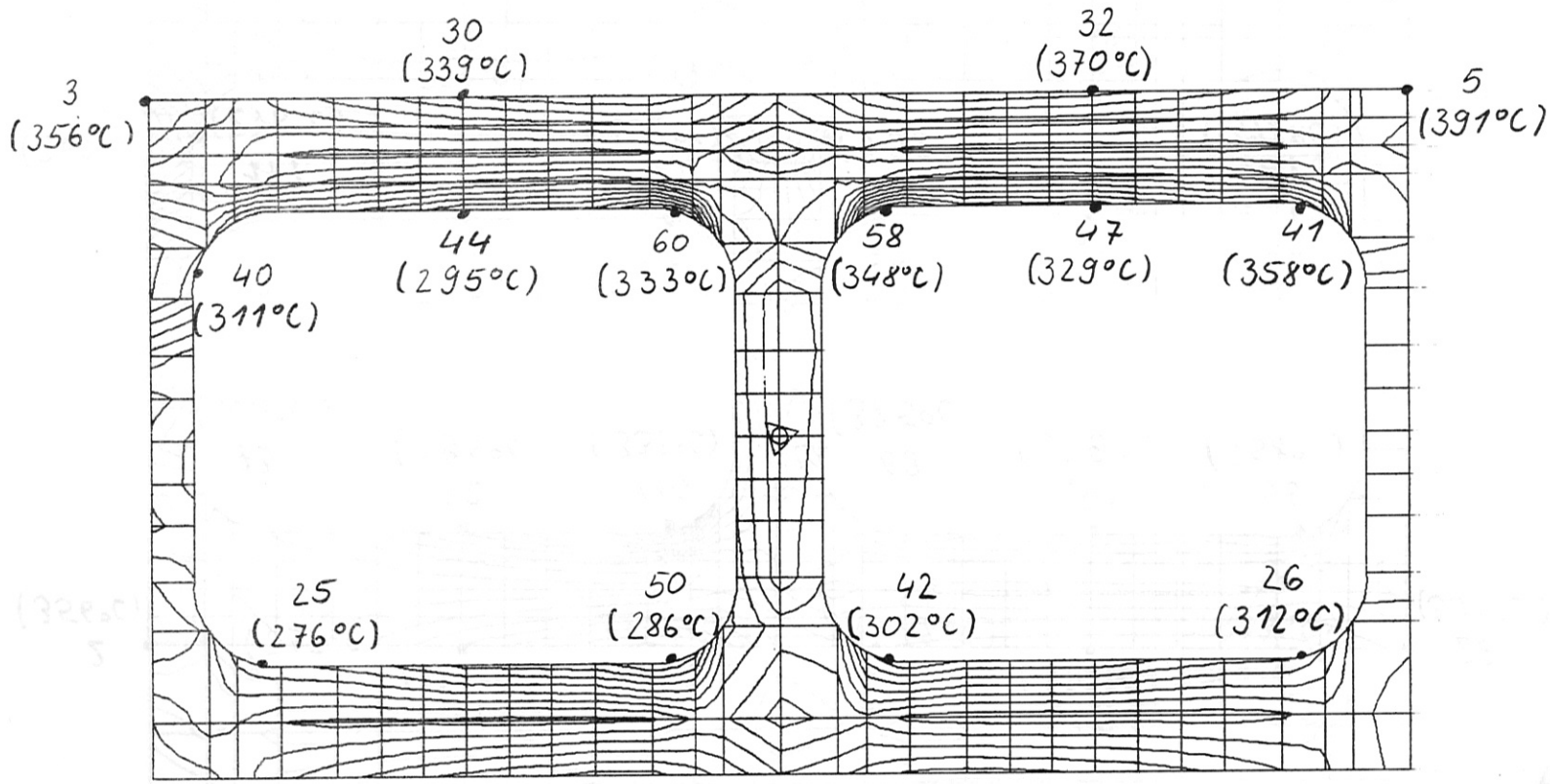

Fig. 49

Case 19 Water cooled thin wall, side supported.
Austenitic steel.

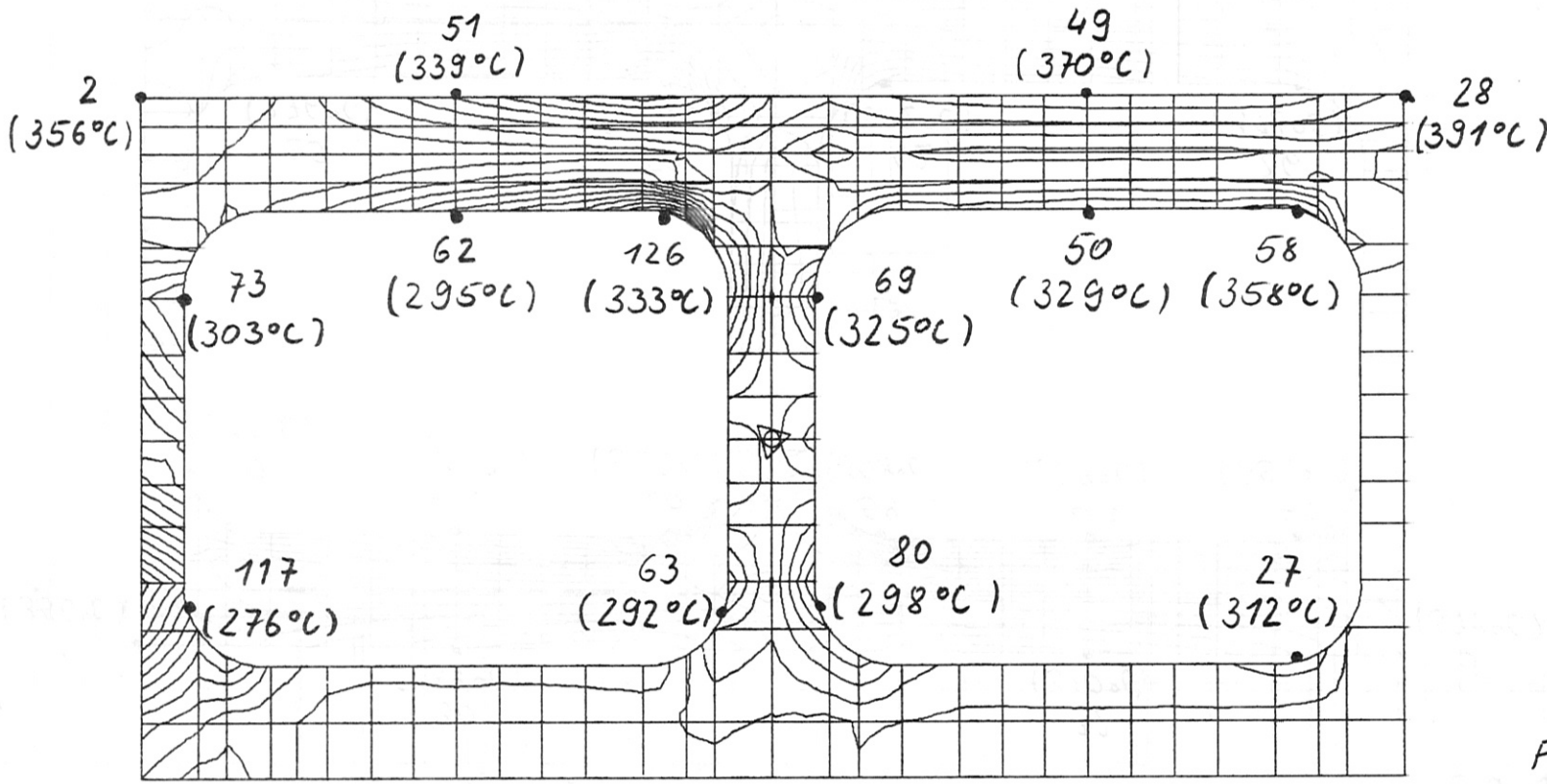

Fig. 50

Case 20 Water cooled thin wall, side and base supported. Austenitic steel.

CONTOURS MISES (MPa)

SCALE REDUCTION
X 1.000
Y 1.000
Z 0.000
LEVEL SIZE
10.00000
EXPONENT
1

UNITS: MM NEW DEG C SEC J —
2D THER. ANALYSIS OF FIRST WALL,RBWFSL
LOADING 3
TEMP. + PRESSURE

DATE
JUL 27.1984
TIME
10:49:21

IPP
GARCHING

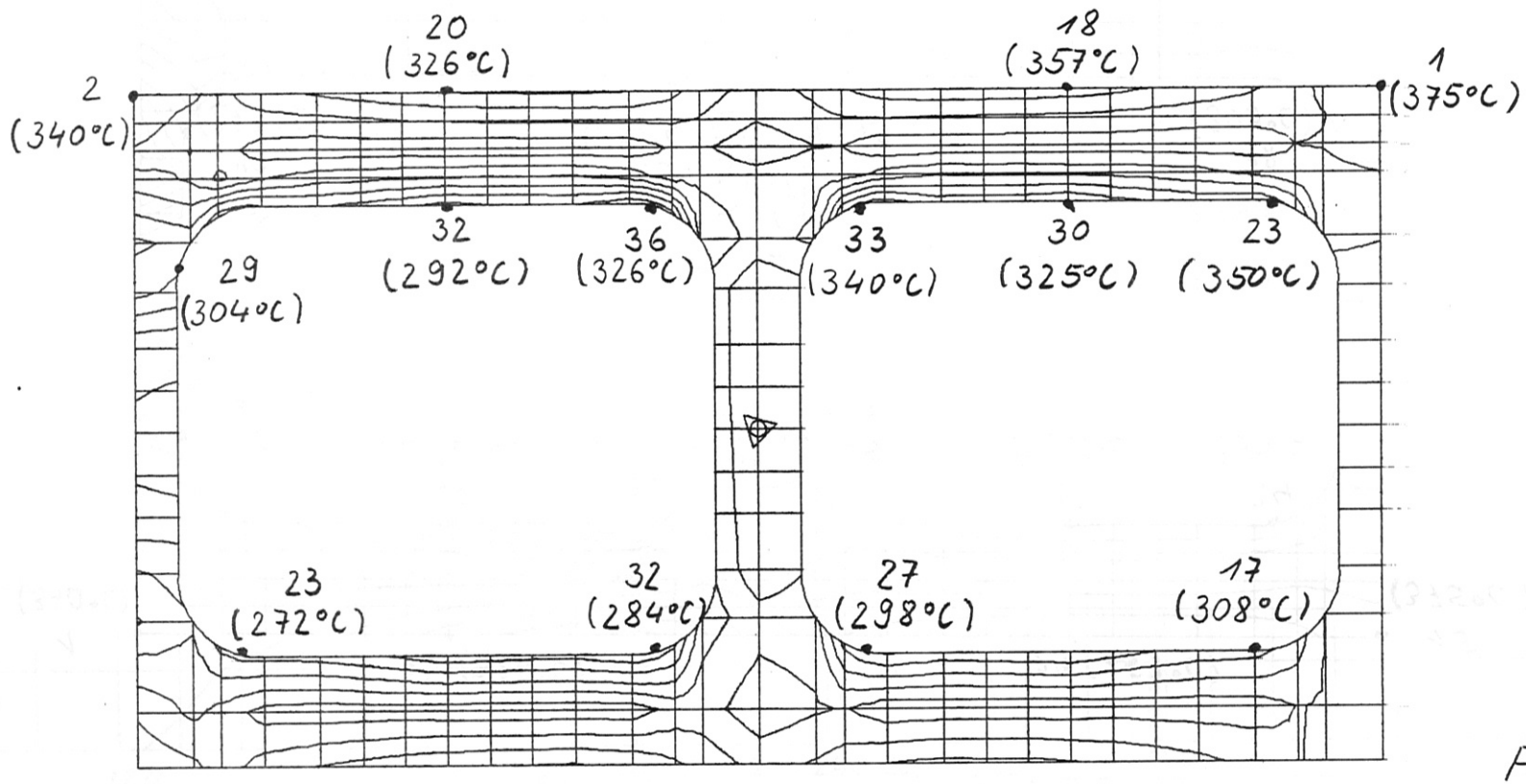

Fig. 51

CONTOURS MISES (MPa)

SCALE REDUCTION
X 1.000
Y 1.000
Z 0.000
LEVEL SIZE
5.00000
EXPONENT
0

UNITS: MM NEW DEG C SEC J —
2D THER. ANALYSIS OF FIRST WALL, RBWPSM
LOADING 3
TEMP. + PRESSURE

DATE
JUL 26,1984
TIME
17:58:05

IPP
GARCHING

Case 21 Water cooled thin wall, side supported
Martensitic steel.

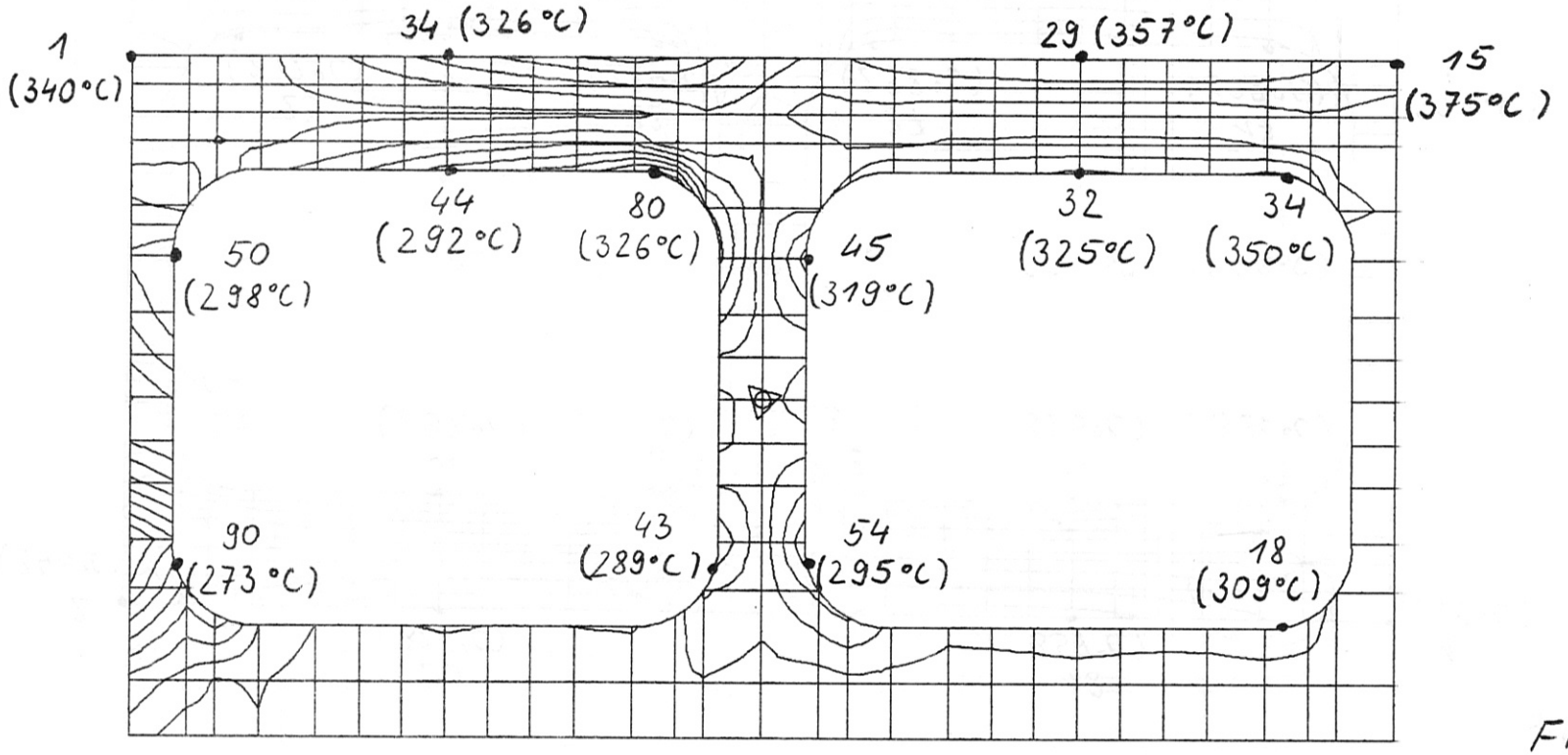

Fig. 52

Case 22 Water cooled thin wall, side and base supported. Martensitic steel.

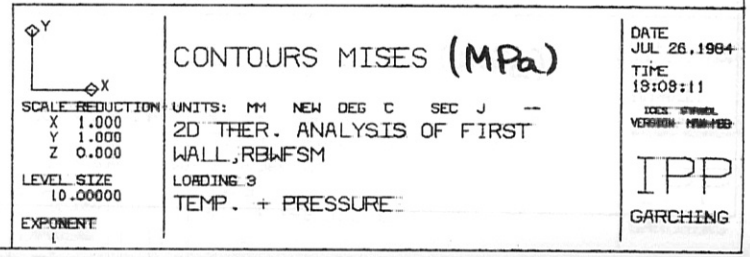

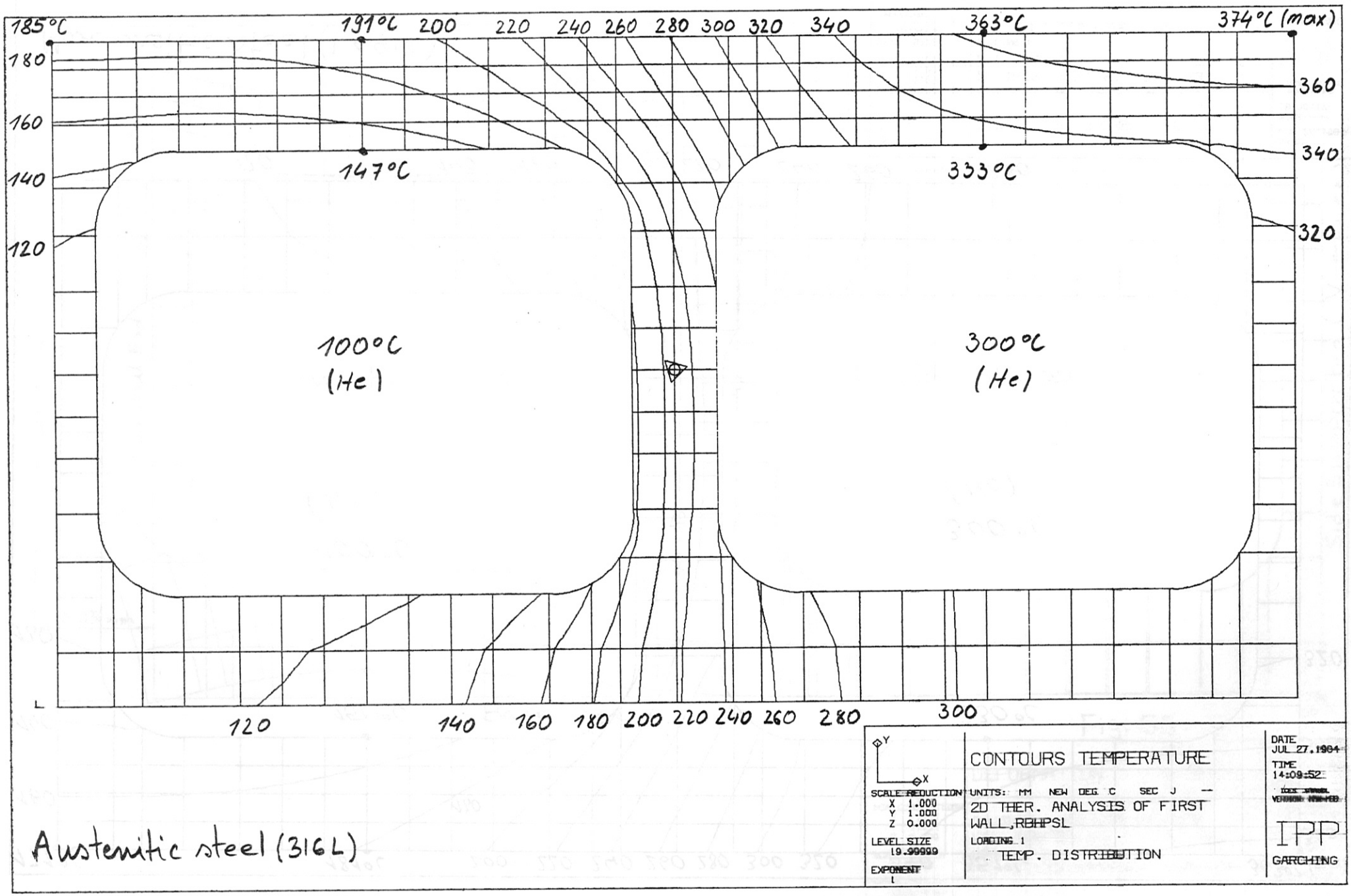

Austenitic steel (316L)

Fig. 53

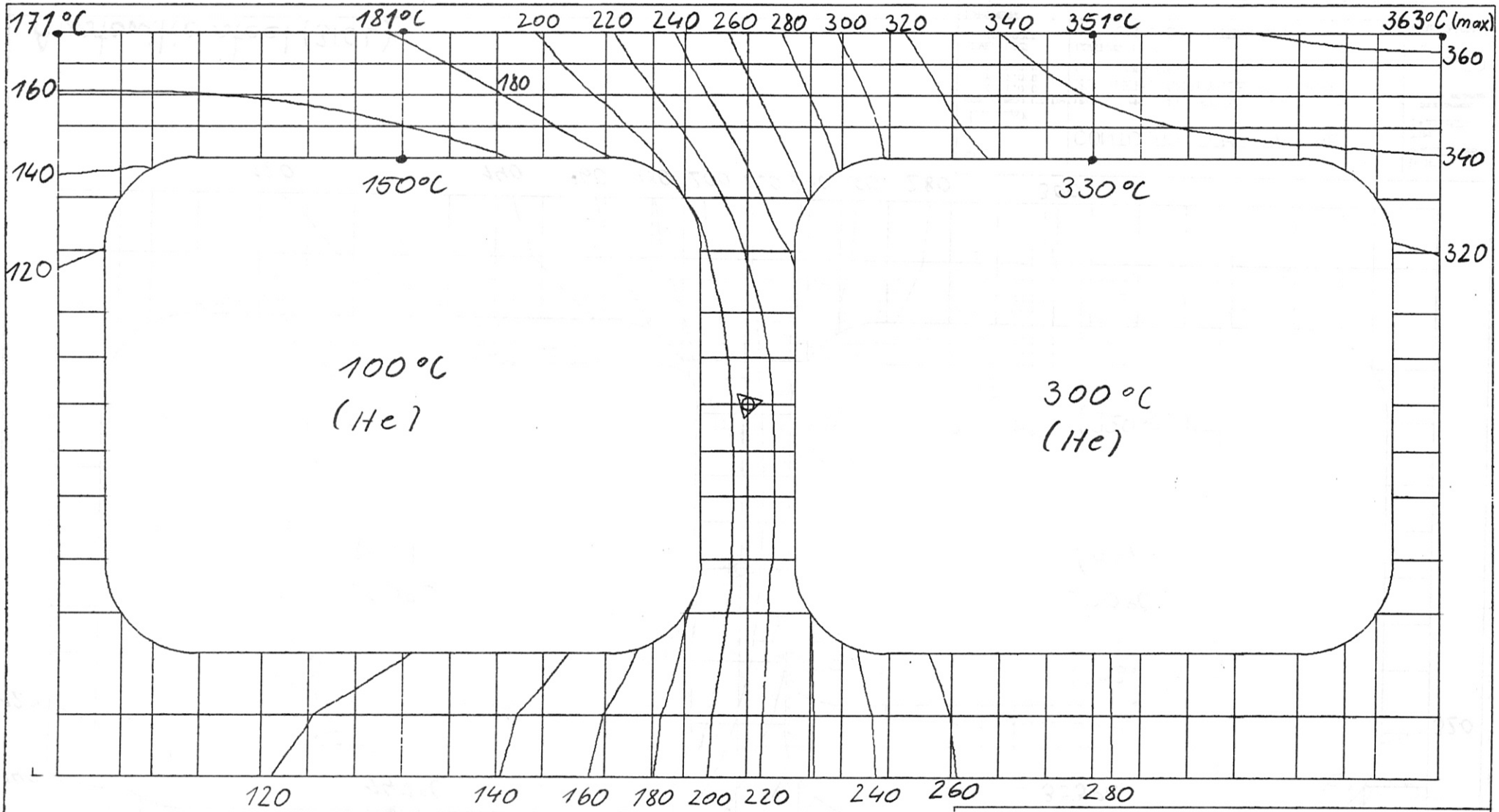

Martensitic steel (1.4914)

Fig. 54

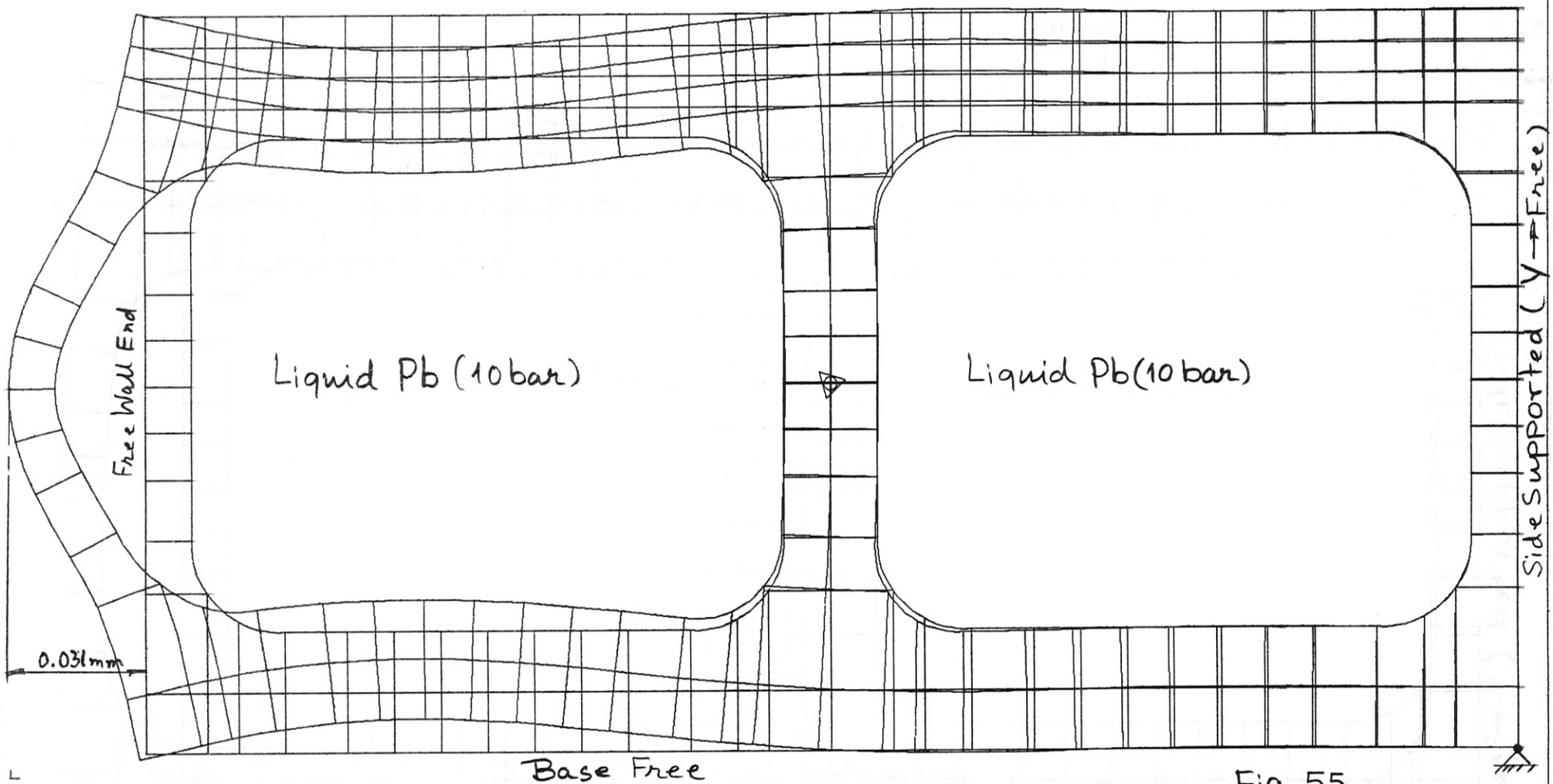

Fig. 55

SCALE REDUCTION
X 1.000
Y 1.000
Z 0.000
SCALE LENGTH
0.10615
RESULT SCALE
1066.76489

DEFORMATION DISPLAC.

2D THER. ANALYSIS OF FIRST WALL,RBWPSL
LOADING 2
FLUID LEAD PRESSURE (N/MM**2)

DATE
JUL 27,1984
TIME
19:00:10

IPP
GARCHING

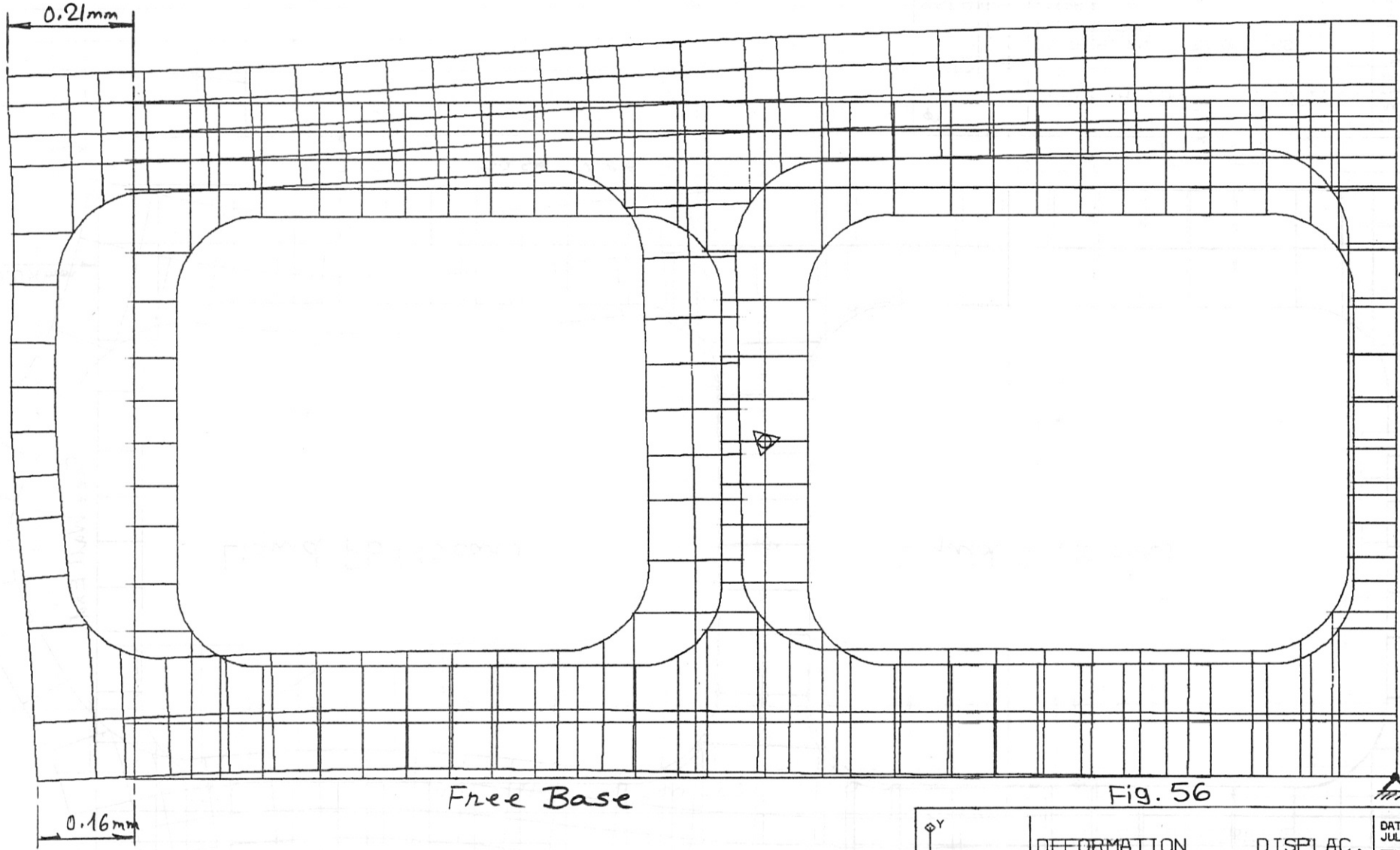

Fig. 56

SCALE REDUCTION
X 1.000
Y 1.000
Z 0.000
SCALE LENGTH
0.19674
RESULT SCALE
20.69617

DEFORMATION DISPLAC.

2D THER. ANALYSIS OF FIRST WALL, RBHPSL

LOADING 3
TEMP. + PRESSURE

DATE
JUL 27.1984
TIME
14:18:29

IPP
GARCHING

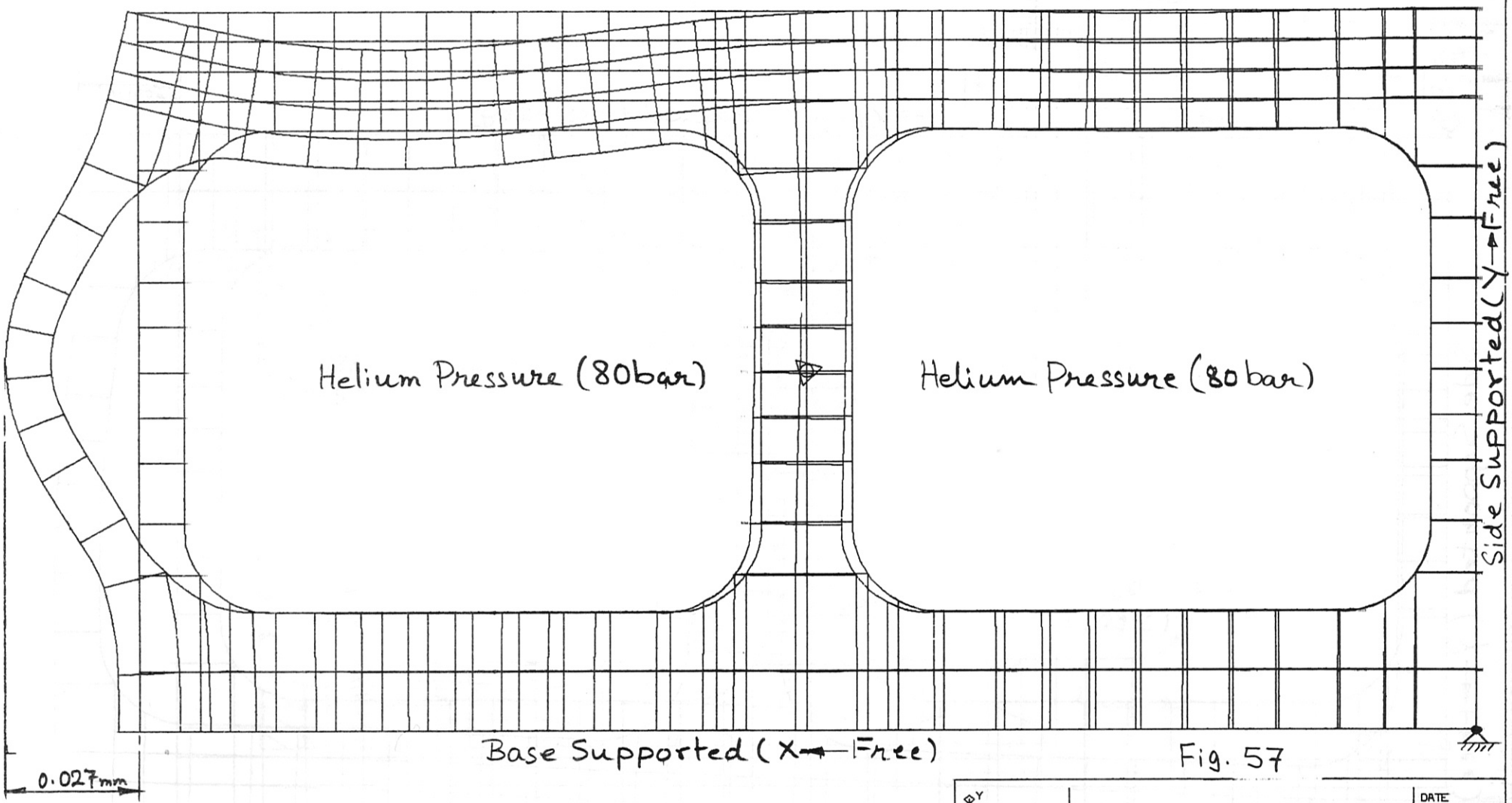

Fig. 57

SCALE REDUCTION
X 1.000
Y 1.000
Z 0.000
SCALE LENGTH
0.19822
RESULT SCALE
167.74458

DEFORMATION DISPLAC.

2D THER. ANALYSIS OF FIRST WALL,RBHFSL
LOADING 2
HELIUM GAS PRESSURE (N/MM**2)

DATE
JUL 27,1984
TIME
19:36:29

IPP
GARCHING

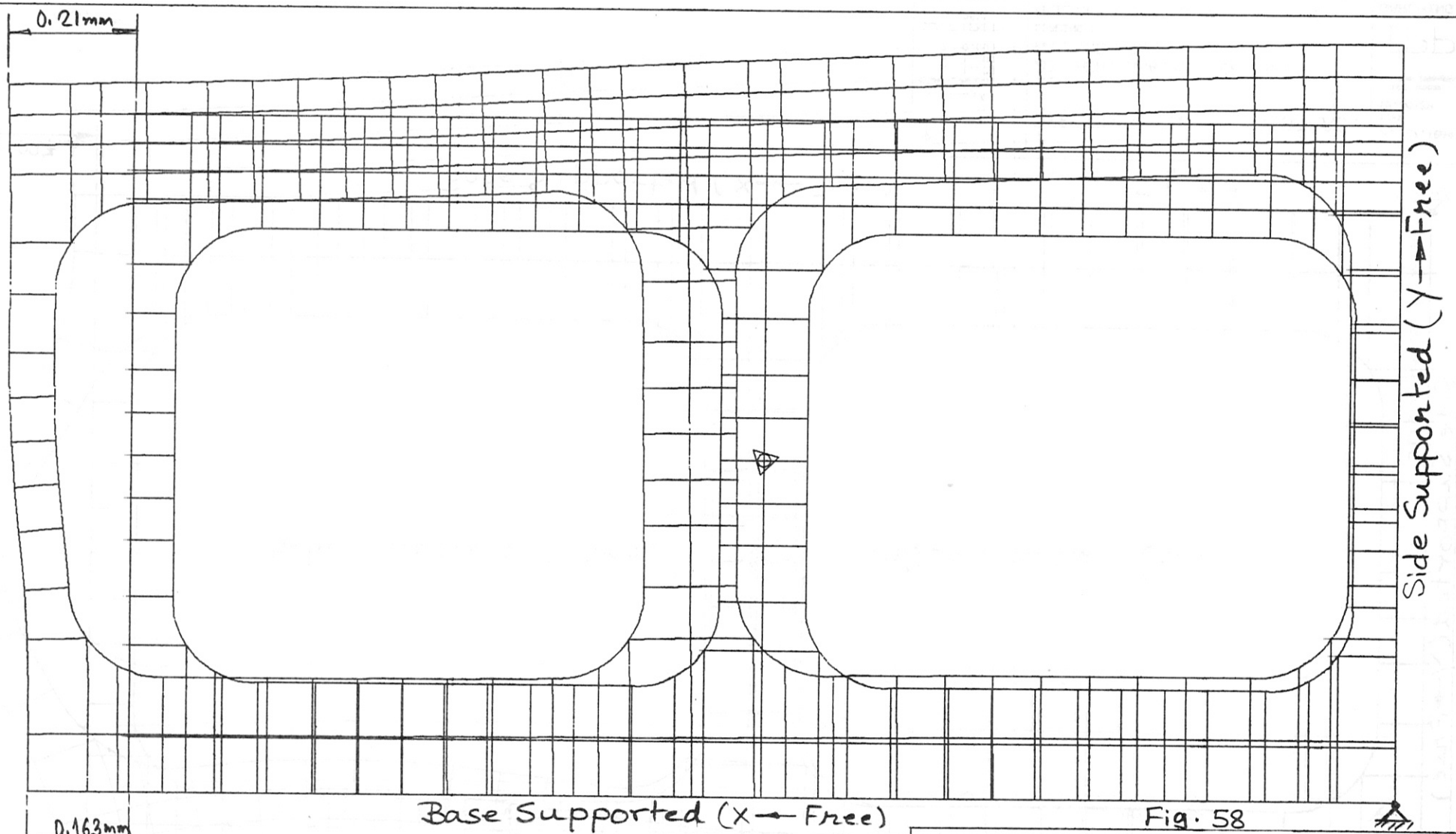

Fig. 58

SCALE REDUCTION
X 1.000
Y 1.000
Z 0.000
SCALE LENGTH
0.19613
RESULT SCALE
21.01266

DEFORMATION DISPLAC.

2D THER. ANALYSIS OF FIRST WALL,RBHFSL
LOADING 3
TEMP. + PRESSURE

DATE
JUL 27.1984
TIME
19:36:52

IPP
GARCHING

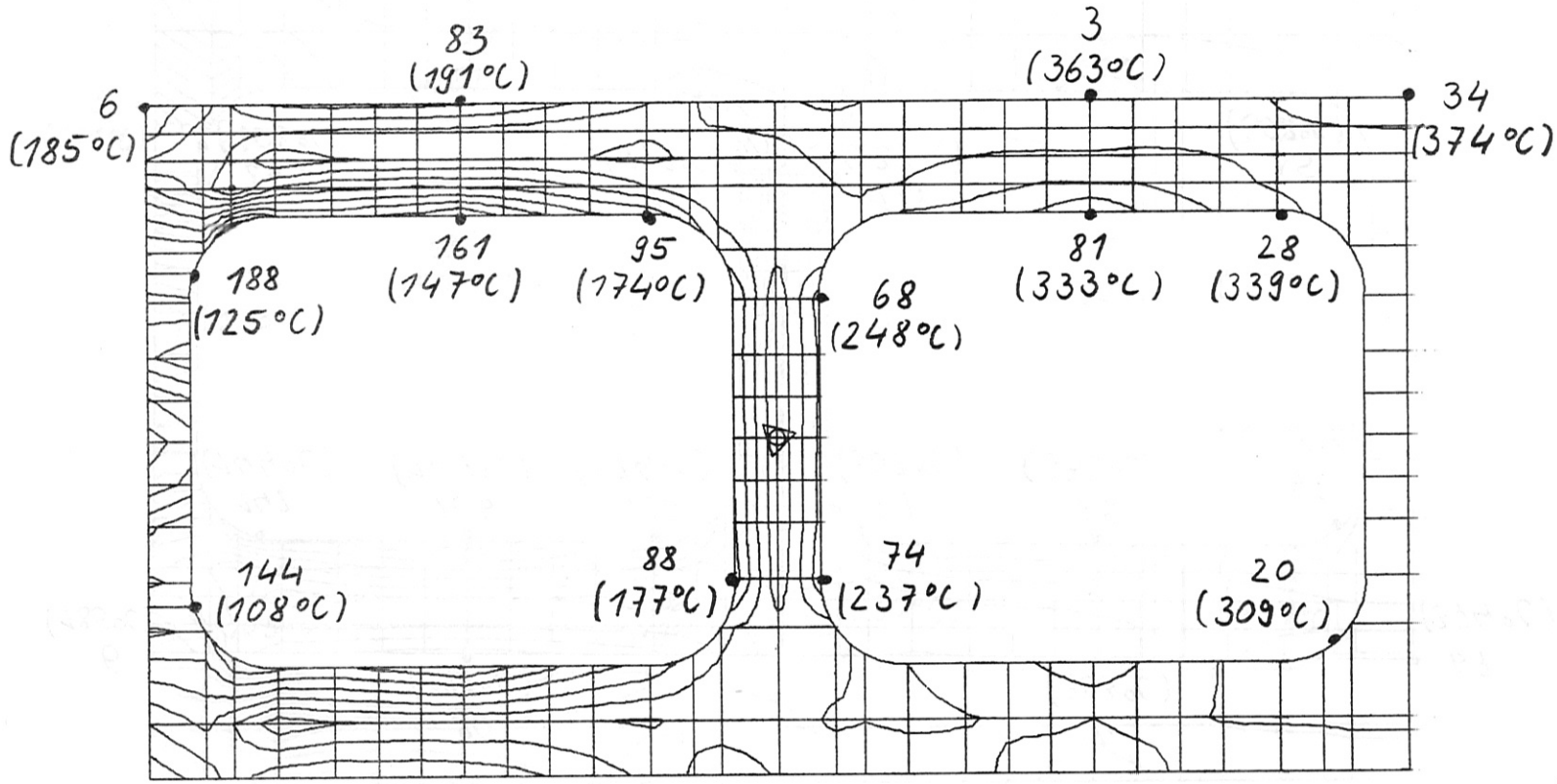

Fig. 59

CONTOURS MISES (MPa)

UNITS: MM NEW DEG C SEC J —
2D THER. ANALYSIS OF FIRST WALL.RBHPSL
LOADING 3
TEMP. + PRESSURE

SCALE REDUCTION
X 1.000
Y 1.000
Z 0.000
LEVEL SIZE
19.99999

DATE
JUL 27.1984
TIME
14:28:04

IPP
GARCHING

Case 23 Helium cooled thin wall, side supported.
Austenitic steel.

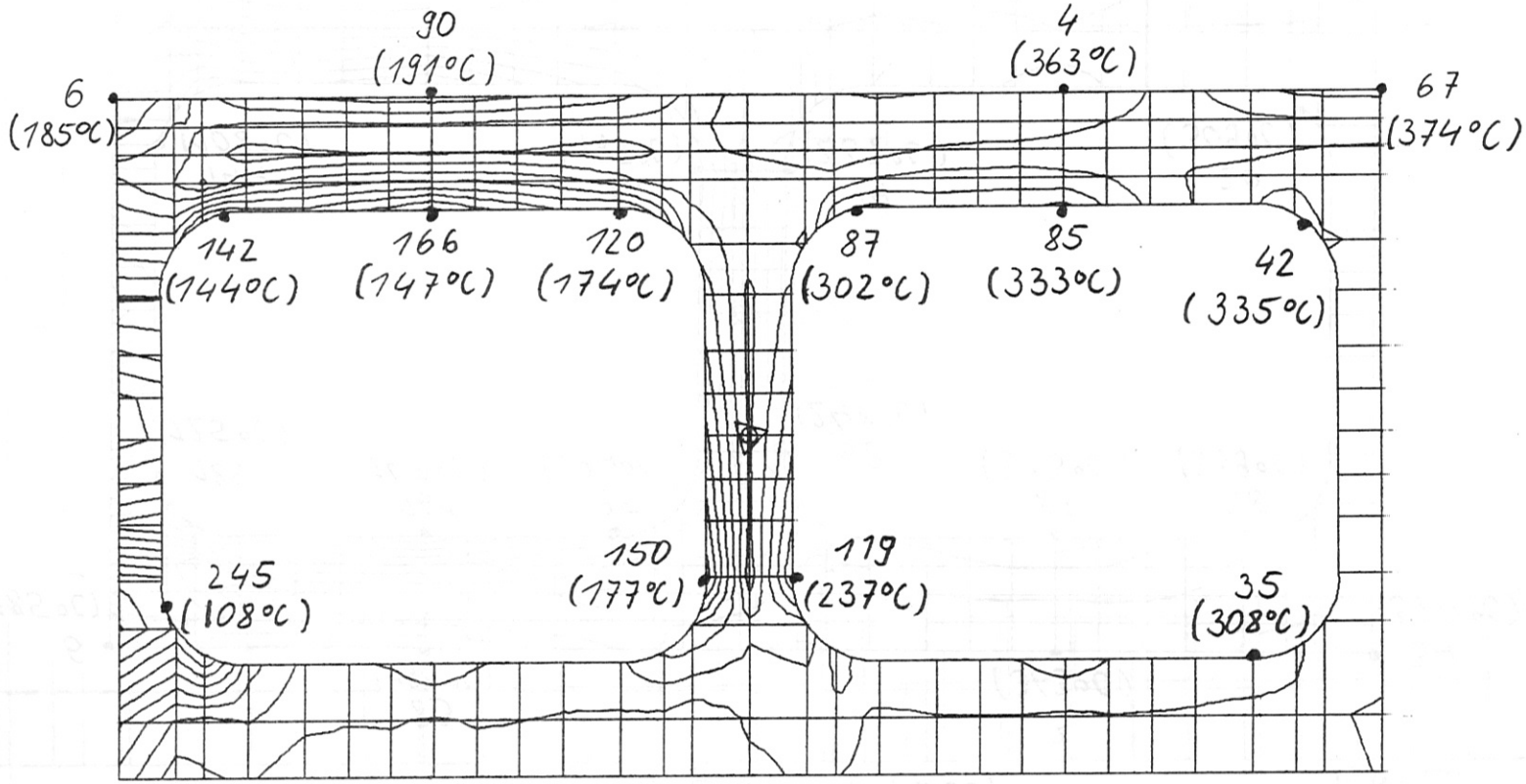

Fig. 60

Case 24 Helium cooled thin wall, side and base supported. Austenitic steel.

SCALE REDUCTION
X 1.000
Y 1.000
Z 0.000
LEVEL SIZE
19.99999
EXPONENT
1

CONTOURS MISES (MPa)
UNITS: MM NEW DEG C SEC J —
2D THER. ANALYSIS OF FIRST WALL, RBHFSL
LOADING 3
TEMP. + PRESSURE

DATE
JUL 27, 1984
TIME
19:52:25

IPP
GARCHING

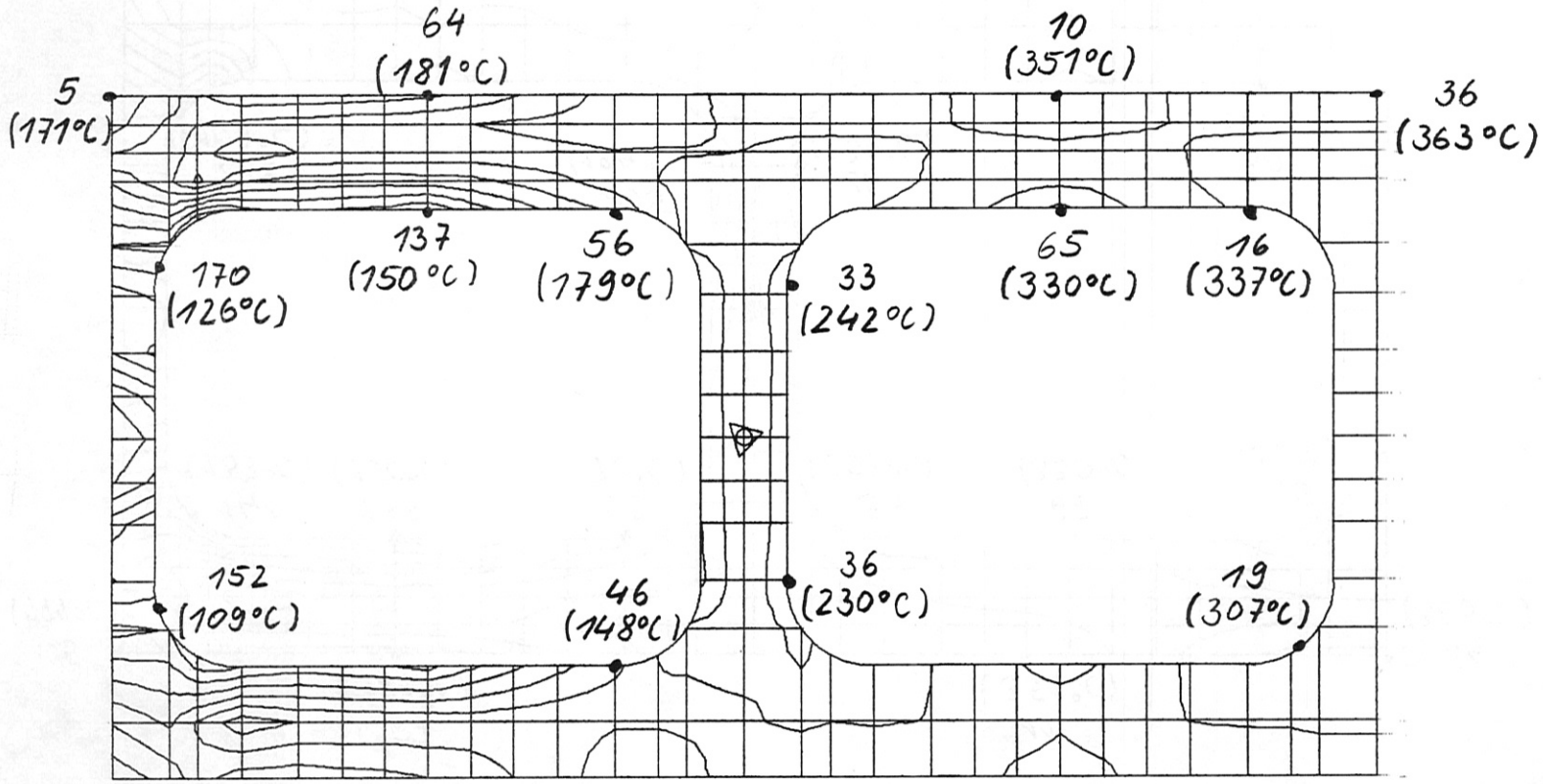

Fig. 61

Case 25 Helium cooled thin wall, side supported.
Martensitic steel.

SCALE REDUCTION X 1.000 Y 1.000 Z 0.000	CONTOURS MISES (MPa)
LEVEL SIZE 9.99999	UNITS: MM NEW DEG C SEC J --
EXPONENT 1	2D THER. ANALYSIS OF FIRST WALL,RBHPSM
	LOADING 3 TEMP. + PRESSURE
	DATE JUL 26.1984 TIME 18:21:24
	IPP GARCHING

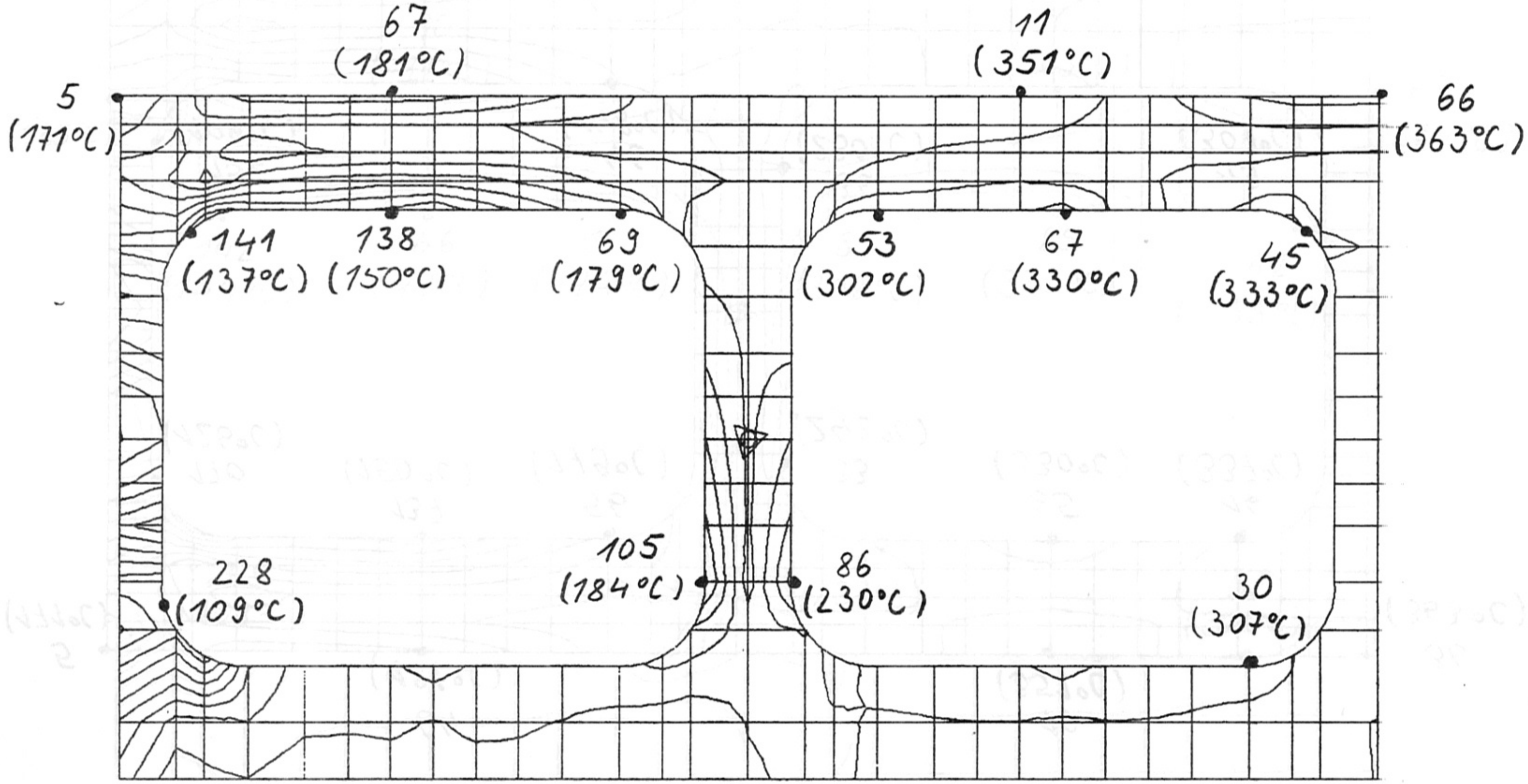

Fig. 62

Case 26 Helium cooled thin wall, side and base supported.
Martensitic steel.

Y X SCALE REDUCTION X 1.000 Y 1.000 Z 0.000 LEVEL SIZE 19.99999 EXPONENT 1	CONTOURS MISES (MPa) UNITS: MM NEW DEG C SEC J -- 2D THER. ANALYSIS OF FIRST WALL,RBHFSM LOADING 3 TEMP. + PRESSURE	DATE JUL 26,1984 TIME 17:18:35 IPP GARCHING